[redacted]

SC-CR-66-2000X

UNCLASSIFIED

FINAL REPORT - -BAYONET PROJECT (U)

1st Review Date: 8-14-97
Authority: ☐ADC ☒ W. Layne
Name:
2nd Review Date: 9/3/97
Authority: ADD
Name: RBCraner

U
Contains Restricted Data
Contains FRD Classified Information
Contains UCNI
Contains
OK for Release

SANDIA SYSTEMATIC DECLASSIFICATION REVIEW
DOWNGRADING OR DECLASSIFICATION STAMP

CLASSIFICATION: U AUTHORITY: R.B. Craner
Emelda Selph 9-11-97
PERSON CHANGING MARKING
REFERENCE: 97SN3351
Carmela Gallegos 9/17/97
PERSON VERIFYING MARKING
DATE: 9/3/97

AUGUST 1966
DAC-59327

PREPARED BY:
R.L. PELLEY
AERO/THERMODYNAMICS SECTION

R.W. SPORING
CONTROLS SECTION

G. F. Lind

APPROVED BY:
G.F. LIND
PROGRAM MANAGER
BAYONET PROGRAM

A.M. GARBLIK
DIRECTOR
ADVANCED MISSILES
AND RE-ENTRY SYSTEMS

[redacted]

UNCLASSIFIED

[redacted]

[redacted]

SC-CR-66-2000X

UNCLASSIFIED

RECORD COPY
Do Not Take From This Room

FINAL REPORT - -BAYONET PROJECT
(U)

AUGUST 1966
DAC-59327

REC'D 9320
C. 3
SEP 9 1966

MISSILE & SPACE SYSTEMS DIVISION
DOUGLAS AIRCRAFT COMPANY, INC.
SANTA MONICA CALIFORNIA

DOUGLAS

UNCLASSIFIED

[redacted]

PREFACE

This document is submitted to the Sandia Corporation, Albuquerque, New Mexico, in compliance with Amendment 6 to Sandia Contract No. 82-7431, dated 10 March 1965. It presents the final report by the Douglas Aircraft Company, Inc., of the results of a 5-month program of wind tunnel tests and preliminary control system studies for a tactical Bayonet missile system.

Requests for further information or assistance will be welcomed by the following Douglas representatives:

- Mr. G. F. Lind, Program Manager
  Santa Monica, California
  Telephone: 213-399-9311, Extension 3096
- Mr. F. R. Ruelke, Contracts Representative
  Santa Monica, California
  Telephone: 213-399-9311, Extension 5102.

ABSTRACT

Means of increasing lift and providing roll control for the Bayonet vehicle were studied. The results indicated that the optimum Bayonet configuration should employ slats, plain flaps, T-tail, and a jet roll control system. These devices should enable Bayonet to obtain a trim lift coefficient of about 1.1 and permit both a supersonic (Mach ≤ 1.2) and a wing station launch.

CONTENTS

	LIST OF FIGURES	ix
	LIST OF TABLES	xiii
	LIST OF SYMBOLS	xv
Section 1	INTRODUCTION	1
Section 2	SUMMARY	5
Section 3	ANALYSIS OF WIND TUNNEL RESULTS	9
	3.1 Longitudinal Stability	14
	3.2 Directional and Lateral Stability	50
	3.3 Roll Control Devices	54
	3.4 Carry and Glide Configuration	59
Section 4	ANALYSIS OF ROLL CONTROL REQUIREMENT	65
	4.1 Introductory Remarks	65
	4.2 Roll Control Analysis	66
	4.3 Mechanization	80
	4.4 Preliminary Roll Control Configuration	84
Section 5	RECOMMENDED ADVANCED BAYONET CONFIGURATION	87
	REFERENCES	89
Appendix	RUN SCHEDULE	91

FIGURES

3-1	Bayonet Wind Tunnel Model Contoured Wing, Slat, Plain Flap, Fairings, and Ailerons 30% Scale	10
3-2	Bayonet Wind Tunnel Model Slab Wing, Jet Flaps, and Jet Roll Control 30% Scale	11
3-3	Run 57	12
3-4	Run 1	13
3-5	Longitudinal Stability	15
3-6	Effect of Slab Wing on Longitudinal Stability-- M = 0.6, i_w = 14°, and 8.4% Horizontal Tail	18
3-7	Effect of Slab Wing on Longitudinal Stability-- Mach No. = 0.8, i_w = 14°, and 8.4% Tail	19
3-8	Effect of Slab Wing on Longitudinal Stability-- M = 1.2, i_w = 14°, and 8.4% Tail	20
3-9	Run 19, PT2	22
3-10	Run 19, PT3	23
3-11	Effect of Slat on Longitudinal Stability-- Mach No. = 0.6, i_w = 14%, and 8.4% Tail	25
3-12	Effect of Slat on Longitudinal Stability-- 8.4% Tail, Mach No. = 0.8, and i_w = 14°	26
3-13	Effect of Slat on Longitudinal Stability-- Mach No. = 1.2, i_w = 14°, and 8.4% Horizontal Tail	27
3-14	Longitudinal Stability with Slat Deflected	28
3-15	Effect of Plain Flap on Longitudinal Stability-- Mach No. = 0.6, Slat Undeflected, i_w = 14°, and 8.4% Tail	30
3-16	Effect of Plain Flaps on Longitudinal Stability-- Mach No. = 0.8, Slats Undeflected, i_w = 14°, and 8.4% Tail	31
3-17	Effect of Plain Flap on Longitudinal Stability-- Mach No. = 1.2, i_w = 14°, 8.4% Tail, and δ_s = 0°	32

3-18 Effect of Deflecting the Slat and Increasing the Horizontal Tail Size on Longitudinal Stability-- $M = 0.6$ and $\delta_F = 40°$ 33

3-19 Effect of Deflecting the Slat and Increasing the Horizontal Tail Size on Longitudinal Stability-- $M = 0.8$ and $\delta_F = 40°$ 34

3-20 Effect of Deflecting the Slat and Increasing the Horizontal Tail Size on Longitudinal Stability-- $M = 1.2$ and $\delta_F = 40°$ 35

3-21 Longitudinal Stability of the Complete Configuration-- $\delta_s = 15°$, $\delta_F = 40°$, and $i_w = 16°$ 37

3-22 Longitudinal Stability of the Complete Configuration-- $\delta_s = 15°$, $\delta_F = 40°$, and $i_w = 16°$ 38

3-23 Effect of Mach Number on Horizontal Tail Effectiveness-- ΔC_M = Pitching Moment Increase Between the 30% Tail and 8.4% Tail 39

3-24 Effect of Mach Number on Horizontal Tail Effectiveness-- ΔC_M = Pitching Moment Increase Between the 30% Tail and 8.4% Tail 40

3-25 Effect of Mach Number on Horizontal Tail Effectiveness-- May 1965 Wind Tunnel Test 41

3-26 Estimated Longitudinal Stability with no Tail and with Assuming Constant Tail Effectiveness 42

3-27 Estimated Longitudinal Stability with no Tail and with Assuming Constant Tail Effectiveness 43

3-28 Trim Normal Force Coefficient Assuming Constant Tail Effectiveness 44

3-29 Effect of Jet Flaps on Longitudinal Stability-- $M = 0.6$, $i_w = 14°$, and Slab Wing 46

3-30 Effect of Jet Flaps on Longitudinal Stability-- $M = 0.8$, $i_w = 14°$, and Slab Wing 47

3-31 Effect of Jet Flaps on Longitudinal Stability-- $M = 1.2$, $i_w = 14°$, and Slab Wing 48

3-32 Effect of Slab Wing on Directional and Lateral Stability--$\beta = -5.0°$, $i_w = 14°$, and 8.4% Tail 51

3-33 Effect of Slat and Flap on Directional Stability-- $M = 0.6$, 8.4% Tail, and $\beta = -5.0°$ 52

3-34 Effect of the Slat and Flap on Directional Stability-- $M = 0.8$, 8.4% Tail, and $\beta = -5.0°$ 53

3-35 Effect of Slat and Flap on Lateral Stability-- $M = 0.6$, 8.4% Tail, and $\beta = -5.0°$ 55

3-36 Effect of Slat and Flap on Lateral Stability-- $M = 0.8$, 8.4% Tail, and $\beta = -5.0°$ 56

3-37	Jet Roll Control	58
3-38	Aileron Effectiveness	60
3-39	Glide Configuration Longitudinal Stability	61
3-40	Carry and Glide Configuration Axial Force Coefficient	63
4-1	Block Diagram--Rolleron Control System	67
4-2	Roll Disturbance--Wing Launch	68
4-3	Block Diagram--Basic Control Configuration	71
4-4	Type II--Typical Roll Transient	74
4-5	Type III--Parameter Sensitivity	76
4-6	Fluidic Roll Control System	85
4-7	Electro/Mechanical Roll Control System	86

TABLES

1-1	Study Goals	2
2-1	Summary of Results	6
4-1	Dispersion--Original Rolleron	69
4-2	Dispersion--Modified Rolleron	69
4-3	Summary--Type I Roll Control	72
4-4	Summary--Type III Roll Control	77
4-5	Summary--Aerodynamic Roll Control	79
A-1	Run Schedule	92

SYMBOLS

C_L	lift coefficient
C_N	normal force coefficient (normal to body centerline); $C_N = C_L$ at zero angle of attack
C_D	drag coefficient
C_M	pitching moment coefficient
C_n	yawing moment coefficient
C_ℓ	rolling moment coefficient
$\bar{c}$	wing mean aerodynamic chord (references length for C_M)
b	wing span (reference length for C_n and C_ℓ)
A	wing area (reference area)
M	Mach number
M. F.	jet magnification factor (ratio of jet thrust plus aerodynamic interaction, to jet thrust)
α	body angle of attack (°)
α_w	wing angle of attack (°)
i_w	wing incidence; angle between wing and body (°)
γ	sideslip angle (°)
δ_s	slat deflection (°)
δ_f	plain flap deflection (°)
$C_{\ell_{\delta_a}}$	rolleron aerodynamic coefficient
C_{l_p}	roll damping coefficient
L_p	aerodynamic damping (1/sec) - $C_{\ell_p} \frac{Ab^2 q\ 57.3}{2V\ I_x}$

I_x	roll moment of inertial (slug - ft^2)
I_δ	rolleron moment of inertia about its hinge line (slug - ft^2)
I_{xy}	rolleron product of inertia about its axis and missile centerline (slug-ft^2)
$\overline{H}$	wheel angular momentum (ft-lb-sec)
V	free-stream velocity (ft/sec)
q	dynamic pressure (lb/ft^2)
P	roll rate (°/sec)
ϕ	roll attitude (°)
ϕ_ϵ	roll attitude error (°)
T_{HM}	rolleron hinge moment (ft-lb/deg) - $C_H Abq$
T_R	rolleron control moment (ft-lb/deg) - $C_{\ell_{\delta_a}} Abq$
β	rolleron viscous damping moment (ft-lb/deg/sec)
L_D	roll disturbance (°/sec^2)
C	control capability (°/sec^2)
K_δ	actuator bandwidth
K_R	rate feedback gain
K_ϕ	attitude error gain
T	thrust (lb)
$\dot{\delta}_L$	aileron rate limit (°/sec)
k	jet reaction amplification factor
ℓ	control lever arm (ft)

Section 1
INTRODUCTION

The feasibility of the Bayonet concept was demonstrated by three successful drop tests of prototype vehicles from January to April 1966. To investigate a weapon design offering greater tactical flexibility, more accuracy, and less delivery aircraft vulnerability, the Sandia Corporation authorized the Douglas Aircraft Company, Inc., to conduct a wind tunnel test, aerodynamic analysis, and stability and control analyses of several high-lift devices and control systems. Analysis of the results is presented in this report, in compliance with Paragraph 3.1.5.3 of the Work Statement, Douglas Report No. SM-52014P, dated March 1966, Reference 1.

Table 1-1 illustrates the goals for a more cost effective Bayonet weapon. Explanations of these are as follows:

1. The ability to launch the Bayonet from wing store positions will permit multiple launches of the weapons on each aircraft mission, providing greater mission effectiveness.
2. The ability to launch at greater aircraft velocities (up to Mach 1.2) will provide increased flexibility of weapon use and reduce delivery aircraft vulnerability.
3. The ability to launch a Bayonet at an altitude lower than 100 ft (and retain an impact angle of 30°) offers better delivery accuracy and also decreases the carrier aircraft vulnerability.

To achieve these goals, interest developed in the following:

1. Increased Lift of up to approximately double the original available lift which allows lower release altitude.
2. A Roll Control System - to compensate for the increased rolling moments resulting from crossflow experienced from wing drop.
3. A Slab Wing - a wing cross-section, which should be easier, and, therefore, cheaper to fabricate, but which would provide lift equal to that obtained from the original contoured wing.

UNCLASSIFIED

Table 1-1

STUDY GOALS

System Goals (For Increased Cost Effectiveness)	Concepts	Techniques
Greater sortie effectiveness	Multiple launch	Roll control
Greater flexibility	Higher A/C velocity	
Reduced A/C vulnerability	Lower release altitude	High-lift devices
Increased accuracy		Roll control
Improved cost	Simplified hardware	Slab wing

UNCLASSIFIED

The Bayonet wing planform was designed from the beginning to be compatible with supersonic carry and launch. Aerodynamic methods for obtaining additional lift were developed in Douglas Report SM-48202 (Reference 2) conducted under Sandia Contract No. 82-7431. Wing-body fairings, leading-edge slats, and trailing-edge flaps were determined to be worthy of further test in the wind tunnel.

The Sidewinder I-C rolleron, roll-retarding system appears to be sufficient to hold the original Bayonet cross-range dispersion to an acceptable value, especially if care is taken to provide symmetrical air flow on the underside of the aircraft fuselage by maintaining symmetry of other external stores near the Bayonet carry position. For drop in the crossflow under a swept wing, however, it was estimated that the rollerons would be marginal or even ineffective.

Work was initiated on 6 April 1966, to investigate the discussed objectives. This work was conducted as Amendment No. 6 to the Sandia Contract No. 82-7431.

Amendment No. 6 involved the following:

1. Wind Tunnel Testing.
   - A. Definition and sizing of the wing tunnel model components and rework of the original 30% scale wing tunnel model to incorporate these components. The components chosen for test were:
     - (1) Leading-edge slats.
     - (2) Trailing-edge plain flaps.
     - (3) Trailing-edge jet flaps.
     - (4) Ailerons.
     - (5) Jet reaction roll control.
     - (6) Slab wing.
     - (7) Wing-body fairings (3).
     - (8) Vertical tail.
     - (9) Larger horizontal tail.
   - B. Test of these components, singly and in various combinations and over a Mach number range from 0.6 to 1.2 (Appendix A and Table 3-1 in Reference 1). Tests were performed in the 8-ft Transonic Wind Tunnel, Cornell Aeronautical Laboratories, Buffalo, New York, June 22 through 24, 1966.

2. Engineering Analysis

   A. Aerodynamic and stability and control analysis of the wind tunnel results, reported herein in Section 3.

   B. Theoretical analysis of the control problem, especially roll control, by use of digital simulation, reported herein in Section 4. This analysis includes considerations of mechanization, to assure continuing interest only in subsystems which could be manufactured reasonably.

Based on the analysis presented in this report, a preliminary configuration is recommended for an Advanced Bayonet (Section 5). An appreciable amount of preliminary design (not within the scope of this work) is required before a final configuration can be selected. The final design will depend on the trades of required performance as a function of obtainable performance. This wind tunnel test and analysis has helped to establish the latter, although additional testing will probably be required before finalization of detailed design of the Advanced Bayonet.

Section 2
SUMMARY

The results of the study are summarized in Table 2-1.

Lift devices are compared to the original, contoured wing, which generates a C_L of 0.65 (0.55 with 30% tail). The slab wing proved to be equivalent to the contoured wing at the high-wing angles of attack under which the Bayonet performs.

High-lift devices can substantially improve the Bayonet performance. By adding slats and plain flaps, and increasing the wing incidence to approximately 20°, a normal force coefficient of approximately 1.1 can be achieved at the subsonic Mach numbers. This lift coefficient is approximately 70% greater than the present Bayonet lift coefficient at Mach 0.8.

To allow the Bayonet high-lift configuration to be launched also at Mach 1.2 with a fixed wing-body configuration, an increase in horizontal tail effectiveness will be required. The wind tunnel test indicated that with the horizontal tail located on the body, the flap is washing out the tail and reducing its effectiveness at the high Mach numbers. It is believed that increased tail effectiveness at the supersonic Mach numbers can be achieved by utilizing a T-tail arrangement (horizontal tail attached to the bottom vertical tail). This arrangement should permit launching both subsonic and supersonic with a fixed wing-body configuration.

If wing launch remains a requirement for Bayonet, it will be necessary to incorporate roll position control. The tests indicate that the jet reaction control is sufficiently effective, with the use of relatively small amounts of thrust. Mechanization of this system is clean, reliable, and inexpensive. Conversely, the aileron proved to be disappointingly ineffective. To make the aileron effective it is estimated that its size would have to be increased

UNCLASSIFIED

Table 2-1

SUMMARY OF RESULTS
Wind Tunnel Tests - June 1966

Lift Device	ΔC_L		Total C_L*	
	Subsonic	Supersonic	Subsonic	Supersonic
Slab wing	0	0	0.55	0.55
Slats alone	0.2	≤0	0.75	<0.70
Flaps--plain	0.4 (Directionally unstable)	0.4	1.0 (Directionally unstable)	0.9
--jet	0.4	0.4	1.05	1.0
Plain flaps and slats	0.50	0.45	1.10	0.96

Roll Control--jet --Effective with small thrust, clean, reliable, inexpensive

--ailerons--Ineffective; low response

Fairings--Ineffective

*With 30% tail, to allow a single wing position for both subsonic and supersonic launch.

UNCLASSIFIED

to approximately 6 times that of the present rollerons, if a cross-range dispersion of 10 ft or less is the requirement. It would be difficult to mechanize that size with the necessary response rates and stiffness. Also, the mechanization is complex, when compared with jet control. Consequently, jet roll control is preferred.

The wing-body fairings tested proved to be ineffective in reducing wing-body interference. Their further consideration is not recommended.

In the opinion of Douglas, there is now a sufficient aerodynamic and stability foundation for preliminary design of an Advanced Bayonet, although further wind tunnel testing of the selected design will be required.

Section 3

ANALYSIS OF WIND TUNNEL RESULTS

Drawings of the Bayonet wind tunnel model are shown in Figures 3-1 and 3-2. Figure 3-1 shows the contoured wing with slat, plain flap, fairings, and ailerons. Figure 3-2 shows the slab wing with jet flaps and jet roll control. Model photographs of these two wings are shown in Figures 3-3 and 3-4. This analysis is based on data transmitted from the Cornell Aeronautical Laboratories, Buffalo, New York, immediately after testing (Reference 4). A formal report of all data by CAL is scheduled for delivery 24 September 1966. A copy of that report will be transmitted to the Sandia Corporation.

The tested model variables were as follows:

1. Wing deflections of 1°, 14°, and 16°. With the wing deflected 1°, the model is in designated carry configuration, whereas the 14° and 16° wing deflections are designated high-lift configuration.
2. Horizontal tail sizes which were 8. 4% and 30% of the wing area. As the small tail (8. 4%) was tested with the majority of the configuration, this tail should be assumed to be part of the configuration under discussion, unless otherwise stated.
3. Three fairings designed to reduce the wing-body interference. One fairing was between the wing and body, another was attached to the body immediately aft of the wing, and the last fairing was used to fill the arrestor hole in the wing (Figure 3-1).
4. Slats deflected 0° and 15°. The slats when undeflected were displaced out from the wing leading edge as shown in Figure 3-1. The slat was designed such that the slat would simply rotate to the designed deflection (15°) when the wing was deployed.
5. Plain flap deflection of 0°, 25°, 40°, and 50°. The flap area was about 20% of the wing area.
6. Jet flaps in which each flap consisted of a slot at the slab wing training-edge through which high-pressure air was ejected. The lift was provided by both the jet thrust and the aerodynamic interaction produced by the jet.

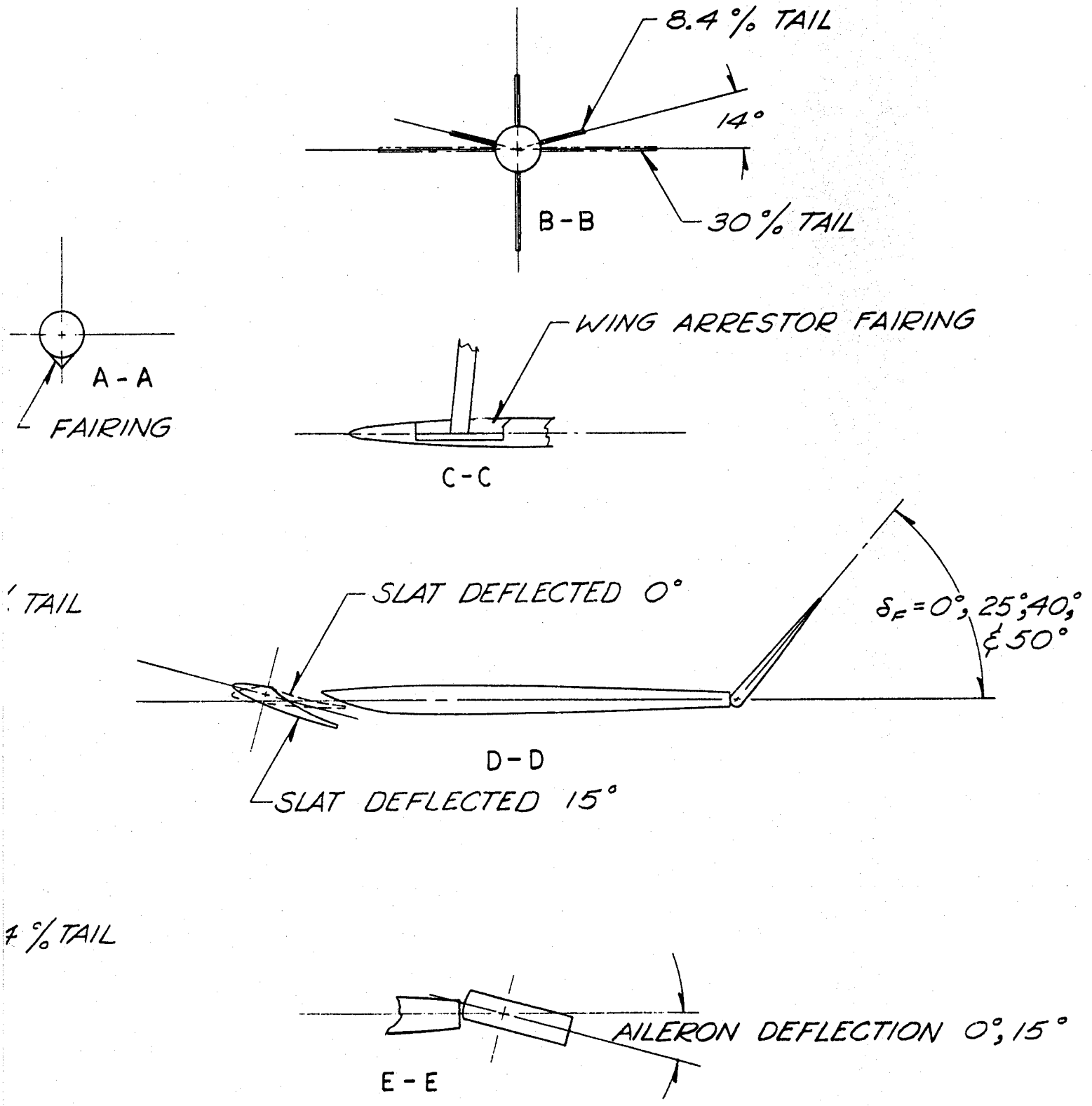

t Wind Tunnel Model Contoured Wing, Slat, Plain Flap, Fairings, and Ailerons 30% Scale

 [redacted]

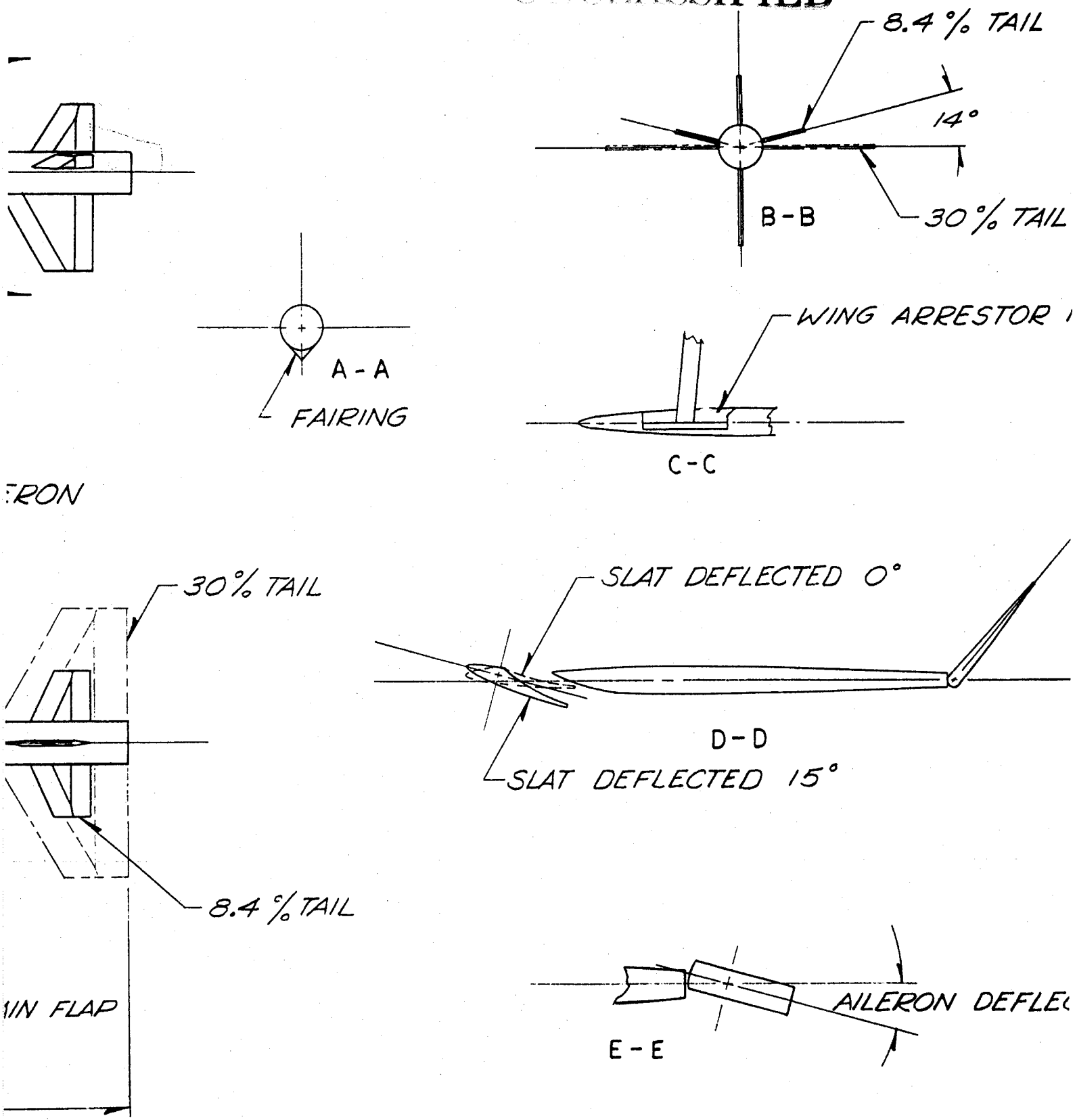

Figure 3-1. Bayonet Wind Tunnel Model Contoured Wing, Slat, Plain Flap, Fairings, and Ailer

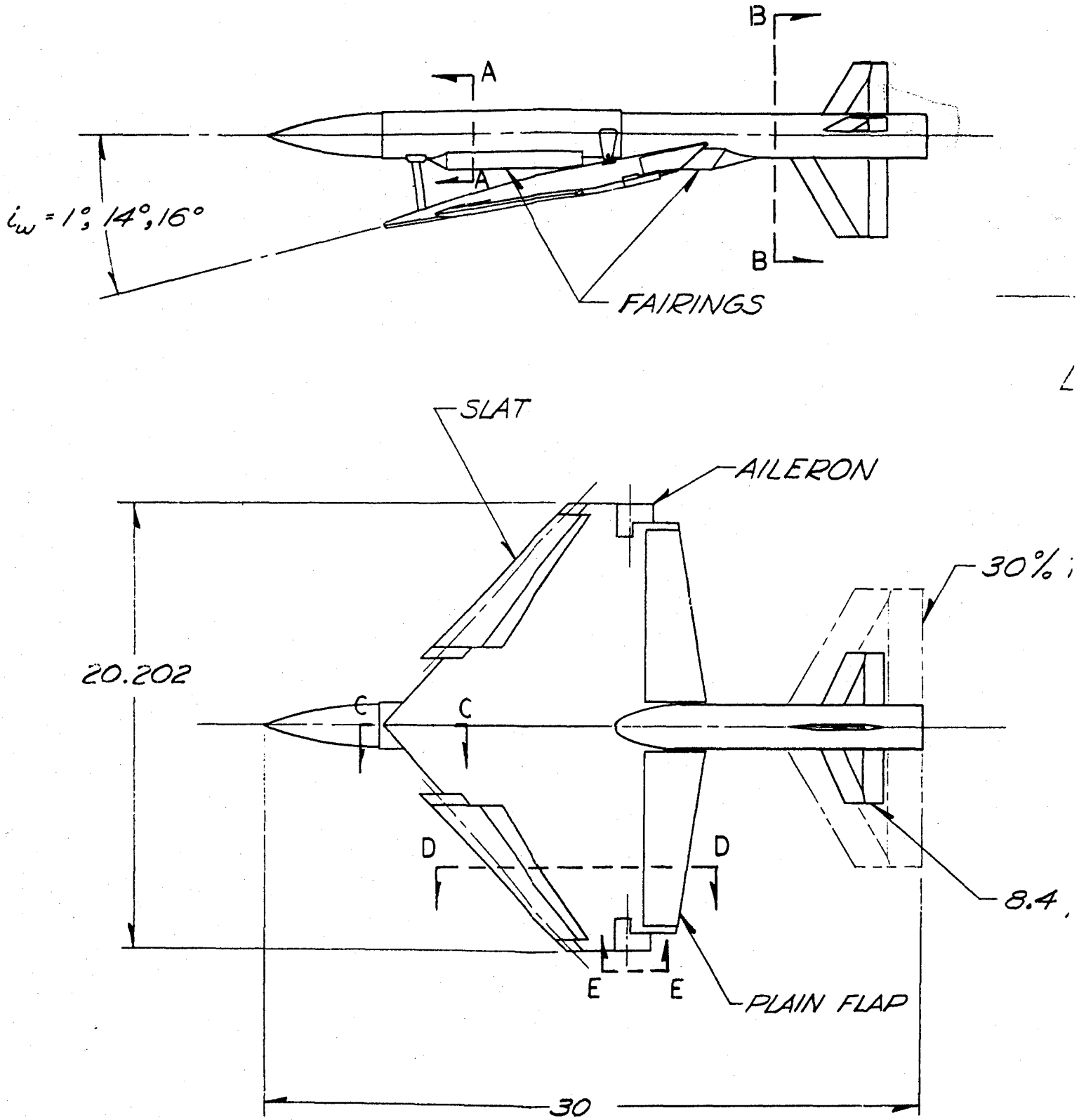

Figure 3-1. Bayonet \

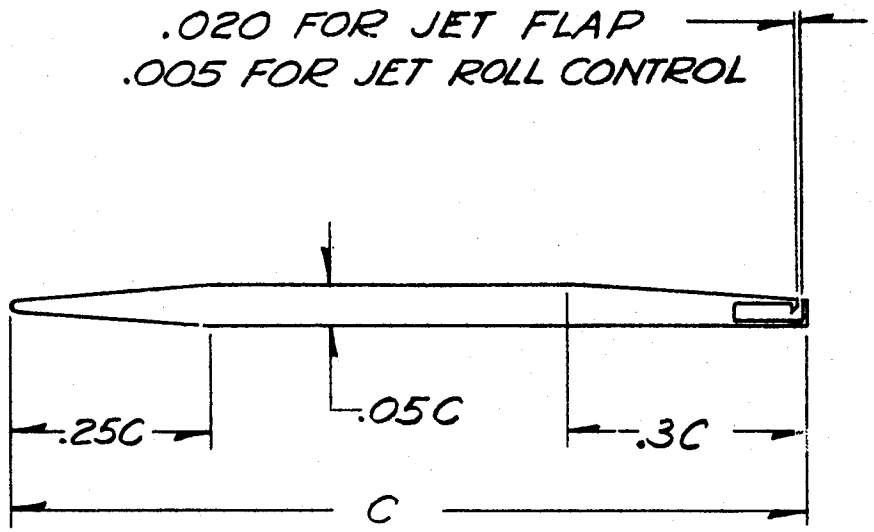

A-A

GAS SUPPLY LINE FOR
JET FLAPS, JET ROLL CONTROL

ntrol 30% Scale

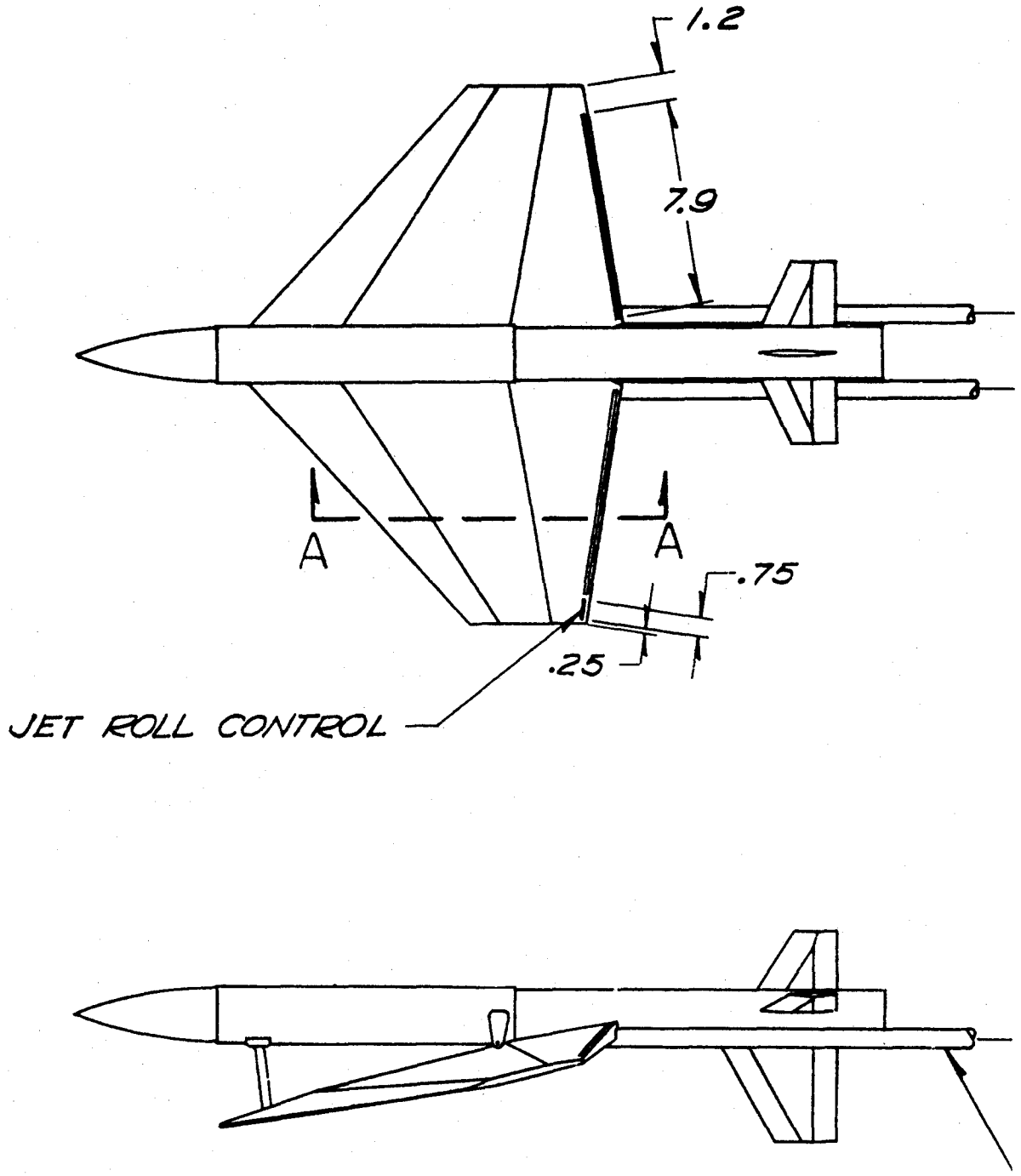

Figure 3-2. Bayonet Wind Tunnel Model Slab Wing, Jet Flaps, and Jet Roll Contr

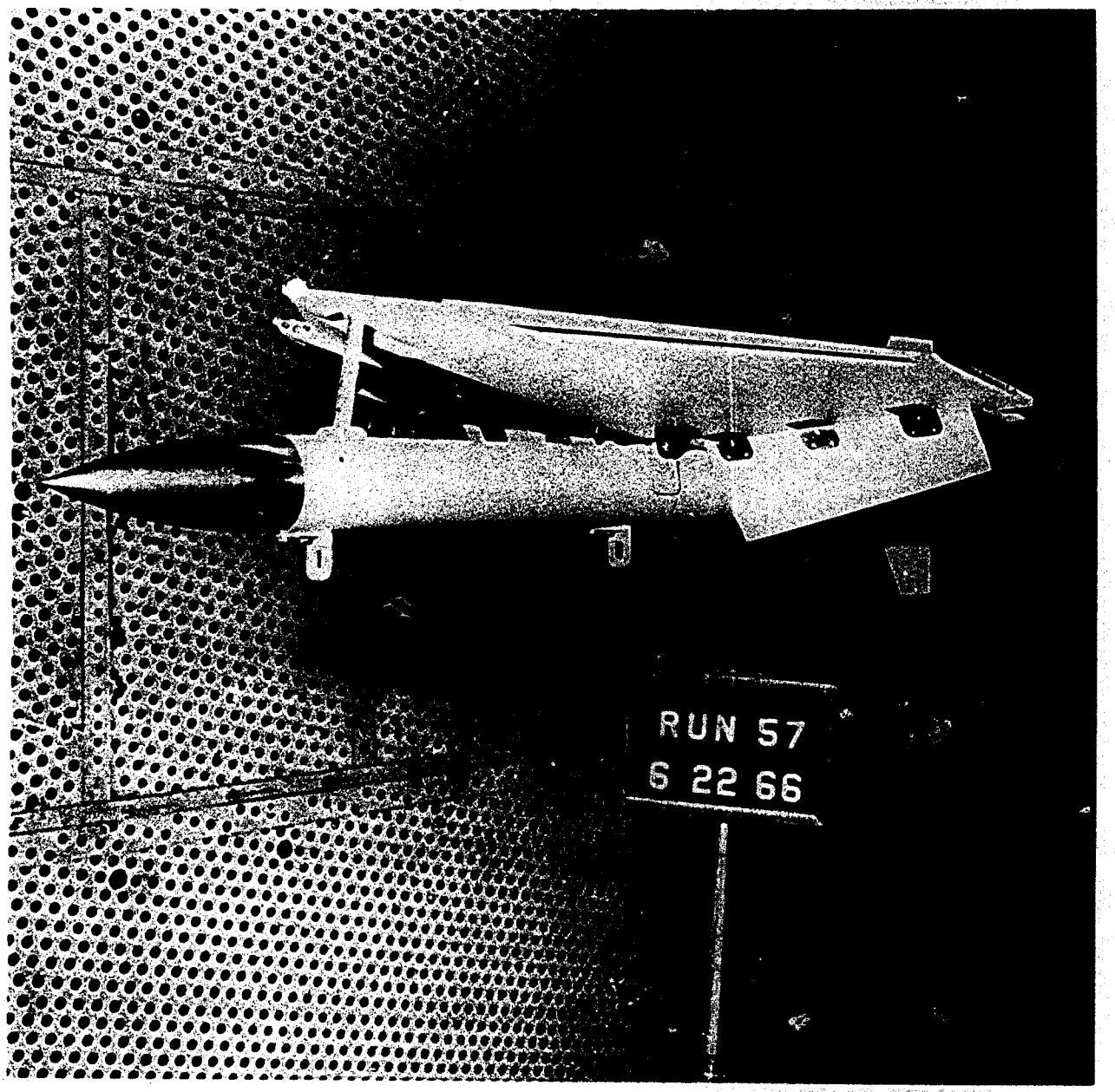

Figure 3-3. Run 57

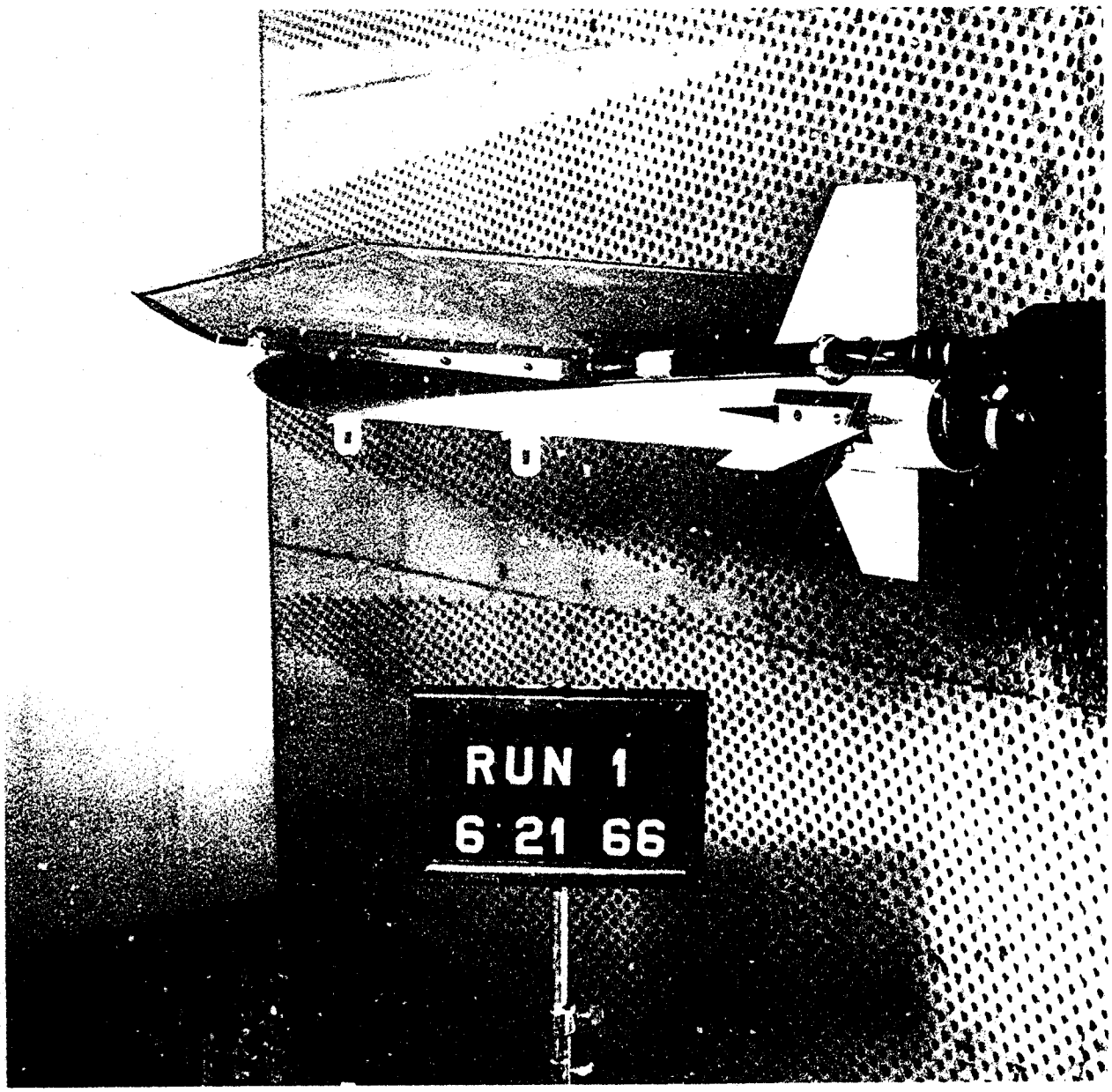

Figure 3-4. Run 1

7. The roll control jet is similar to the jet flap, except that the roll jet was located near the wing outboard tip. Because the aerodynamic interaction is believed to be considerably higher on the windward side than on the leeward side, the roll jet air was only ejected on the windward side. Therefore only one roll jet was required and it was placed on the wing left hand side. Both the air for the jet flap and the roll jet were supplied through lines that were attached to the slab wing training edge (Figure 3-2).
8. The aileron was deflected either 0° or 15° (the left side +15° and the right side -15°). Each aileron area was 19.7 in.^{2} (full scale) and was hinged so as to minimize the aerodynamic hinge moments. The aileron area was about 80% larger than the present Bayonet rolleron area.
9. A slab wing with a straight-sided profile was tested to determine if it could produce approximately the same lift as the contoured wing. The slab wing was thickened on the leeward side trailing-edge to accommodate the ducting required for the roll jet and jet flap.

On all configurations, a boundary-layer trip was attached to the leeward side of the wing. Also on all configurations, both vertical tails were included on the model. The center of gravity (CG) was assumed to be at station 38.13 of the full scale vehicle (21.67 in. behind the wing apex with the wing undeflected). Except for those dimensions given in Figures 3-1 and 3-2, all dimensions, pressures, and thrusts presented in this report are for the full-scale Bayonet.

The wing tunnel test run schedule is presented in Appendix A. The test parameters were as follows:

1. Mach number: 0.6, 0.8, 0.95, 1.0, 1.1, and 1.2.
2. Angle of attack: -8° to +8°.
3. Sideslip angle: 0 and -5°.
4. Reynolds number: 1.2×10^6.

3.1 LONGITUDINAL STABILITY

As considerable use is made of longitudinal stability curves, a discussion on how to use them and what they reveal is warranted. A longitudinal stability curve with some hypothetical data is provided in Figure 3-5. This figure shows the effect of both changes in horizontal tail size and CG. Because of the increased tail load, an increase in the horizontal tail size results in a reduction in total normal force and an increase in the pitching moment.

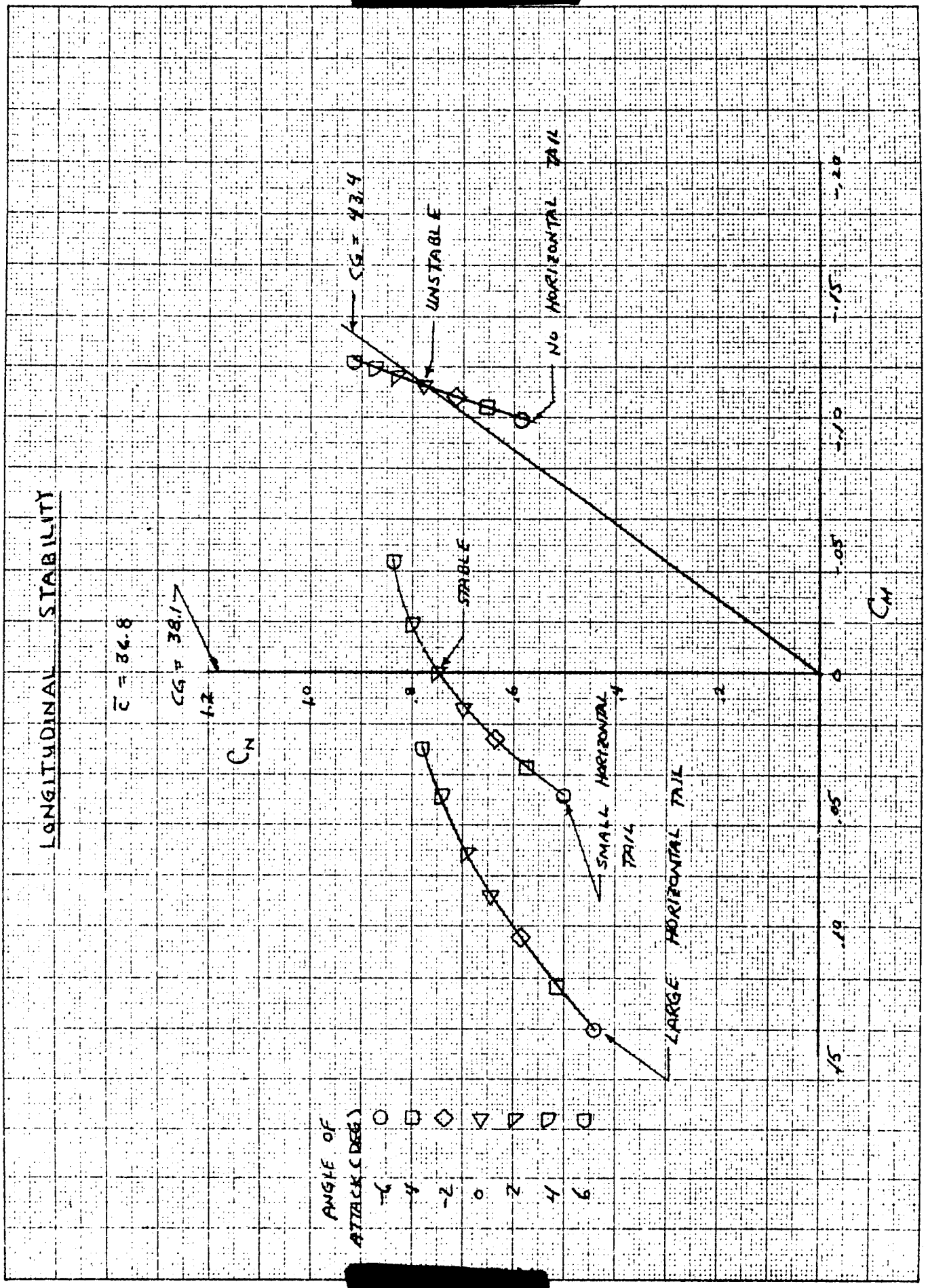

Figure 3-5. Longitudinal Stability

Since trim only occurs when $C_M = 0$, the only trim condition, with CG at station 38, is the small tail configuration at $\alpha = 2°$. To trim the vehicle at other angles of attack and other tail sizes, the CG must be moved. To determine the proper CG for other trim conditions, a straight line is drawn from the curve origin ($C_M = C_N = 0$) to the desired trim condition. The resulting CG is then equal to $(CG)_{original} - (\partial C_M / \partial C_N)\ \overline{C}$ where:

$CG_{original}$ = the CG for which the basic curves were drawn

In this example it is equal to 38

$\frac{\partial C_M}{\partial C_N}$ = inverse slope of the straight line

$\overline{C} = C_M$ reference length

The slope of the data curve at trim relative to the trim CG line then determines the longitudinal stability. A configuration is longitudinally stable if the quantity

$$\frac{\partial C_M}{\partial C_N}\text{ data at trim point} - \frac{\partial C_M}{\partial C_N}\text{ trim CG line}$$

is negative. For example: the configuration with the small horizontal tail is stable at $\alpha = 2°$, whereas the no-tail configuration is unstable at $\alpha = 0°$.

Another variable that will affect longitudinal stability is a change in wing incidence. An increase in wing incidence will result in an increase in pitching moment and a slight reduction in normal force. This effect is similar to an increase in horizontal tail size. Therefore, the longitudinal stability data at one wing incidence, based on the same wing angle of attack, should be similar to the data at another wing incidence if the horizontal tail size is adjusted. Because the wing dominates the normal force coefficient, a change in wing incidence will change the angle of attack. The data at $\alpha = 4°$ with a 16° wing incidence is approximately equivalent to the data at $\alpha = 0°$, 20° wing incidence with a slight adjustment in tail size, because the wing angle of attack is held constant. In summary, it is believed that changes in wing incidence will have relatively little effect on longitudinal stability.

3.1.1 Slab Wing

The results of the aerodynamic study on high-lift devices for Bayonet (Reference 2) indicated that the wing lift is relatively insensitive to the wing cross-section. Therefore, a slab wing with straight line sections was tested in a wind tunnel to determine if a simpler and less expensive wing could be employed on Bayonet. This wing is shown in Figure 3-2. On the leeward side trailing edge, the wing was thickened to accommodate the air duct for the jet flaps and jet roll control, as noted previously. With the flow mostly separated at high angles of attack near the wing leeward side trailing edge, it was expected that the thickened portion of the wing would have only a small affect on lift.

The longitudinal stability for both the slab wing and contoured wing at $M = 0.6$, 0.8, and 1.2 are shown in Figures 3-6, 3-7, and 3-8. The contoured wing data was obtained from the previous Bayonet wind tunnel test (June 1965). This data are presented in Reference 3. Since this prior data was for a 16° wing incidence, an estimate of the contoured wing aerodynamics at 14° wing incidence was required. The estimated contoured wing C_N and C_M data, shown in Figures 3-6 through 3-8 are estimated to be accurate to within ±0.01. These figures show that at small wing angles of attack, the slab wing generated slightly less lift than the contoured wing. At high-wing angles of attack, the two wings produced approximately the same lift. The lift reduction at low-wing angles of attack is probably caused by the wing trailing-edge thickening on the leeward side. This requirement for thickening would be reduced, or eliminated, if only the jet aileron is selected in final design.

The slab wing also resulted in a positive increment in the pitching moment at subsonic Mach numbers. What is causing this effect is unknown. Some possible causes are (1) change in the downwash on the tail, (2) thickening of the wing trailing-edge, (3) center of pressure shift because of the wing profile, and, (4) downwash loads on the air lines for the jet flaps and jet roll control. Because of the positive pitching moment increment, the slab wing probably would require a smaller horizontal tail for trim than the contoured wing. The smaller tail would increase the slab wing configuration total lift by about 0.02.

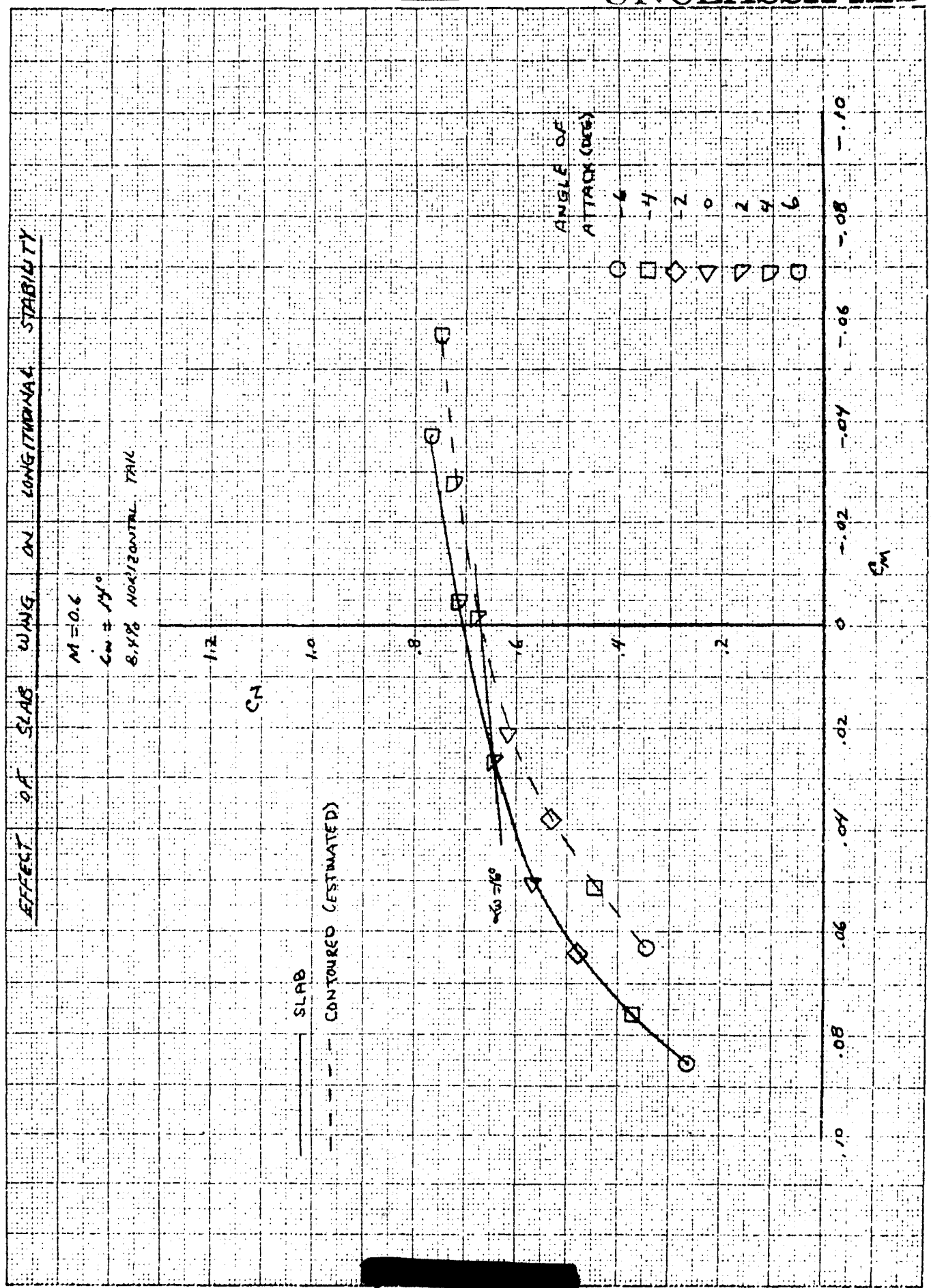

Figure 3-6. Effect of Slab Wing on Longitudinal Stability-- M = 0.6, i_w = 14°, and 8.4% Horizontal Tail

UNCLASSIFIED

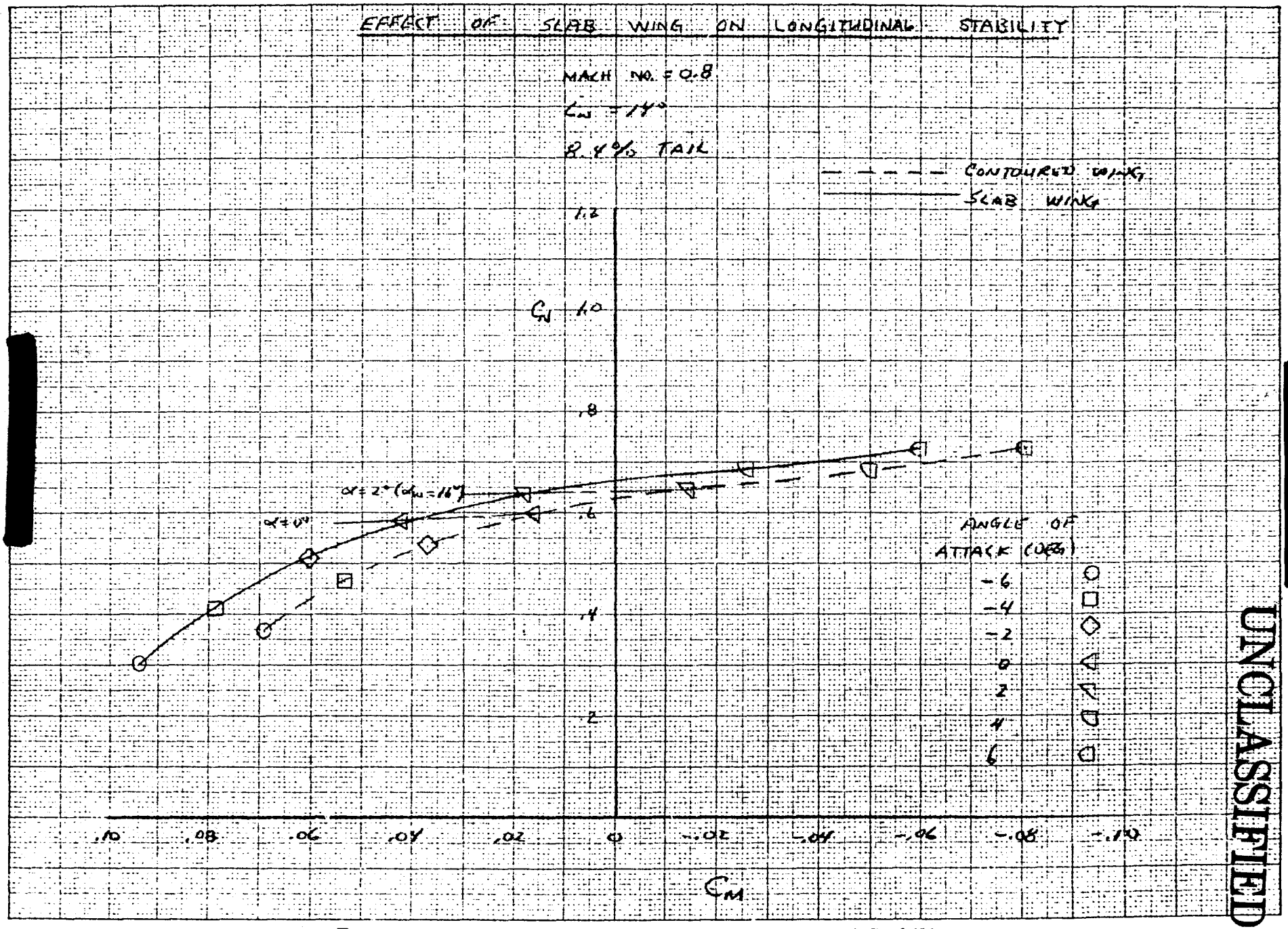

Figure 3-7. Effect of Slab Wing on Longitudinal Stability--
Mach No. = 0.8, i_w = 14°, and 8.4% Tail

UNCLASSIFIED

UNCLASSIFIED

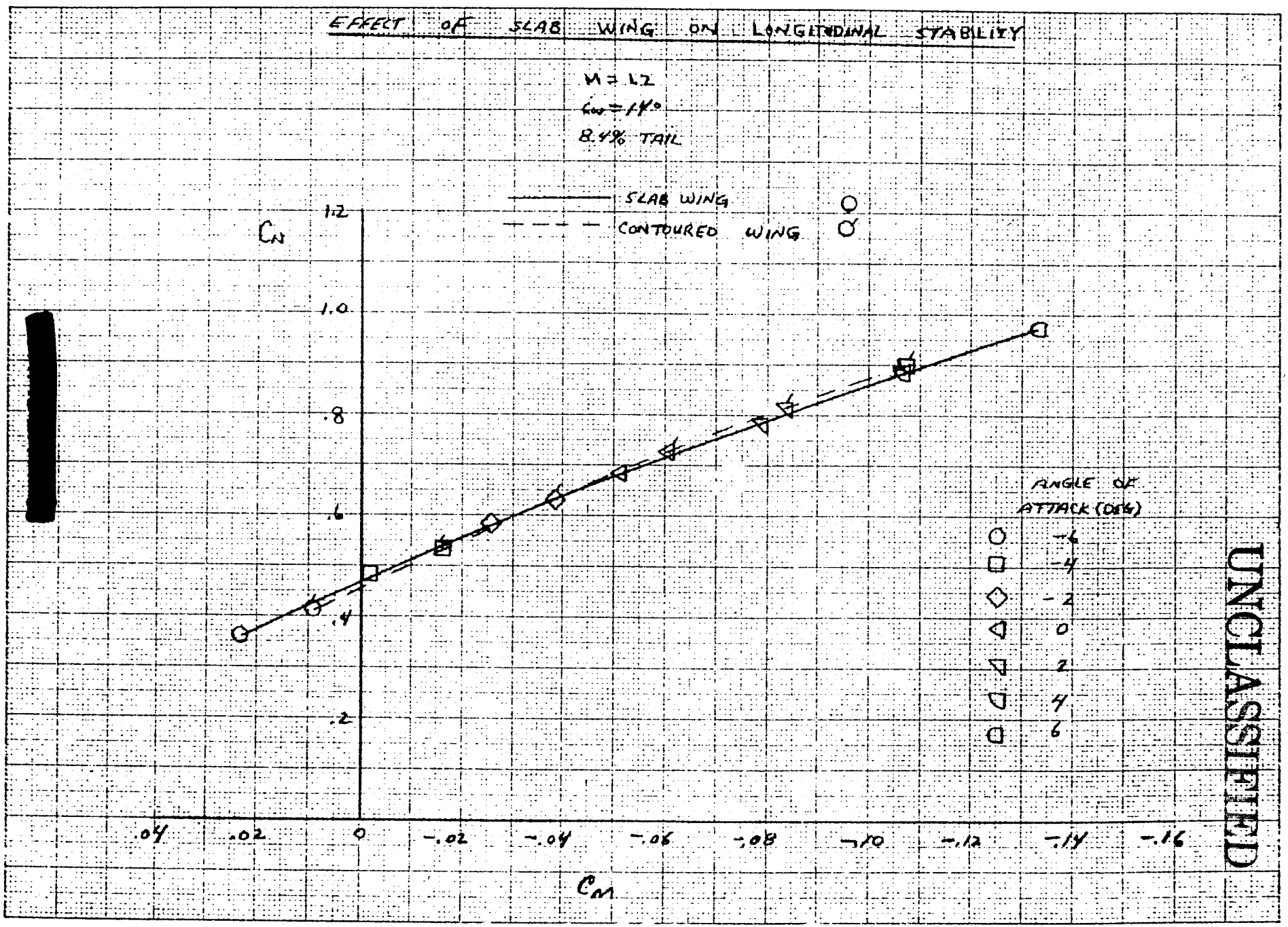

Figure 3-8. Effect of Slab Wing on Longitudinal Stability--
M = 1.2. i = 14°. and 8.4% Tail

UNCLASSIFIED

Because the slab wing produced approximately the same trim lift as the contoured wing, the slab wing is recommended for the advanced Bayonet configuration because of its simpler fabrication requirements.

3.1.2 Fairings

The results of the May 1965 Bayonet wind tunnel test revealed that removal of a fairing between the wing and body resulted in a slight increase in lift and a significant increase in directional stability. This fairing was designed to reduce the carry drag, but with the wing deployed, the fairing increased the blockage between the wing and body. To reduce interference between the wing and body, three fairings were designed and wind tunnel tested. These fairings are shown in Figure 3-1. One fairing was located between the wing and body, and another fairing was positioned on the body immediately aft of the wing. Both fairings were wedge-shaped and were designed to reduce wing-body blockage or the body crossflow drag (negative lift). The third fairing filled the wing arrestor hole and was designed to prevent any interference caused by this hole.

To more fully understand the flow interference, the model was run at $M = 0.8$, $\alpha = 0°$ with oil. Pictures of the oil flow results are shown in Figures 3-9 and 3-10. These pictures show that the wing is inducing a strong cross-wash on the body near the wing pivot point.

Because the previous test indicated that the interference was the largest at Mach 0.8, the three fairings were only tested at this Mach number. The results of the wind tunnel test on all three fairings indicated that they had little, if any, effect on any of the missile aerodynamics (Reference 4). Why the fairings had no effect is not understood because the oil flow pictures indicated significant wing-body interference. Because the effects of the fairings were insignificant, they are not recommended for the Advanced Bayonet configuration.

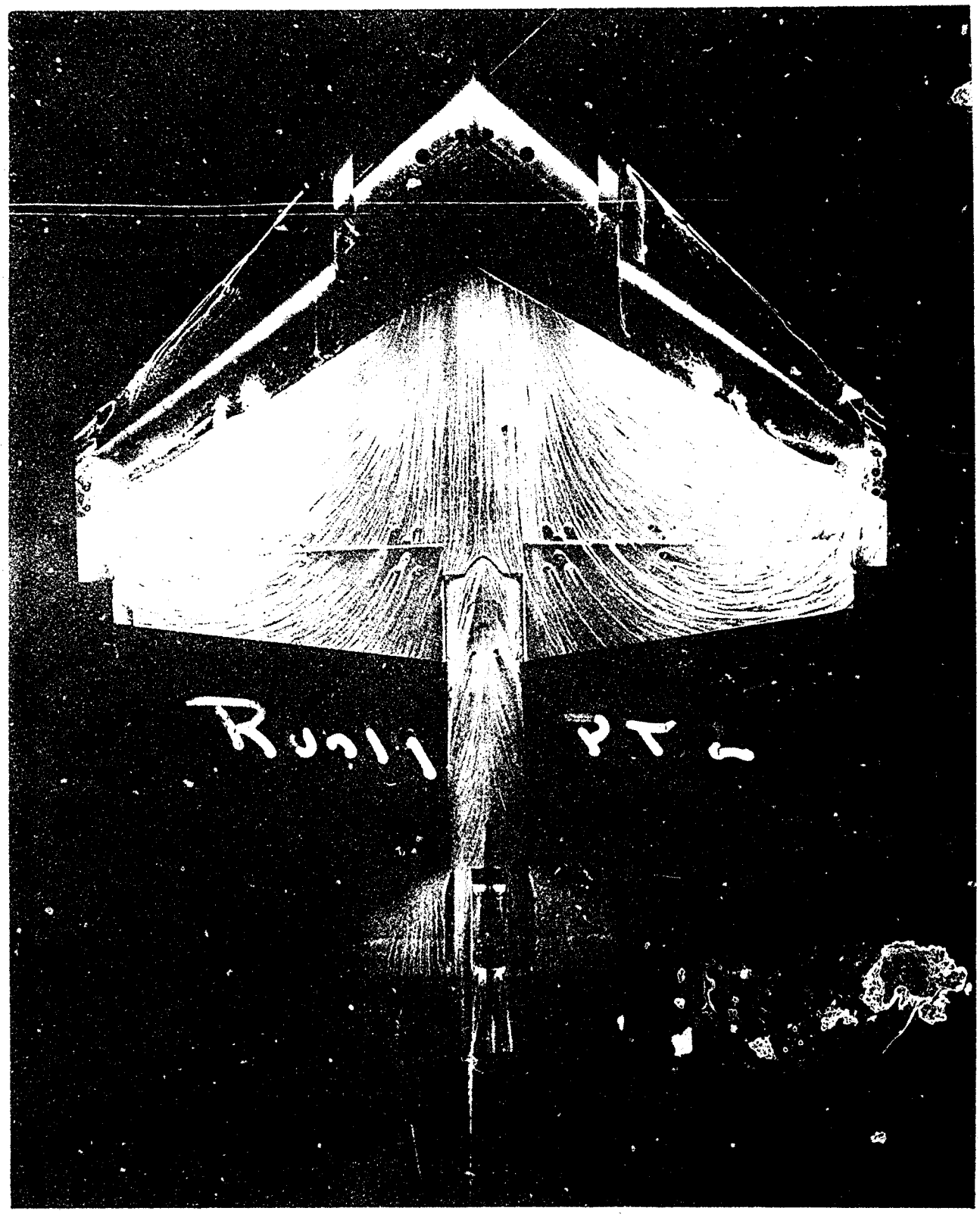

Figure 3-9. Run 19, PT2

[redacted]

Figure 3-10. Run 19 PT3

[redacted]

3.1.3 Slats

The slat is shown in Figure 3-1. The slat was designed so that when the wing was deployed, the slat airloads would cause the slat to rotate about its hinge point to the desired deflection (15°). This design resulted in the slat being translated forward and slightly upward from the wing when the slat was undeflected. In the carry position (i_w = 1°), the slat chord was designed to be approximately parallel to the wing chord to reduce carry drag.

The effect of both the deflected and undeflected slat on longitudinal stability at Mach 0.6, 0.8, and 1.2 are shown in Figures 3-11, 3-12, and 3-13. Again, the basic wing data (no slats) were obtained from the May 1965 wind tunnel test. The effect of the undeflected slat at the subsonic Mach numbers was to increase normal forces by approximately 10%. This lift increase is caused by the undeflected slat acting as a leading-edge chord extension.

Deflecting the slat provided a further lift increase at the subsonic Mach numbers. At Mach 1.2, the slat resulted in a small reduction in lift. The longitudinal stability at the three Mach numbers with the slat deflected is shown in Figure 3-14. This figure shows that with a 14° wing incidence, the configuration had not attained maximum trim lift. To maximize trim lift, the wing incidence should be increased. At 18° wing incidence this would result in a trim lift coefficient at α = 0° of about 0.85. This lift coefficient is approximately 30% greater than the present Bayonet trim lift coefficient. With a CG chosen to provide subsonic trim at α = 0°, i_w = 18°. the trim angle of attack at Mach 1.2 would be roughly -12° (-8° angle of attack, -4° wing incidence change), which is unacceptable It should be noted that the configuration is statically stable at Mach 1.2, which would allow launching at 1.2 with a CG transfer or by repositioning the wing. But, because of the large center of pressure travel, the slat only configuration cannot be successfully flown at both subsonic and supersonic Mach numbers with a fixed configuration.

UNCLASSIFIED

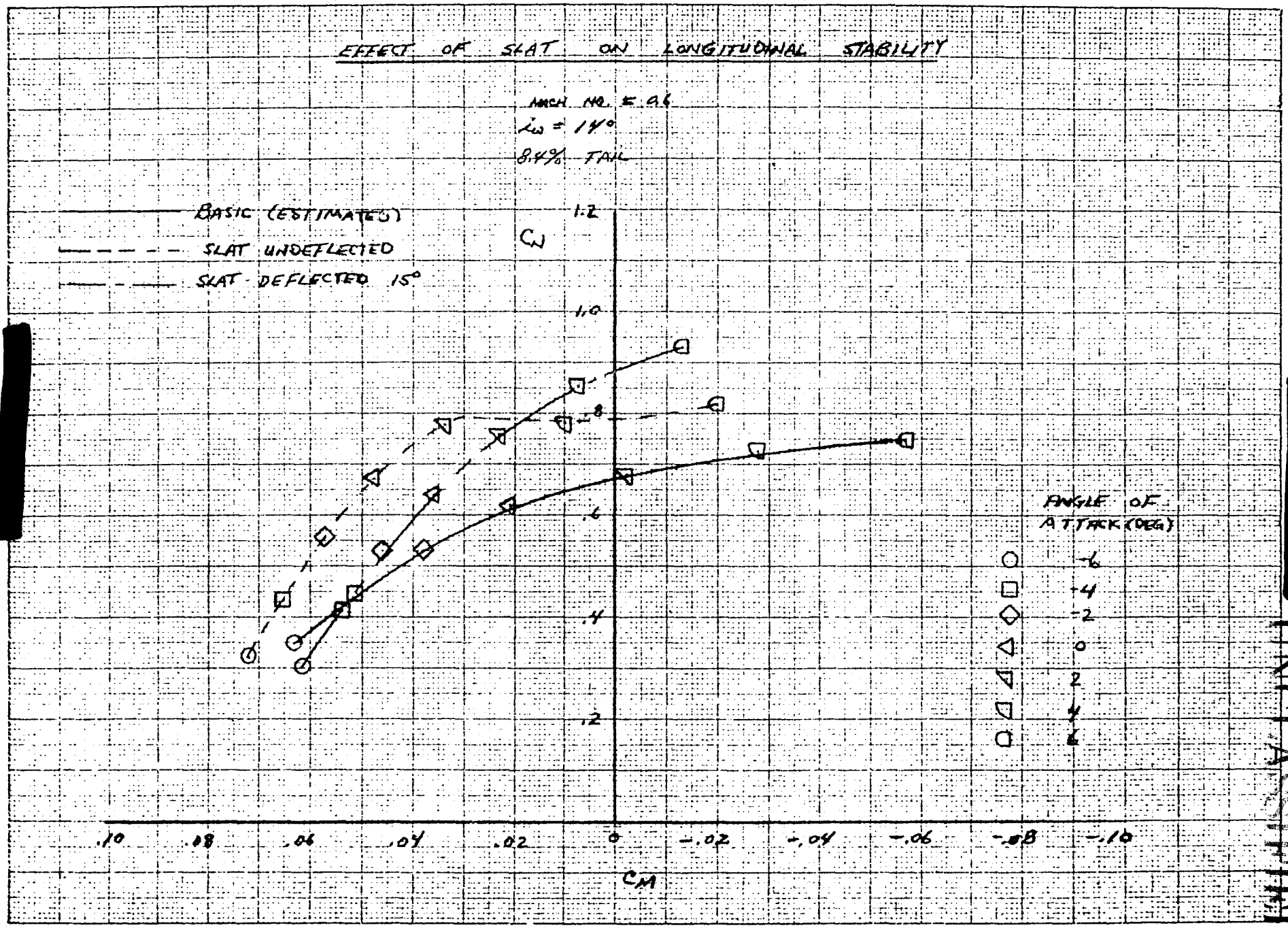

Figure 3-11. Effect of Slat on Longitudinal Stability--
Mach No. = 0.6, i_w = 14%, and 8.4% Tail

UNCLASSIFIED

UNCLASSIFIED

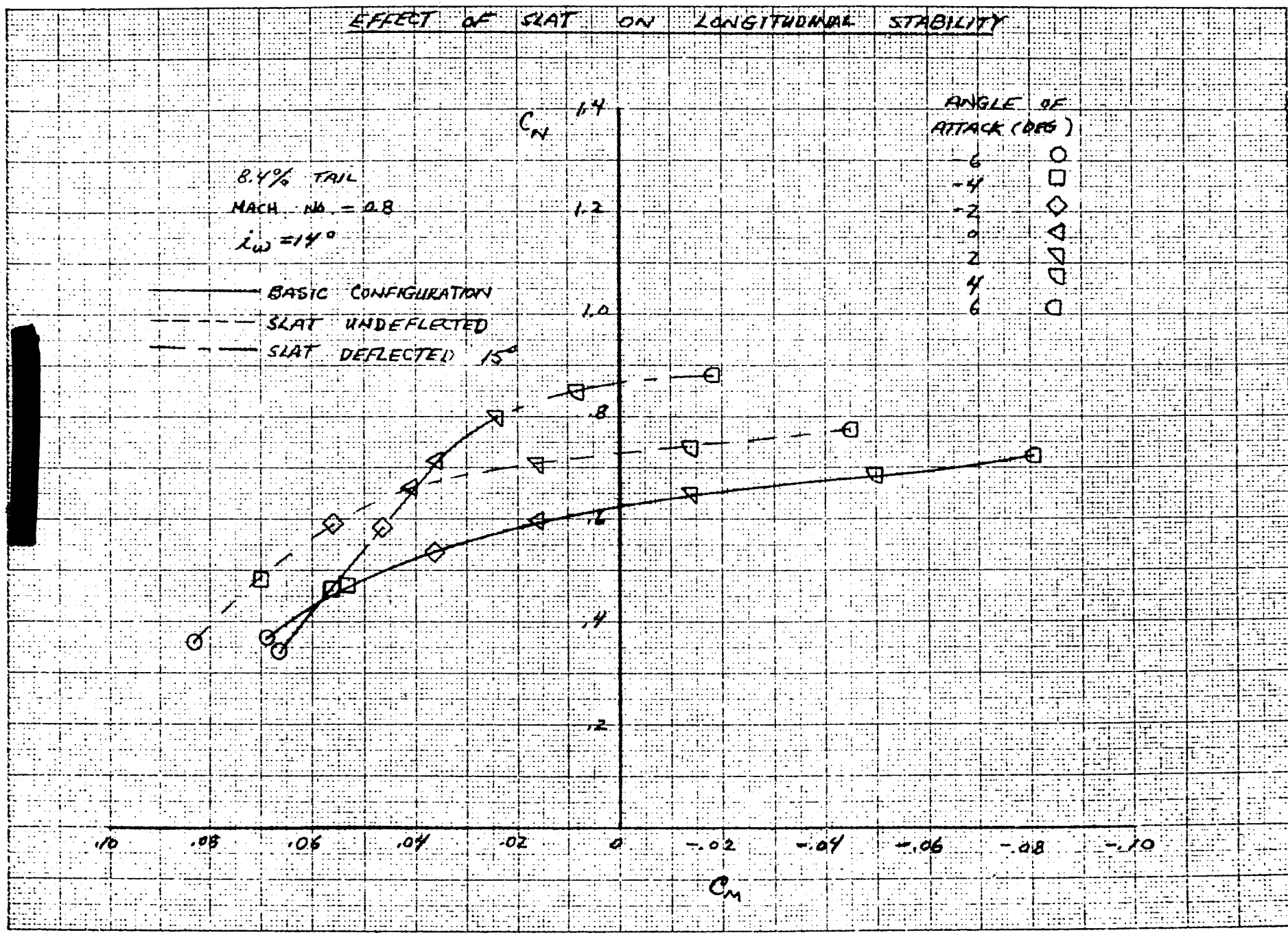

Figure 3-12. Effect of Slat on Longitudinal Stability--
Mach No. = 0.8, i_w = 14°, and 8.4% Tail

UNCLASSIFIED

UNCLASSIFIED

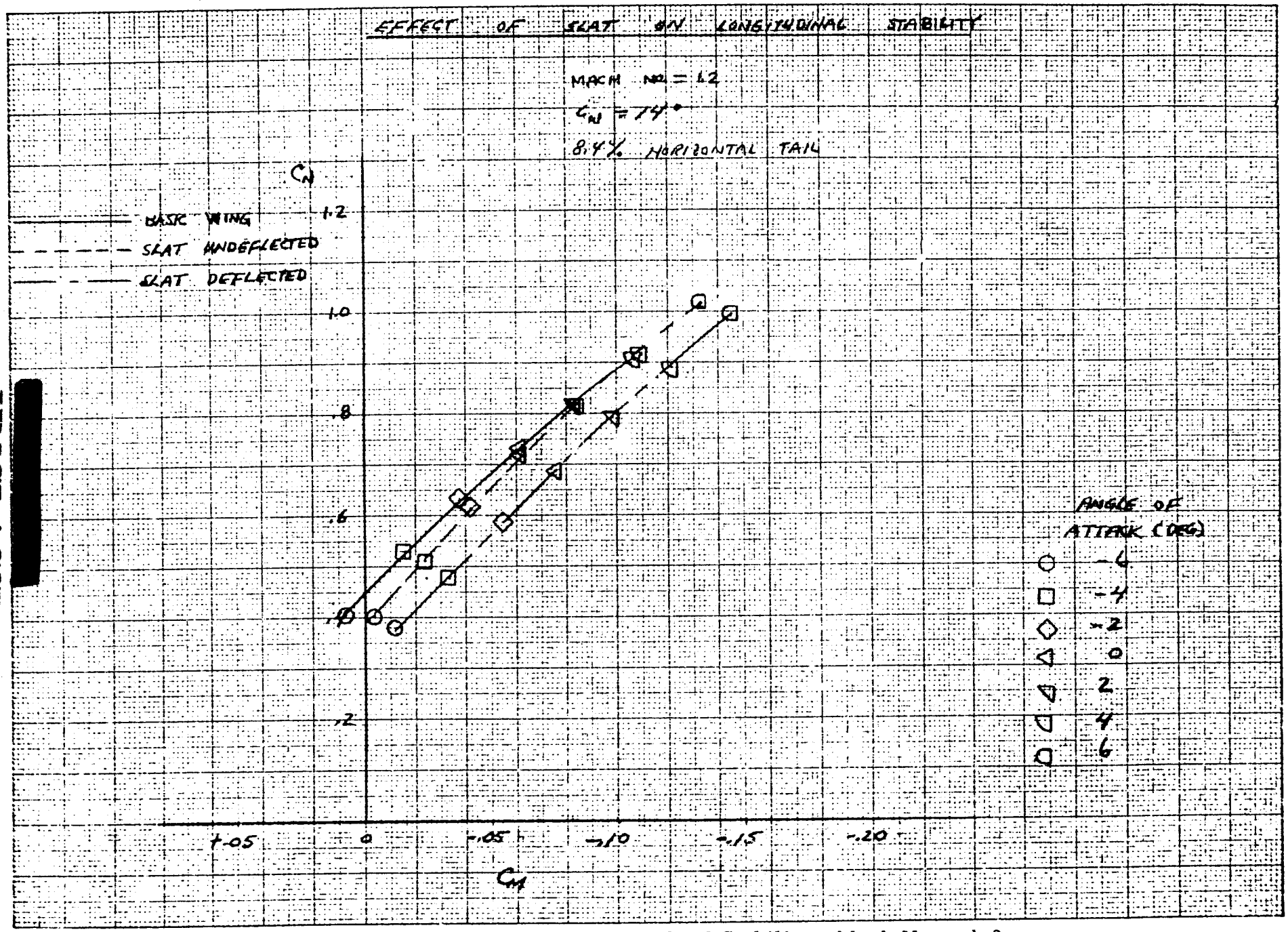

Figure 3-13. Effect of Slat on Longitudinal Stability--Mach No. = 1.2, i_w = 14°, and 8.4% Horizontal Tail

UNCLASSIFIED

UNCLASSIFIED

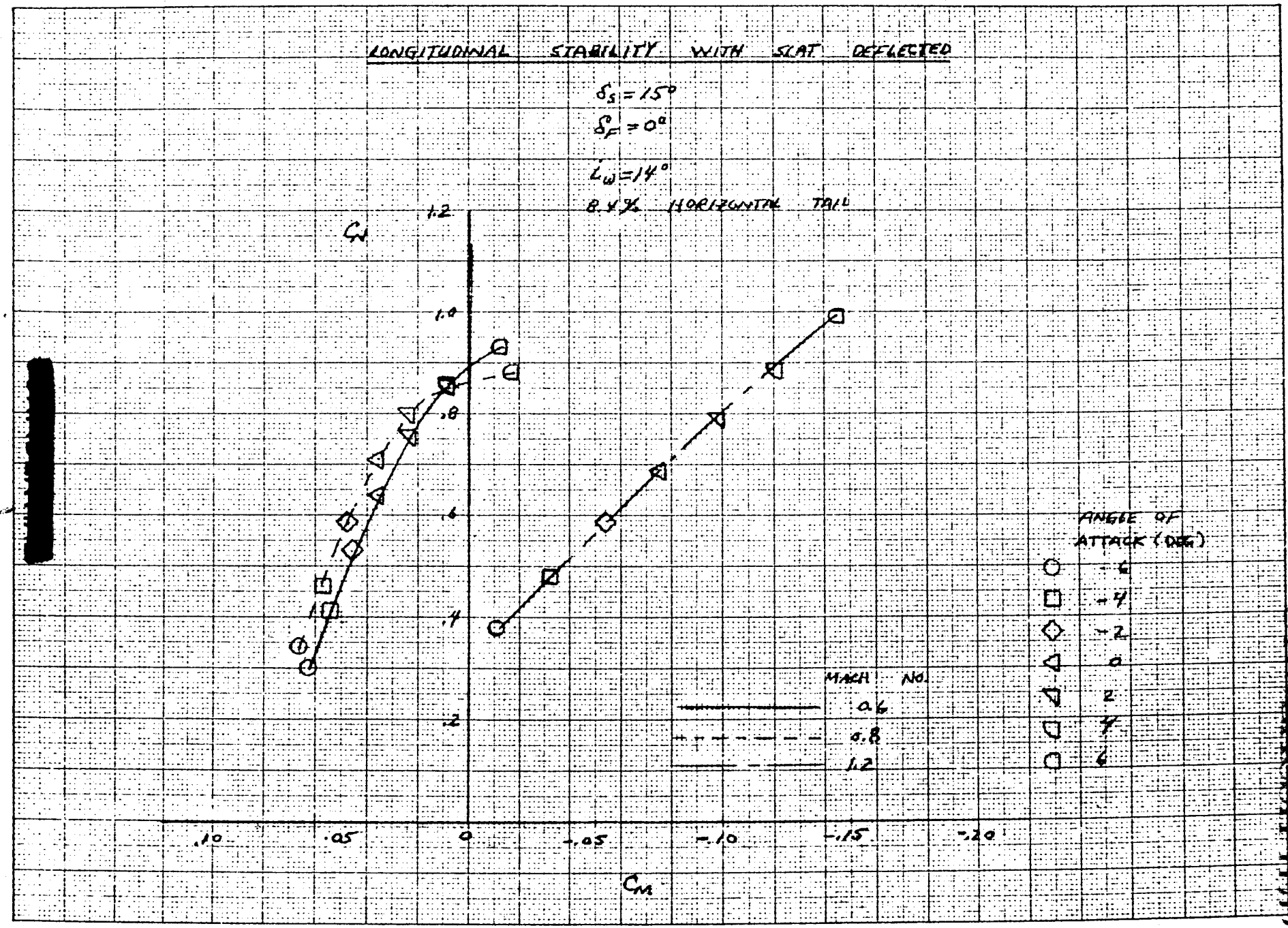

Figure 3-14. Longitudinal Stability with Slat Deflected

UNCLASSIFIED

3.1.4 Plain Flaps

Figures 3-15, 3-16, and 3-17 show the effect of flap deflection at Mach 0.6, 0.8, and 1.2. This configuration was tested with the small horizontal tail, a 14° wing incidence, and the slat undeflected. These figures show that the normal force with the flaps deflected 40° and 50° were approximately equal. Also, these two deflections produced a normal force, which was only slightly greater than the 25° flap. The flaps at all Mach numbers produced a lift increment of approximately 0.4. From this data, a flap deflection of 40° was chosen for the remaining runs on the contoured wing.

At zero angle of attack, this configuration attained a trim lift coefficient of approximately 1.1. As this configuration included the slat in the undeflected position, which produced a lift increase at the subsonic Mach number, a flap alone configuration (without the slat) would have less lift than that shown in Figures 3-15 and 3-16. Removing the slat would probably reduce the subsonic lift by approximately 0.05. As shown in Figures 3-15, 3-16, and 3-17, the configuration is unstable at Mach 1.2 and is unstable at low angles of attack in the subsonic Mach number regime. To prevent this longitudinal instability, it is estimated that the horizontal tail size should be increased to approximately 12% wing area or greater.

3.1.5 Plain Flaps and Slats

Figure 3-18 shows the effect of increasing wing incidence by 2° (to 16°) and deflecting the slat 15° at Mach 0.6 with an 8.4% horizontal tail and the flap deflected 40°. This figure also shows the effect of increasing the horizontal tail size to 30% with $\delta_s = 15°$, $\delta_f = 40°$, and $i_w = 16°$. Figures 3-19 and 3-20 show the same information at Mach 0.8 and 1.2.

Based on the same wing angle of attack, Figures 3-11, 3-12, 3-18, and 3-19 show that deflecting the slat 15° at the subsonic Mach numbers, resulted in a smaller lift increase when the flap was deflected 40° than when the flap was undeflected. At Mach = 0.8 with a 16° wing angle of attack ($\alpha = 2°$), the slat increased C_N by 0.1 when the flap was undeflected, whereas with the flap deflected, the total lift increase resulting from deflecting the slat was about 0.03.

UNCLASSIFIED

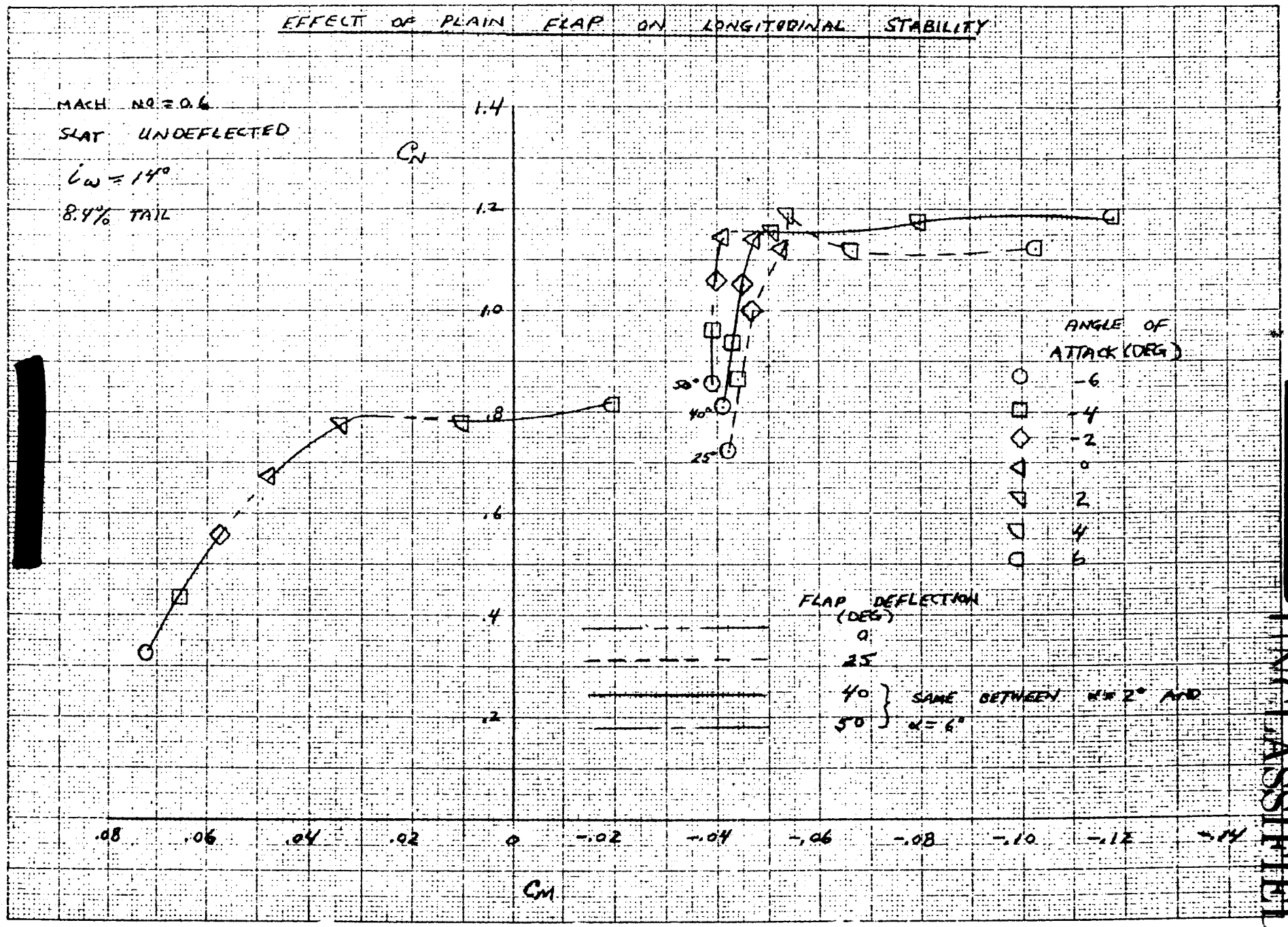

Figure 3-15. Effect of Plain Flap on Longitudinal Stability--Mach No = 0.6, Slat Undeflected, i_w = 14°, and 8.4% Tail

UNCLASSIFIED

UNCLASSIFIED

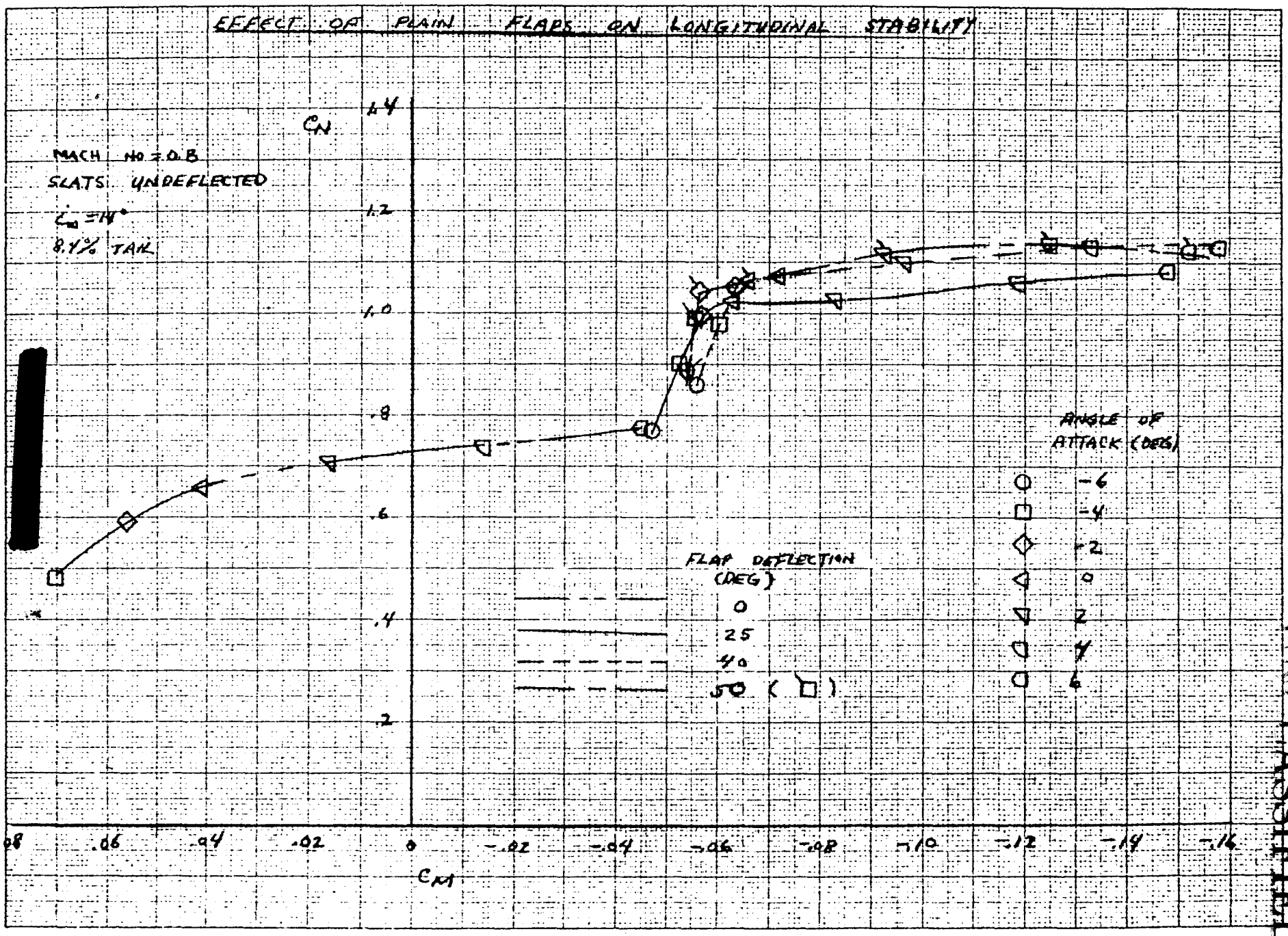

Figure 3-16. Effect of Plain Flaps on Longitudinal Stability--Mach No. = 0.8, Slats Undeflected, i_w = 14° and 8.4% Tail

UNCLASSIFIED

UNCLASSIFIED

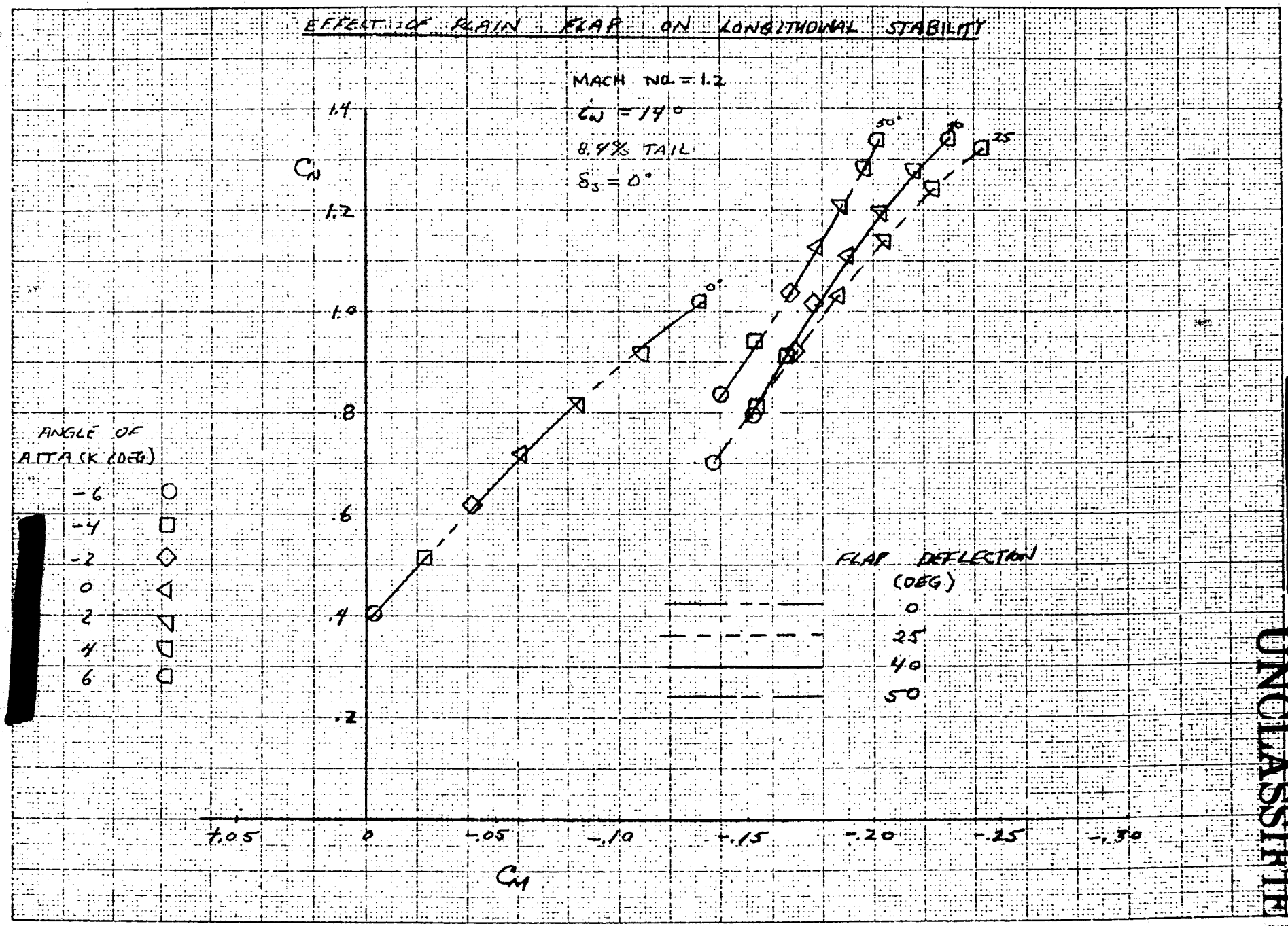

Figure 3-17. Effect of Plain Flap on Longitudinal Stability--Mach No. = 1.2, i_w = 14°, 8.4% Tail, and δ_s = 0°

UNCLASSIFIED

UNCLASSIFIED

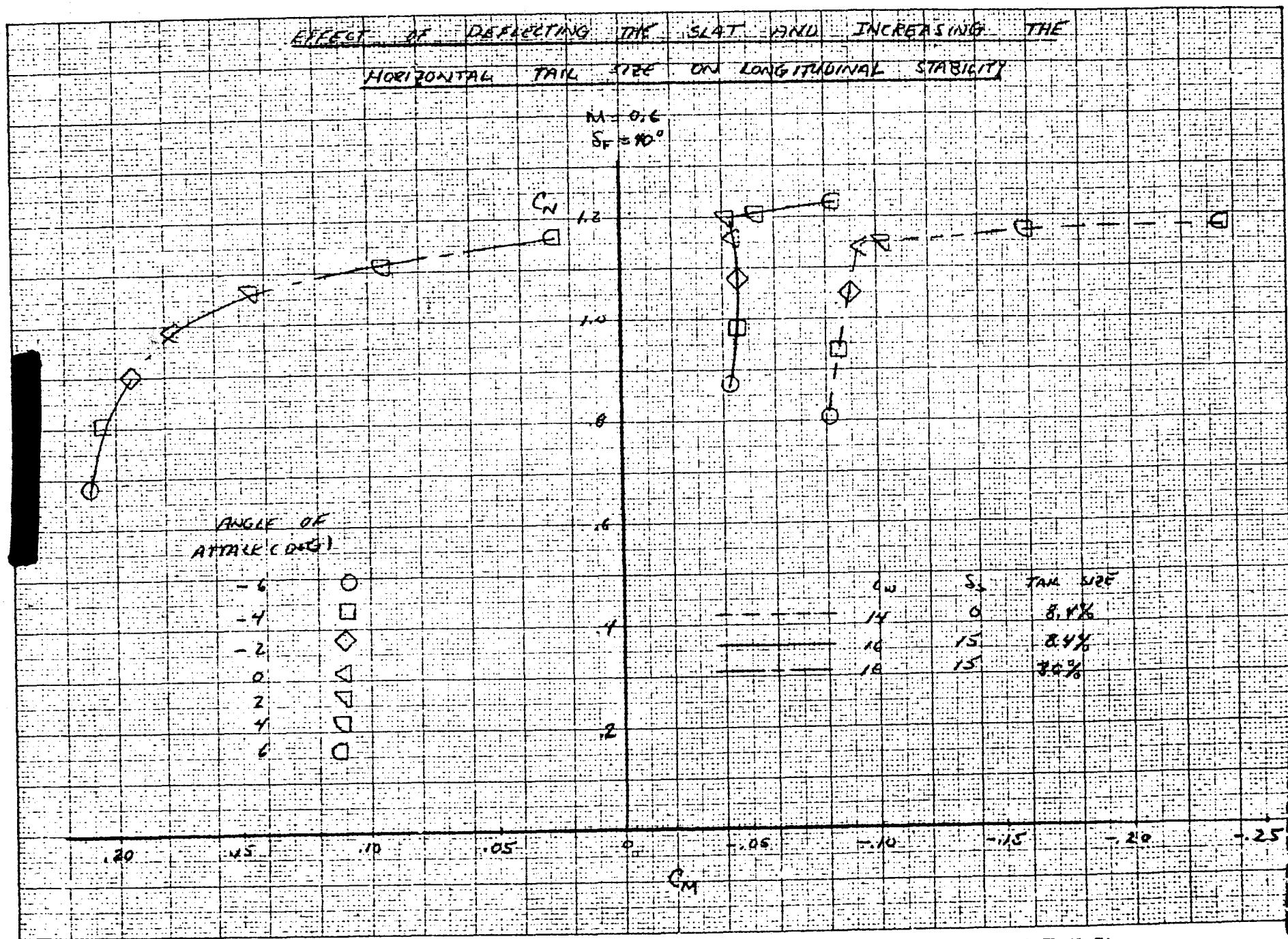

Figure 3-18. Effect of Deflecting the Slat and Increasing the Horizontal Tail Size on Longitudinal Stability-- M = 0.6 and δ_F = 40°

UNCLASSIFIED

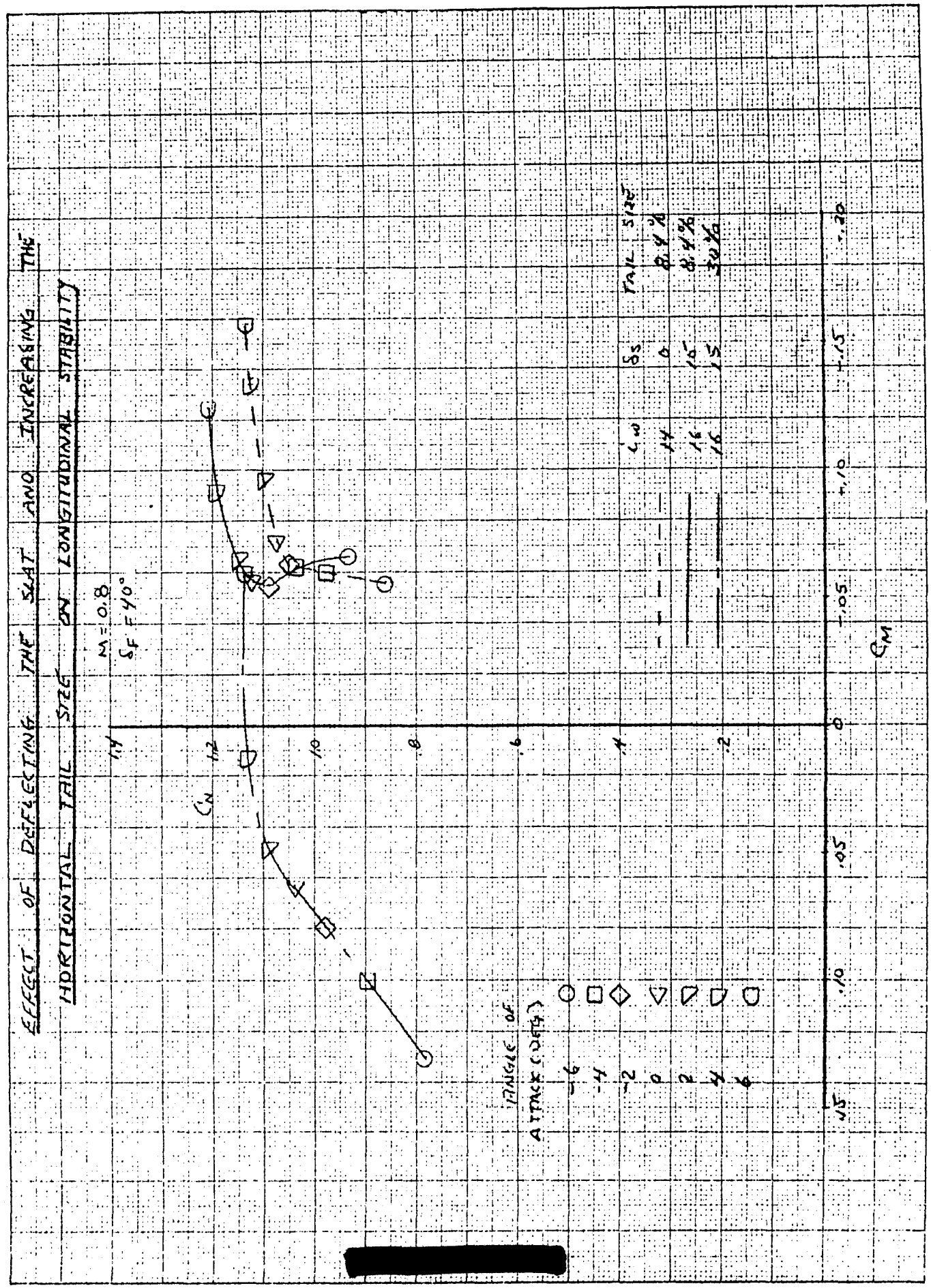

Figure 3-19. Effect of Deflecting the Slat and Increasing the Horizontal Tail Size on Longitudinal Stability-- M = 0.8 and δ_F = 40°

UNCLASSIFIED

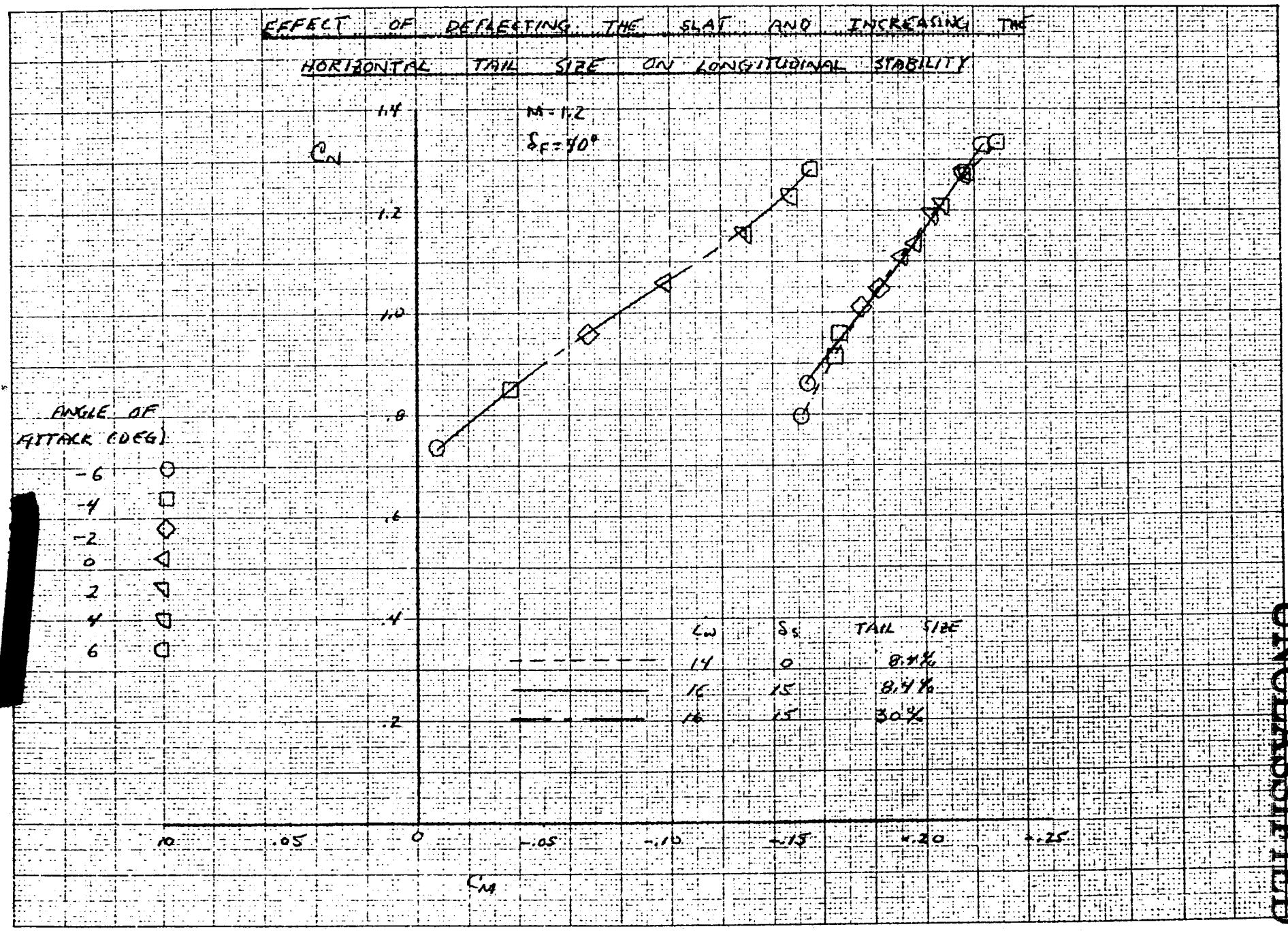

Figure 3-20. Effect of Deflecting the Slat and Increasing the Horizontal Tail Size on Longitudinal Stability-- M = 1.2 and δ_F = 40°

UNCLASSIFIED

Figures 3-21 and 3-22 show the effect of increasing the horizontal tail size at Mach 0.6, 0.8, 0.95, 1.0, 1.1, and 1.2. These figures show that generally an increase in Mach number resulted in a reduction in horizontal tail effectiveness. This change in tail effectiveness is more clearly shown in Figures 3-23 and 3-24, which show the pitching moment difference between the 8.4% tail and 30% tail as a function of angle of attack and Mach number. The tail effectiveness from the May 1965 wind tunnel test is shown in Figure 3-25. Figure 3-25a shows ΔC_M caused by changing the body length from 83 in. to 100 in. and Figure 3-25b shows the pitching moment change between the 12% tail and no tail. This figure shows that the horizontal tail effectiveness was roughly independent of the Mach number. The change in tail effectiveness on the present test is believed to be caused by the flap washing out the tail at the higher Mach numbers. The tail effectiveness change results in too-large of a center of pressure travel to permit launching both subsonic and supersonic with a fixed configuration. Although if the launch Mach number is known, the missile could be successfully flown by repositioning the wing.

The data also suggest that if a constant tail effectiveness could be achieved, the trim angle of attack variations would be sufficiently small to permit both a subsonic and supersonic launch with a fixed configuration. This is shown in Figures 3-26 and 3-27. These figures show the estimated longitudinal stability at Mach numbers from 0.6 to 1.2, assuming a tail effectiveness which is equal to the 30% tail at Mach 0.6. Assuming a 20° wing incidence and choosing a CG to trim at approximately $\alpha = 0°$ at Mach 0.6 and 0.8, the trim angle of attack Mach 1.2 would be about -3.5°. Because of the high drag coefficient ($C_D \approx 0.45$), the impact Mach number for a Mach 1.2 launch is about Mach 1.01. This impact Mach number has a trim angle of attack equal to approximately -0.7°, which should provide good impact conditions.

It is believed that the constant tail effectiveness can be achieved by going to a T-tail arrangement (the horizontal tail attached to the bottom vertical tail). This arrangement should remove the tail from the flap wake, thereby increasing the tail effectiveness at the higher Mach numbers.

Figure 3-28 shows the estimated trim normal force coefficient assuming a constant tail effectiveness (data taken from Figures 3-26 and 3-27). With

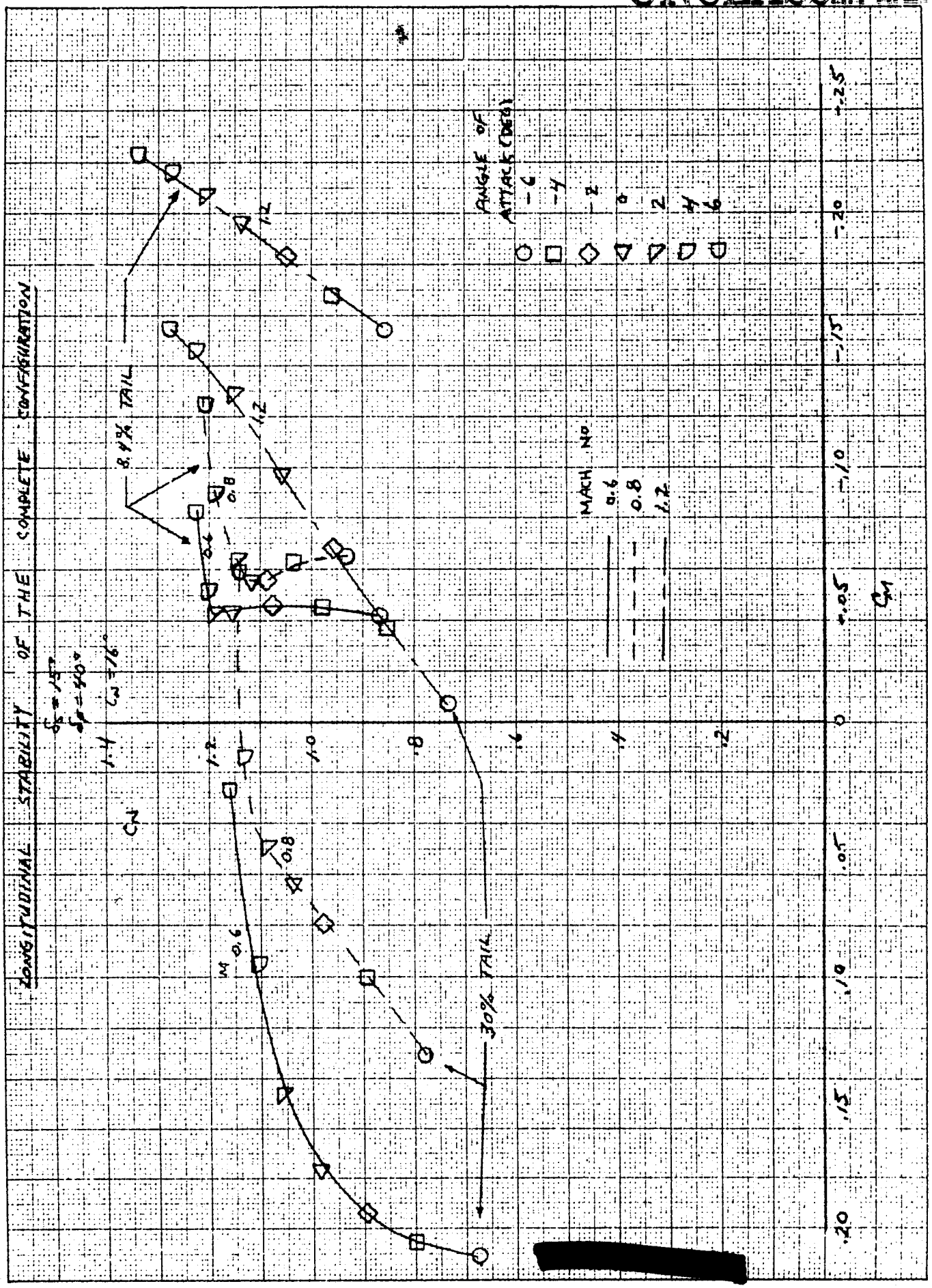

Figure 3-21. Longitudinal Stability of the Complete Configuration--
$\delta_s = 15°$, $\delta_F = 40°$, and $i_w = 16°$

UNCLASSIFIED

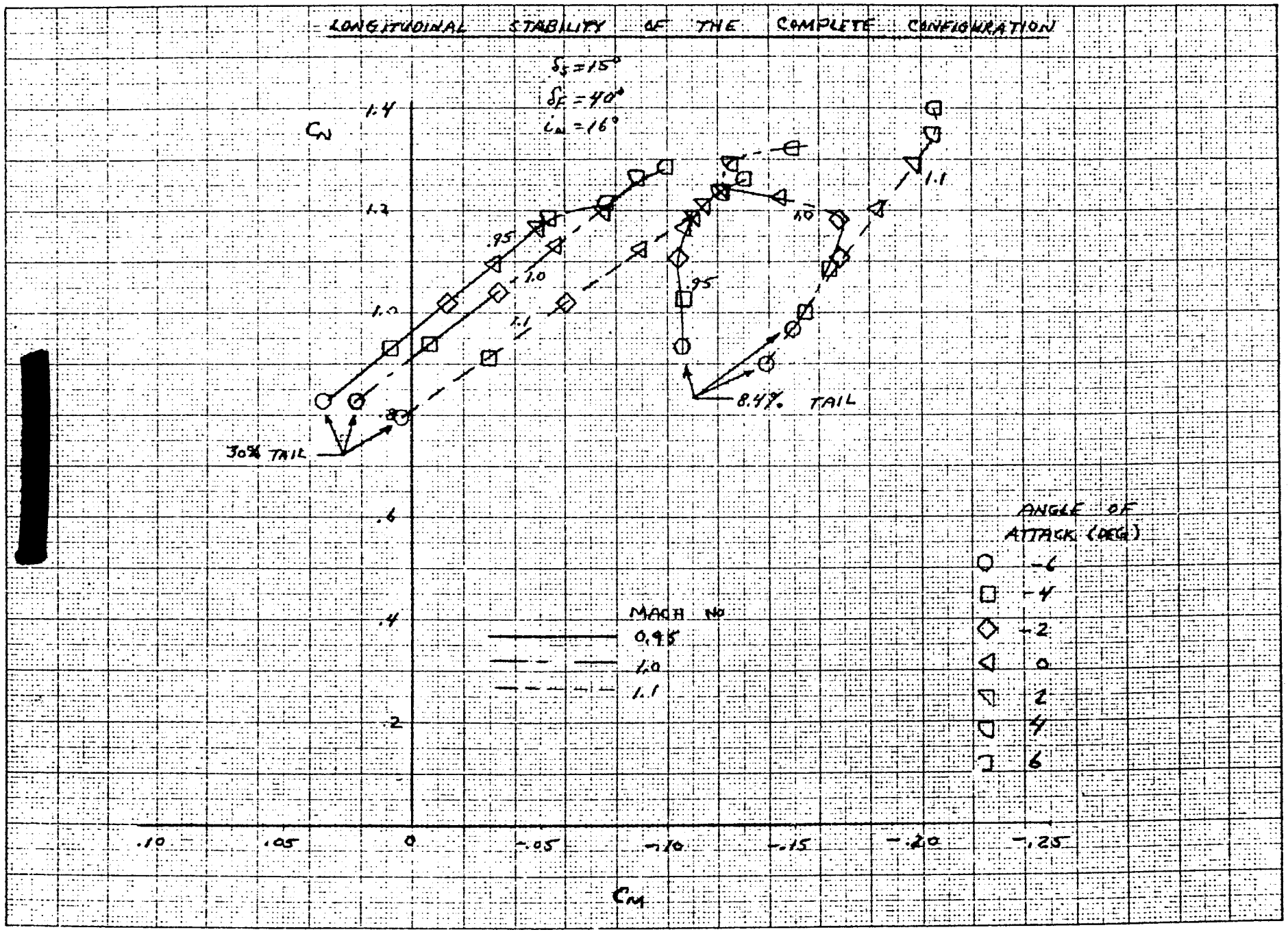

Figure 3-22. Longitudinal Stability of the Complete Configuration--
$\delta_S = 15°$, $\delta_F = 40°$, and $i_W = 16°$

UNCLASSIFIED

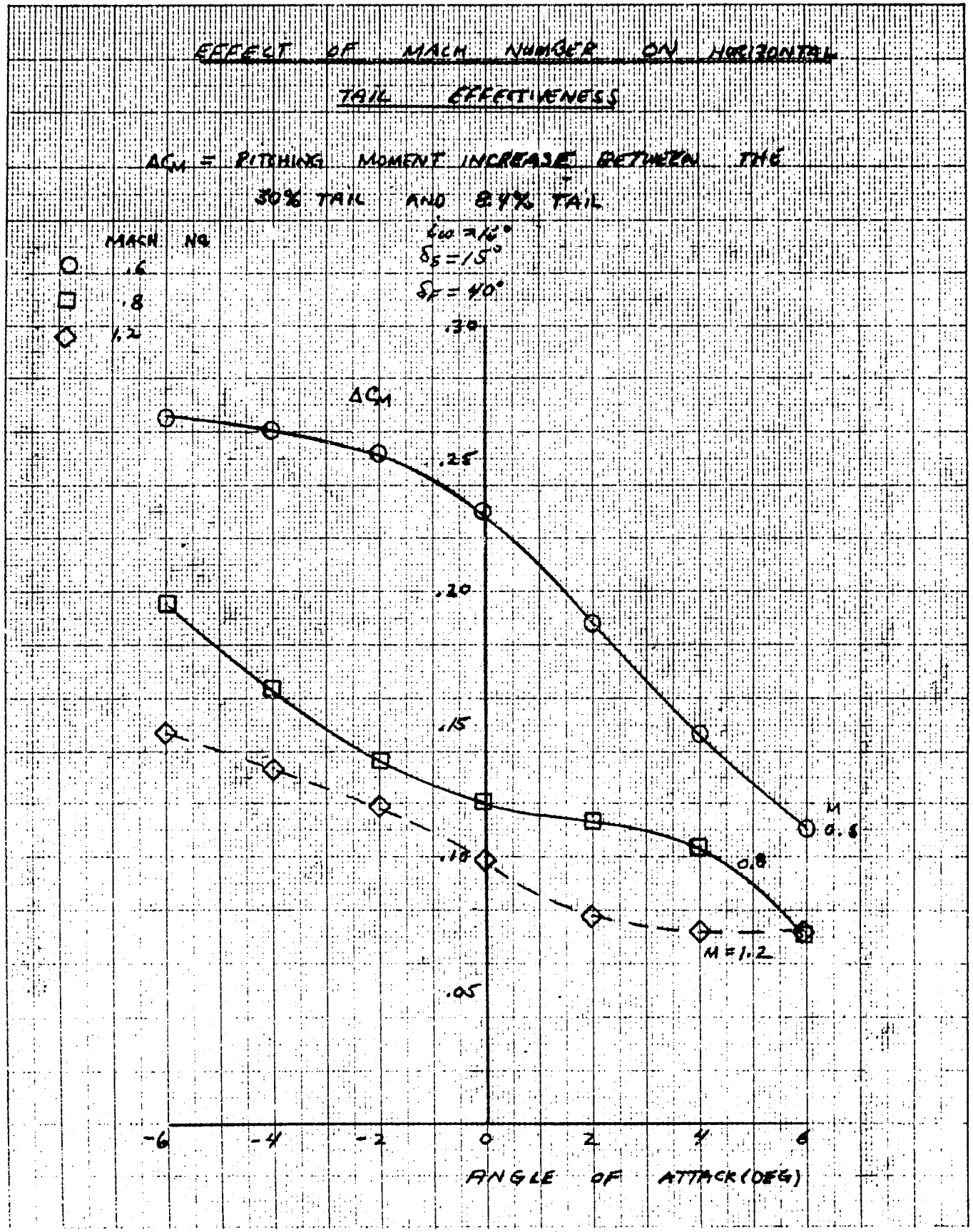

Figure 3-23. Effect of Mach Number on Horizontal Tail Effectiveness-- ΔC_M = Pitching Moment Increase Between the 30% Tail and 8.4% Tail

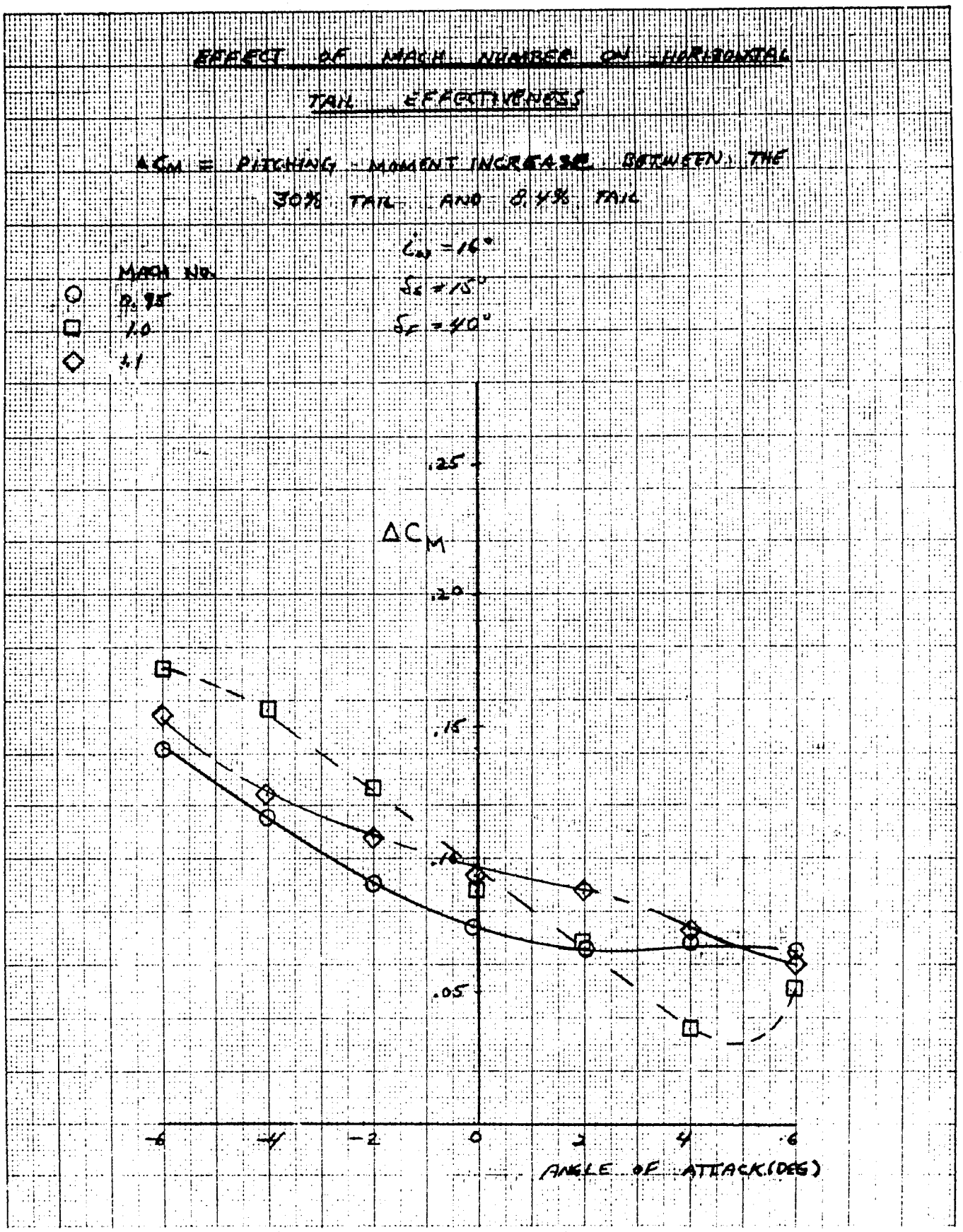

Figure 3-24. Effect of Mach Number on Horizontal Tail Effectiveness-- ΔC_M = Pitching Moment Increase Between the 30% Tail and 8.4% Tail

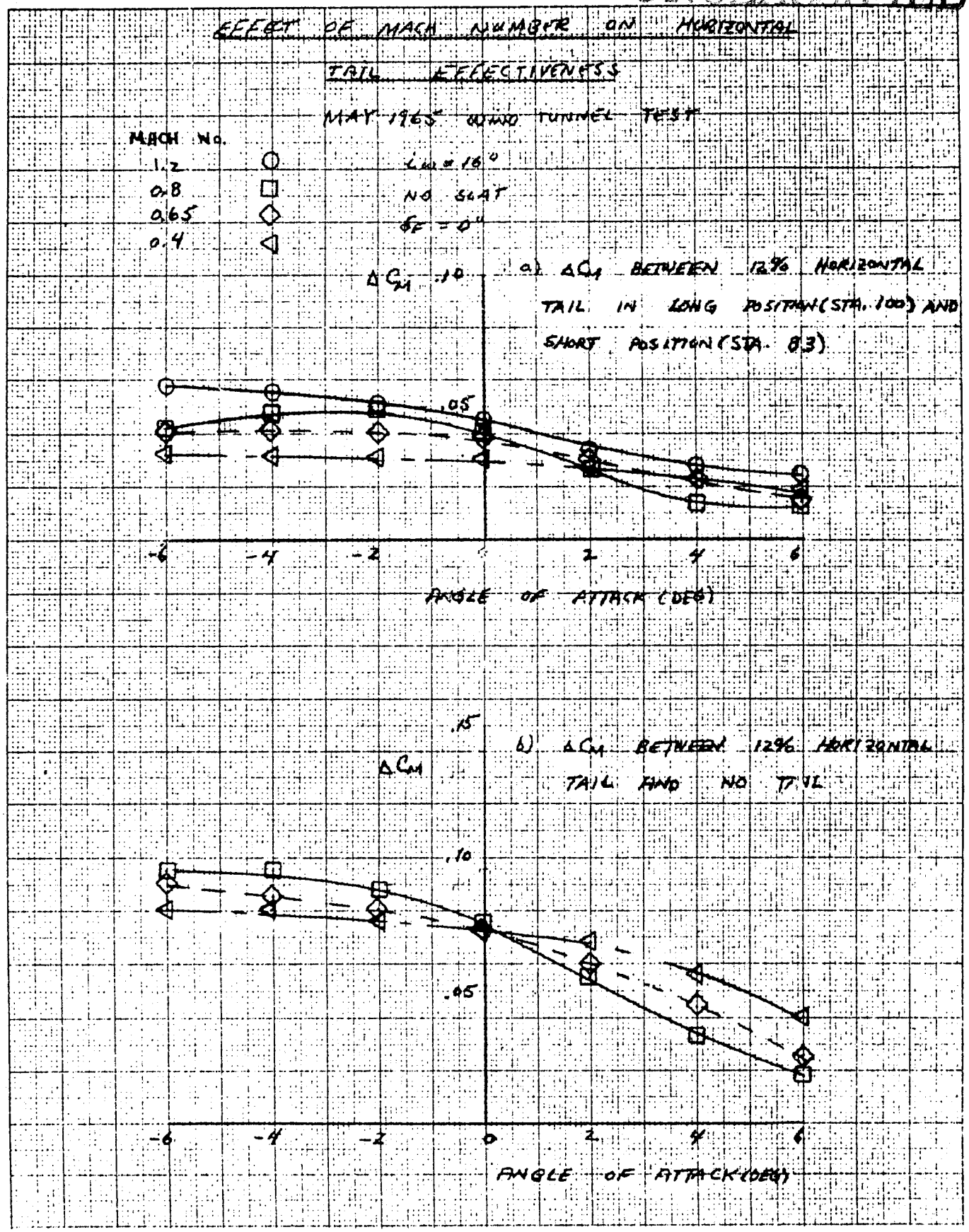

Figure 3-25. Effect of Mach Number on Horizontal Tail Effectiveness--May 1965 Wind Tunnel Test

UNCLASSIFIED

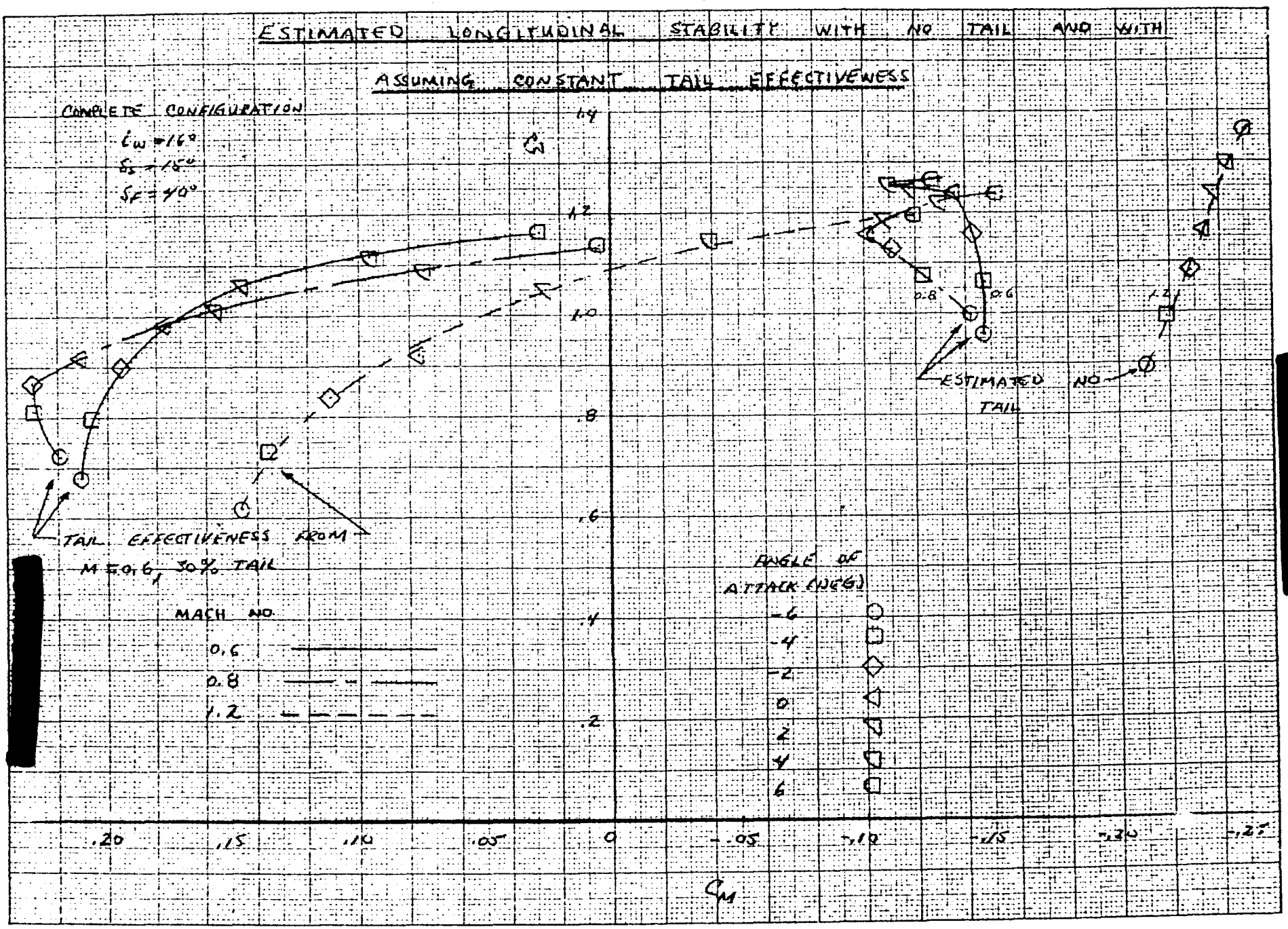

Figure 3-26. Estimated Longitudinal Stability with no Tail and

UNCLASSIFIED

UNCLASSIFIED

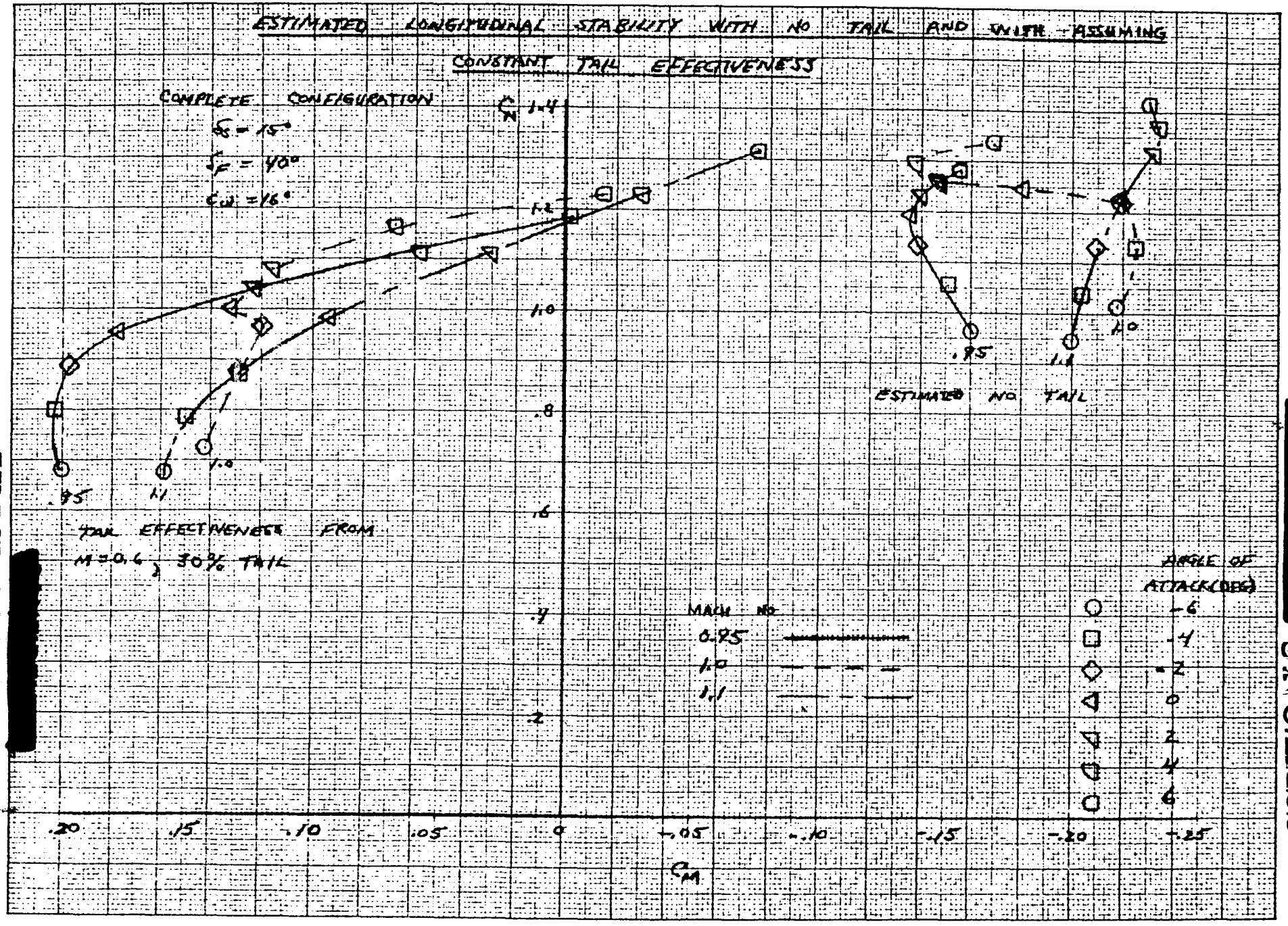

Figure 3-27. Estimated Longitudinal Stability with no Tail and with Assuming Constant Tail Effectiveness

UNCLASSIFIED

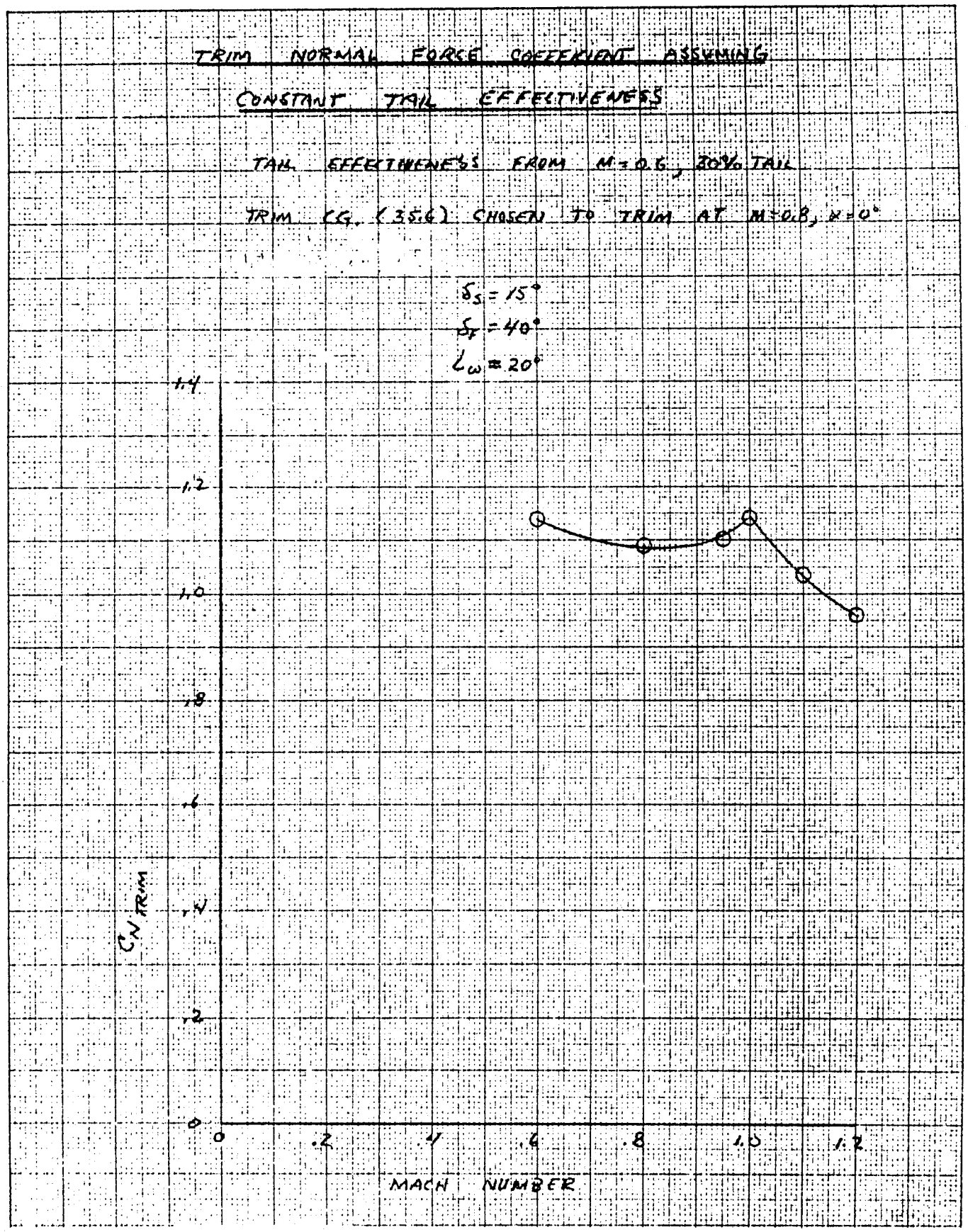

Figure 3-28. Trim Normal Force Coefficient Assuming Constant Tail Effectiveness

slats and flaps deflected, the estimated trim normal force coefficient is approximately 1.1 at the subsonic Mach numbers. This is slightly less than the 1.2 C_N estimated from Reference 2. The difference is because Reference 2 assumed that the incremental lift caused by the slat and flap could be added separately, whereas the results of this test showed that there is some lift interference between the slat and flap.

3.1.5 Jet Flaps

Another method of obtaining lift is through the use of a jet flap. This flap configuration is shown in Figure 3-2. The jet consists of a high-pressure air supply which is ejected through a slot at the trailing-edge on the windward side of the slab wing. In the tests, the slot was about 0.070 in. wide and extended from the wing trailing-edge inboard position to about 4 in. from the wing tip. For simulation purposes, the jet supply pressure on the flight vehicle was assumed to be approximately 1650 psi at Mach 1.2. At Mach 0.6 and 0.8, the jet pressure was assumed to be 225 psi and 330 psi.

Figures 3-29, 3-30, and 3-31 show the effect of the jet flaps on longitudinal stability at Mach 0.6, 0.8, and 1.2. The jet resulted in an incremental lift coefficient of about 0.5 at all Mach numbers. The jet magnification factors at Mach 0.6, 0.8, and 1.2 were about 4.7, 5.1 and 2.5. The jet magnification factor is defined as the ratio of: Jet thrust plus aerodynamic interaction, to jet thrust. For example, at Mach 0.6, the jet induced aerodynamic lift was approximately 3.7 times the jet thrust.

Although the jet flaps resulted in a slightly greater lift increase then the plain flaps, the jet flaps are not recommended because of their complexity. Because the amount of jet thrust is roughly proportional to the dynamic pressure, large variations in thrust are required; for example, a factor of 10-1 between Mach 1.2 and M 0.5. Assuming a solid propellant, this would require extremely large changes in burn rate or dumping the excess thrust overboard. To determine the thrust requirements, measurement of dynamic pressures, either directly or indirectly, is required.

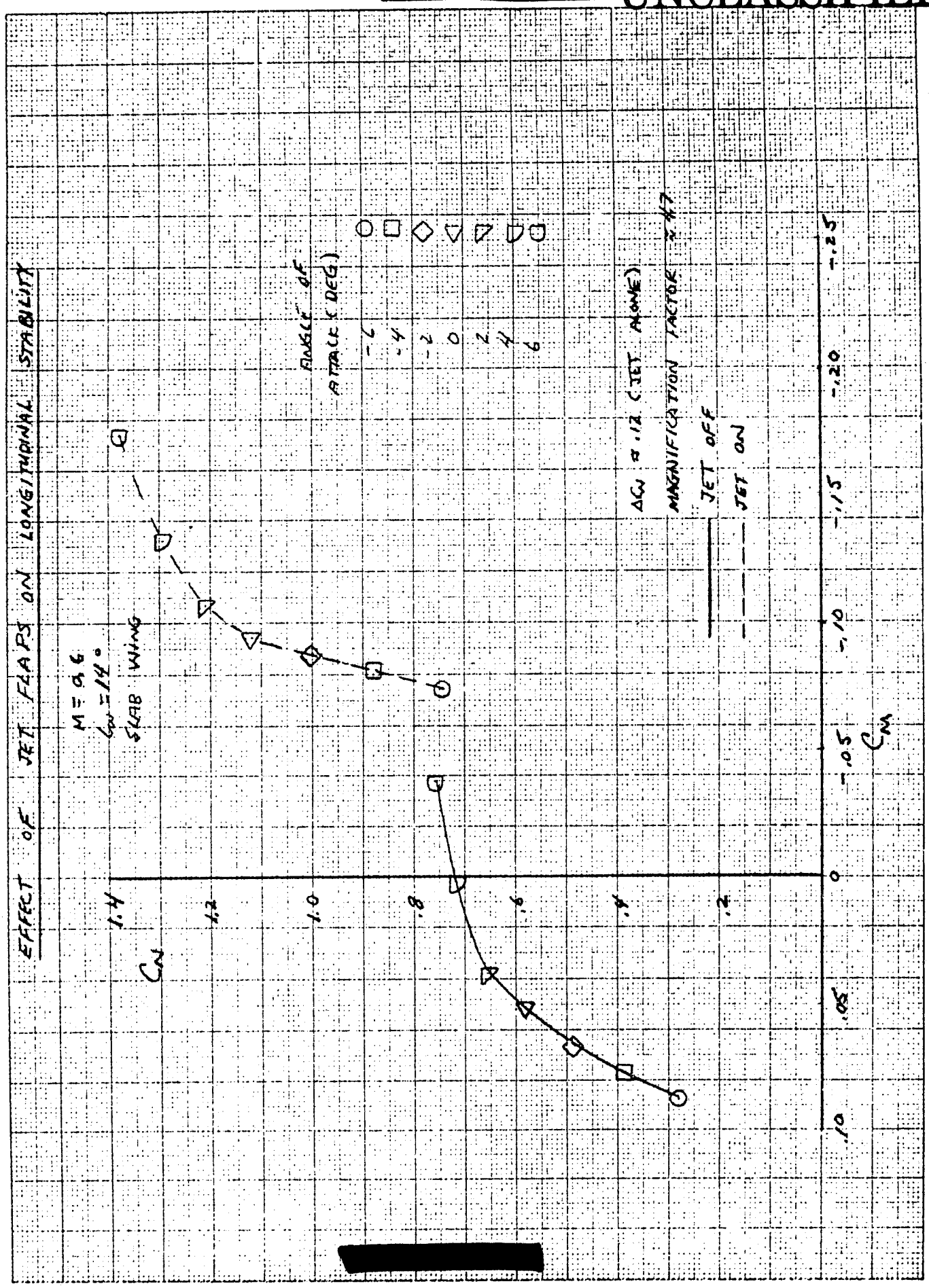

Figure 3-29. Effect of Jet Flaps on Longitudinal Stability--
M = 0.6, i_w = 14°, and Slab Wing

UNCLASSIFIED

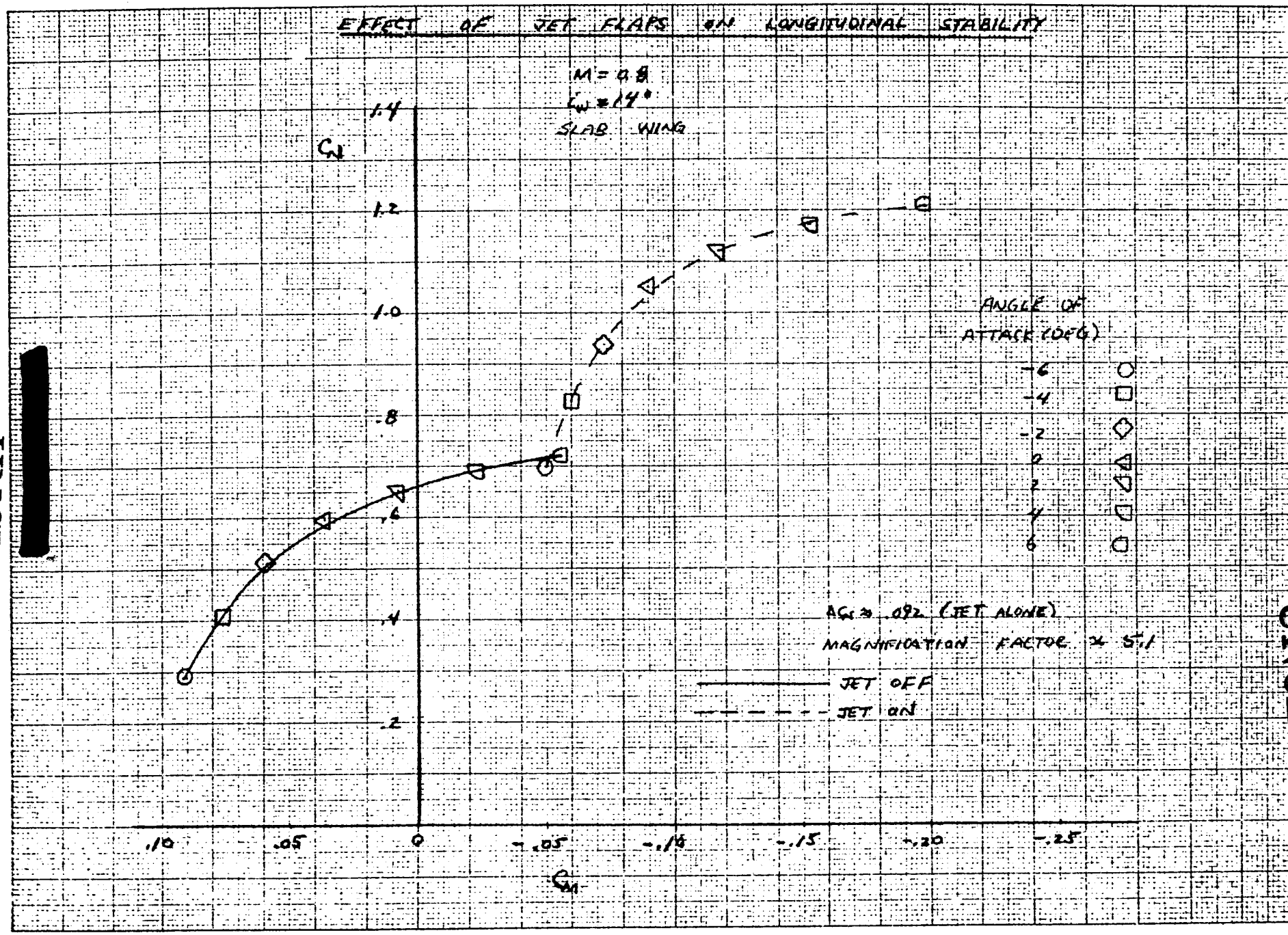

Figure 3-30. Effect of Jet Flaps on Longitudinal Stability--
M = 0.8, i_w = 14°, and Slab Wing

UNCLASSIFIED

UNCLASSIFIED

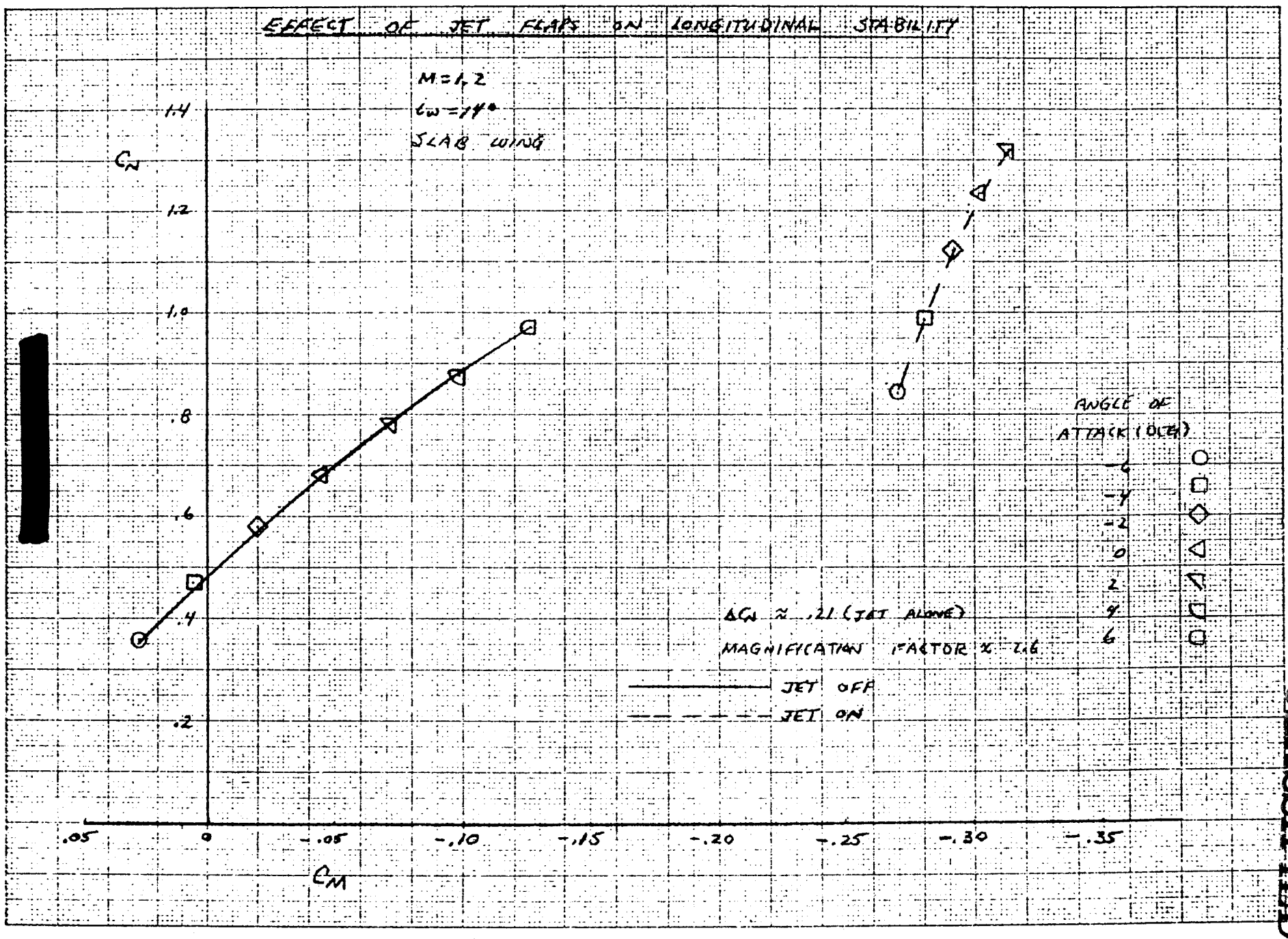

Figure 3-31. Effect of Jet Flaps on Longitudinal Stability--
M = 1.2, i_w = 14°, and Slab Wing

UNCLASSIFIED

The size of a hot gas generator required to produce 5,500 lb of thrust for 0.6 sec was investigated; The jet flap propulsion requirements at Mach 1.2. Olin Mathieson's Omax lb-27 ammonium perchlorate solid propellant was selected for this study because of its clean burning, high-performance characteristics.

Results of this study concluded the following:

1. The propellant flow rate (W) required is 30.4 lb/sec.
2. The propellant weight (W) required for 0.6 sec is 18.3 lb.
3. The inert weight (W_i), i.e., gas generator case, insulation and igniter assembly would be approximately 22 lb.
4. The gas generator size would be 5 in. outside diameter by 39.5 in. overall length. The total weight would be approximately 40 lb.

Although preliminary design may be required before final conclusions should be drawn, it is seen that the weight and volume requirements for the jet flap gas generator are marginally compatible with the basic Bayonet configuration. Also the burning of the gas supply results in CG variations with flight time which would present problems in trim angle of attack variations.

3.1.7 Pitch Control

Another possible means of reducing the trim angle of attack variations is through use of a pitch control system. This system would probably involve deflecting or placing a flap on the horizontal tail. Measurement of dynamic pressure, Mach number, or preferably body angle of attack would be required to determine the proper deflection in flight. Because of horizontal tail wash-out, when mounted on the body, it would also be desireable to attach the horizontal tail to the bottom vertical tail in order to increase the pitch control effectiveness. A pitch control system would not be recommended, because of its complexity, unless the necessary increase in horizontal tail effectiveness cannot be achieved.

3.2 DIRECTIONAL AND LATERAL STABILITY

3.2.1 Slab Wing

The slab wing directional and lateral stability at Mach 0.6, 0.8, and 1.2 is shown in Figure 3-32. This configuration was directionally stable at Mach 0.6 and 0.8 up to, 4.6° and 3.1° angle of attack. At Mach 1.2, the slab wing configuration was directionally stable at all angles of attack tested. Although the Bayonet vehicle at low velocities can achieve sufficient angles of attack to become unstable ($\alpha \geq 3.1°$), the missile instability is for a relatively small duration such that the flight characteristics are not seriously affected. Reference 5, Subsection 3.3.2.

The slab wing lateral stability is shown in Figure 3-32. One of the design criteria for Bayonet was to minimize this stability in order to reduce the vehicle roll perturbations caused by winds and yaw angles. Figure 3-32 shows that the configuration is laterally stable. This level of stability is approximately equal to that on the present Bayonet configuration and has an acceptable value. With the addition of roll control, the configuration will become less sensitive to lateral stability. Although a direct comparison is not possible between the slab and contoured wing (May 1965 data) because of a change in wing incidence and the addition of another vertical tail, the data in Figure 3-32 is similar to the contoured wing data in Reference 1.

3.2.2 Slats and Flaps

The wind tunnel data, Reference 4, showed that all Bayonet configurations tested had good directional stability between Mach 0.95 and Mach 1.2. Figures 3-33 and 3-34 show the effect of both flap and slat deflection on directional stability at Mach 0.6 and 0.8. A comparison between these figures and Figure 3-32 shows that the contoured wing with the slat undeflected has larger directional stability than the slab wing. The contoured wing with $\delta_s = 0°$ increases the angle of attack at which the configuration becomes unstable by approximately 1°. Because it is believed that the slab and contoured wings are approximately aerodynamically equivalent, the directional stability difference is probably

UNCLASSIFIED

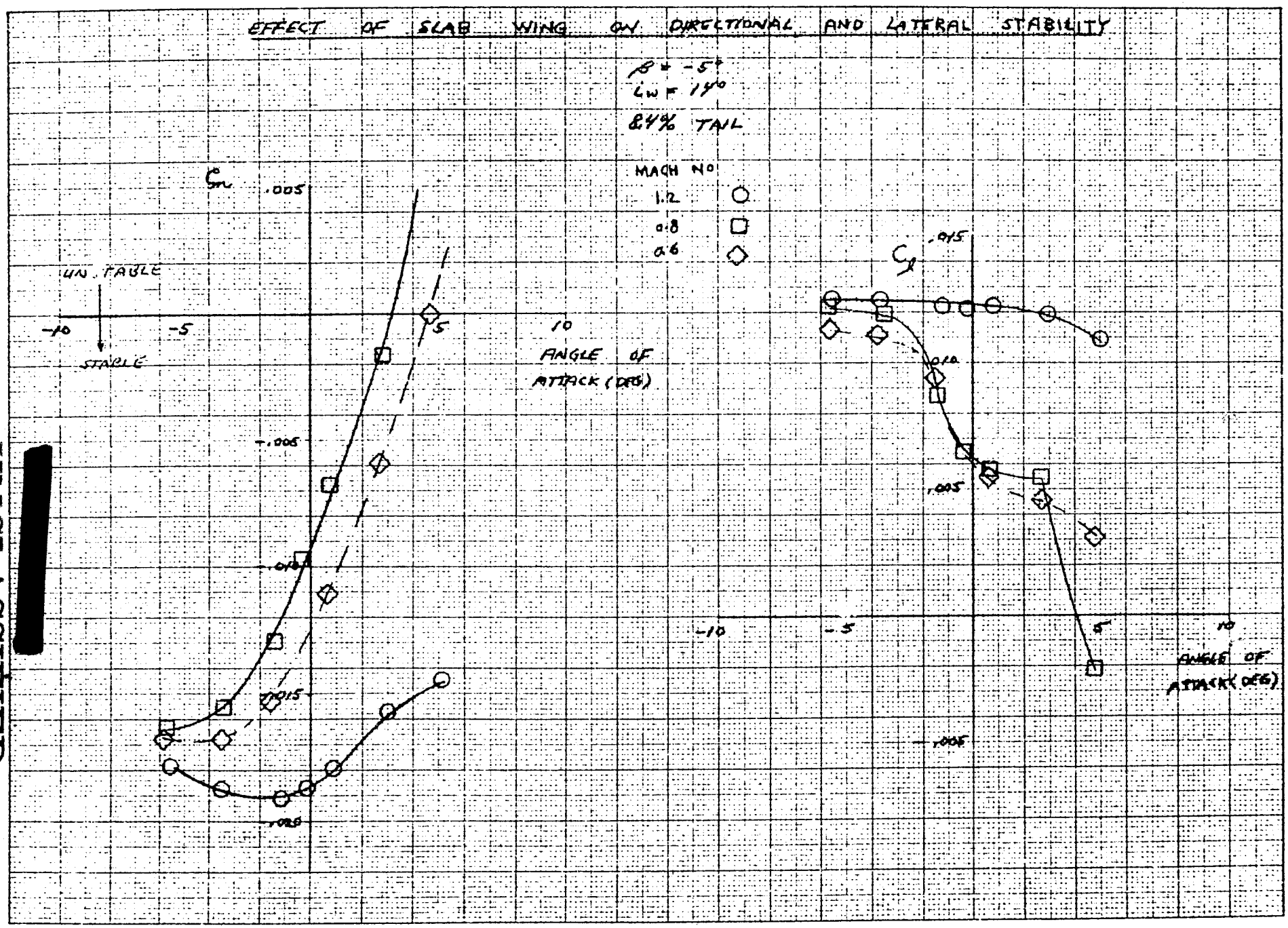

Figure 3-32. Effect of Slab Wing on Directional and Lateral Stability--
$\beta = -5.0°$, $i_w = 14°$, and 8.4% Tail

UNCLASSIFIED

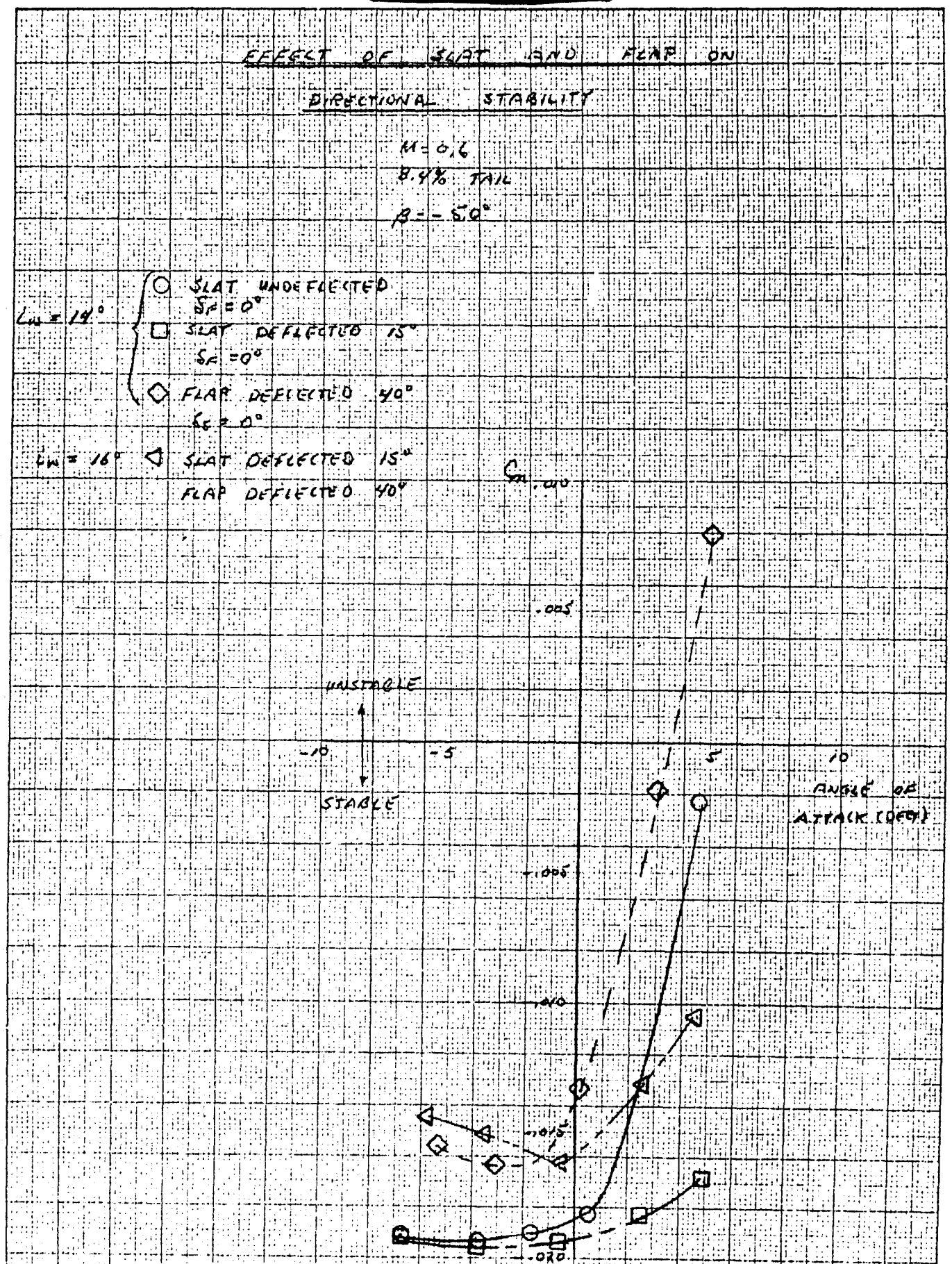

Figure 3-33. Effect of Slat and Flap on Directional Stability--
M = 0.6, 8.4% Tail, and β = -5.0°

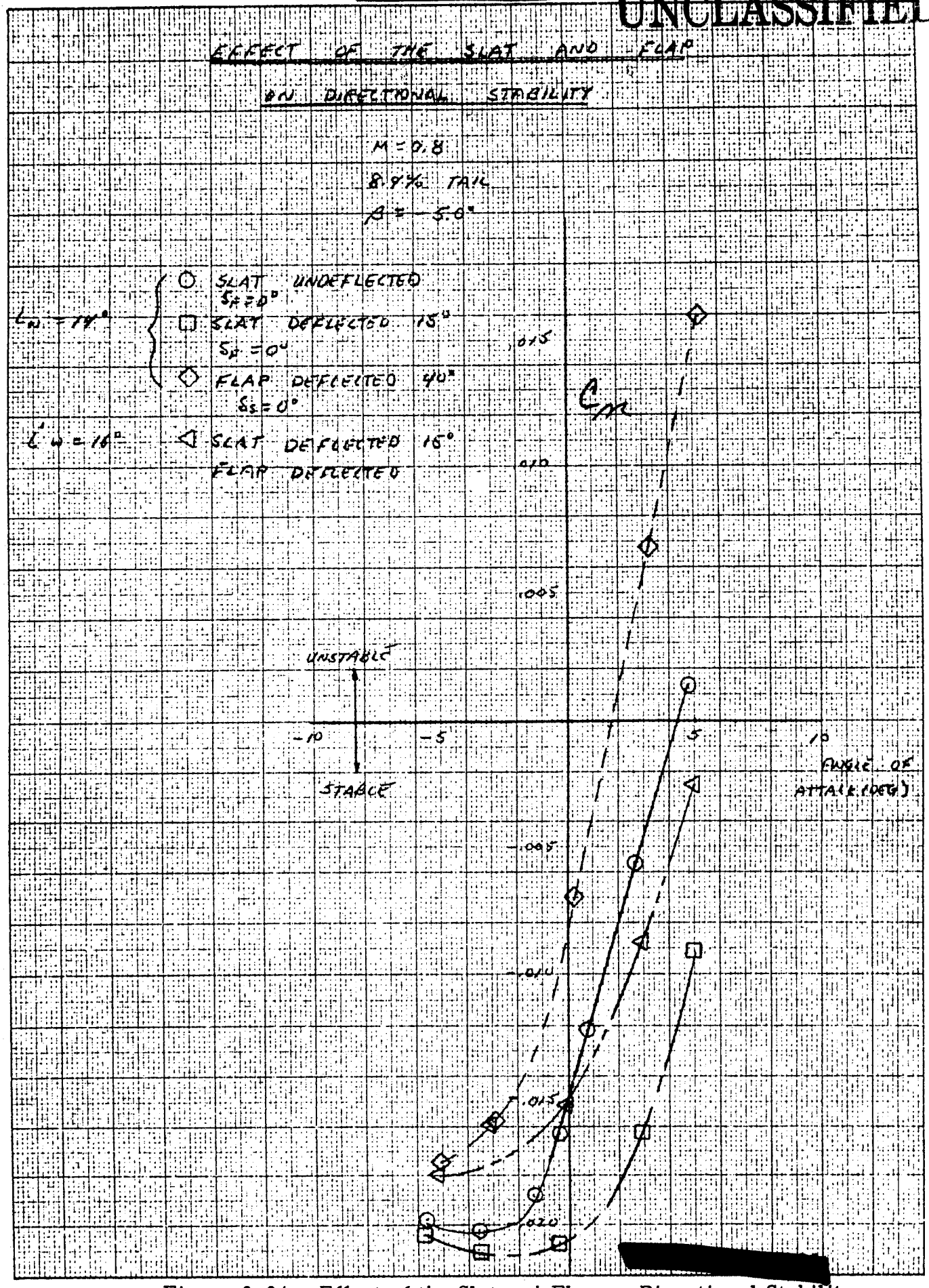

Figure 3-34. Effect of the Slat and Flap on Directional Stability--
M = 0.8, 8.4% Tail, and β = -5.0°

due to the undeflected slat. That is, the undeflected slat reduced the leeward side flow separation (evidenced by the lift increase) thereby increasing the vertical tail effectiveness.

As shown in Figures 3-33 and 3-34, deflecting the slat (with the flap undeflected) resulted in a considerable increase in directional stability. This increase is also caused by the slat reducing the flow separation on the wing leeward side. Deflecting the flap by 40° (δ_s = 0°) resulted in a considerable reduction in directional stability. This is caused by the flap washing out the vertical tails. At Mach 0.6 and 0.8, the flap configuration became directionally unstable at 3.3° and 1.8° angle of attack. As this flap data is with the slat undeflected, the flap directional stability without a slat would probably be less (by approximately 1°) than that shown in Figures 3-32 and 3-33. This would mean that the basic wing with flap alone would have too little directional stability to be flown successfully. In addition, it is desirable to increase the wing incidence (for greater lift) from 14° to approximately 20°, which would further reduce directional stability. This increase in wing incidence cannot be achieved unless the vertical tail effectiveness can be increased considerably.

An increase in tail effectiveness by increasing vertical tail size is somewhat limited because of carry aircraft compatibility. The increase in tail effectiveness can be achieved by using a deflected slat in combination with the flap. Figures 3-32 and 3-33 show that deflecting the slat with δ_f = 40° resulted in a large increase in directional stability. This level of stability should allow increasing the wing incidence to about 18° or 20°.

The effect of slat and flap deflection on lateral stability at Mach 0.6 and 0.8 are shown in Figures 3-35 and 3-36. The effect of these deflections on lateral stability was similar to their effect on directional stability.

3.3 ROLL CONTROL DEVICES

3.3.1 Jet Roll Control

The jet roll control was similar to the jet flap. The roll jet (Figure 3-2) consisted of a slot about 0.017 in. wide at the wing tip trailing-edge. The

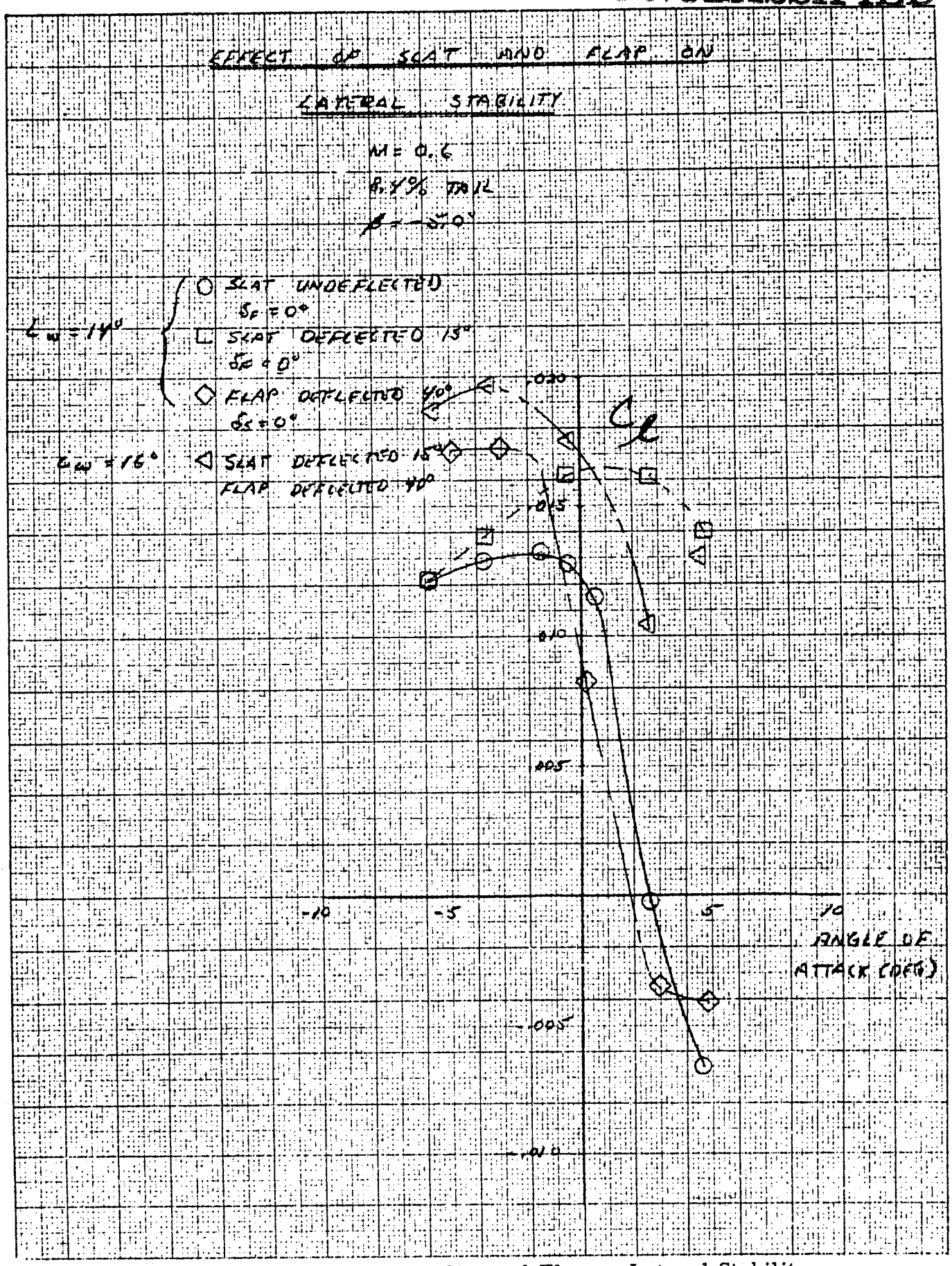

Figure 3-35. Effect of Slat and Flap on Lateral Stability--
M = 0.6, 8.4% Tail, and β = -5.0°

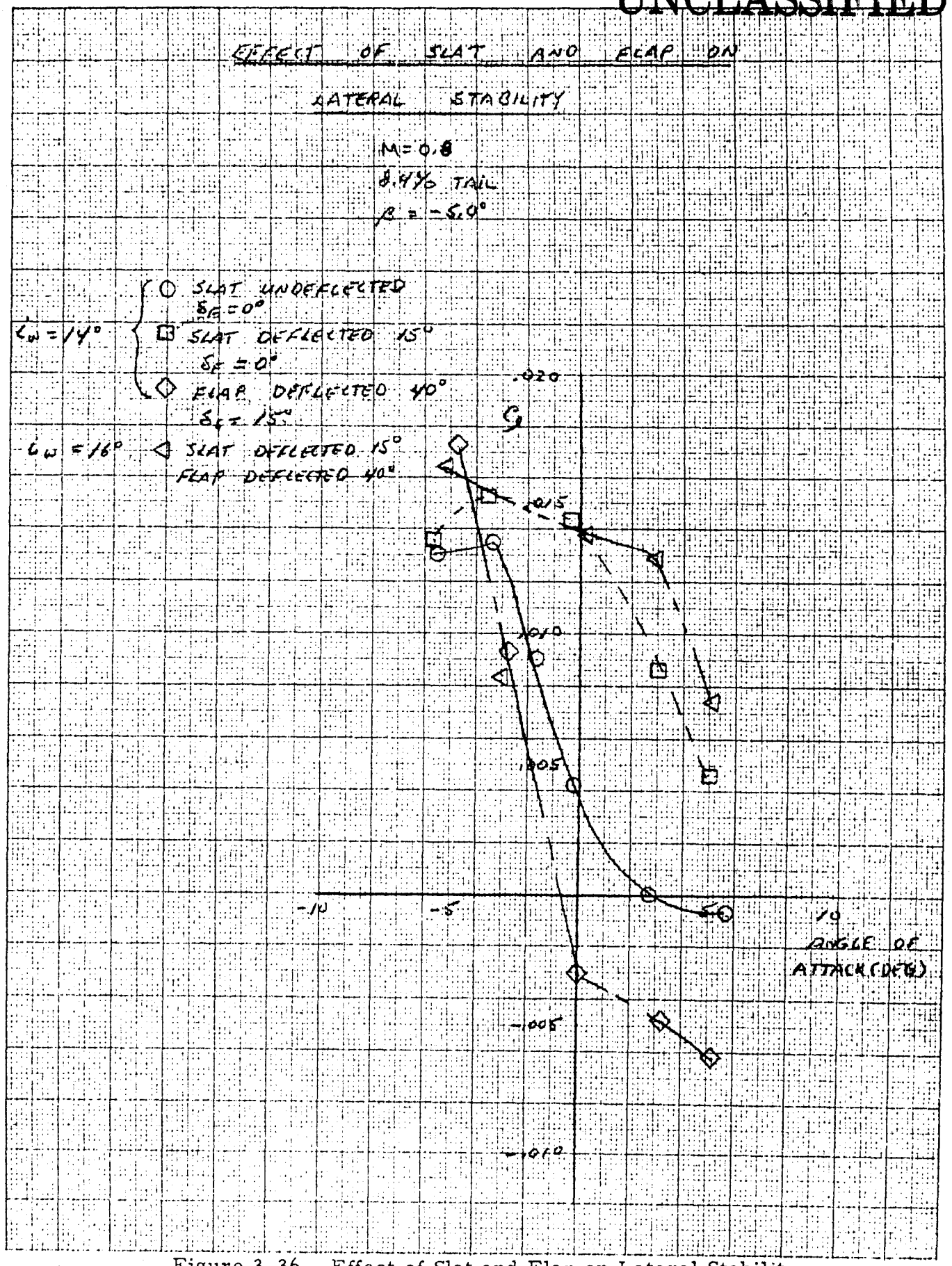

Figure 3-36. Effect of Slat and Flap on Lateral Stability--
M = 0. 8.4% Tail, and β = -5.0°

slot extended approximately from the wing tip to about 3.3 in. from the tip. To increase the aerodynamic interaction, the air jet was ejected only on the wing windward side. This design required only one jet for testing. It was located on the wing left hand side (to produce negative roll). For simulation purposes, the jet on the flight article was assumed to produce 50 lb of thrust. The supply pressure was assumed to be 1,500 psi.

The jet induced rolling moment at Mach 1.2 and 0.8 is shown in Figure 3-37. While the roll data at Mach 1.2 appears to be valid, the data at Mach 0.8 was questionable. During the tests, variations in jet flap plenum pressures on the side opposite the activated roll control plenum were observed. This was caused by the test setup, which allowed some of the air supply to escape into the tunnel near the model base. The escaping air appeared to have no effect at Mach 1.2, but at Mach 0.8, the air appeared to have a slight effect on the missile aerodynamics. The escaped air seemed to reduce the jet-induced rolling moment. At Mach 0.6, the escaped air had such a large effect on the aerodynamics that the roll data was not usable.

At Mach 1.2, the roll jet magnification factor was about 2.5. This is almost identical to the jet flap magnification factor at Mach 1.2. The roll jet magnification factor at Mach 0.8 was approximately 3.4, which is less than the jet flap magnification factor. The data suggest that this reduction in roll magnification factor is partly caused by the escaping gas. Without this interference, it is believed that the roll and jet flap magnification factor would be approximately equal at Mach 0.8.

Based on the assumption that the roll and jet flap magnification factors are approximately equal, an estimate of the roll control was made. This estimate shown in Figure 3-37 assumes that the jet is producing 50 lb of thrust. Because of the reduced dynamic pressure, the roll control increases with a reduction in Mach number. Fortunately, this roll control trend is similar to the induced rolling moment coefficient resulting from a wing launch.

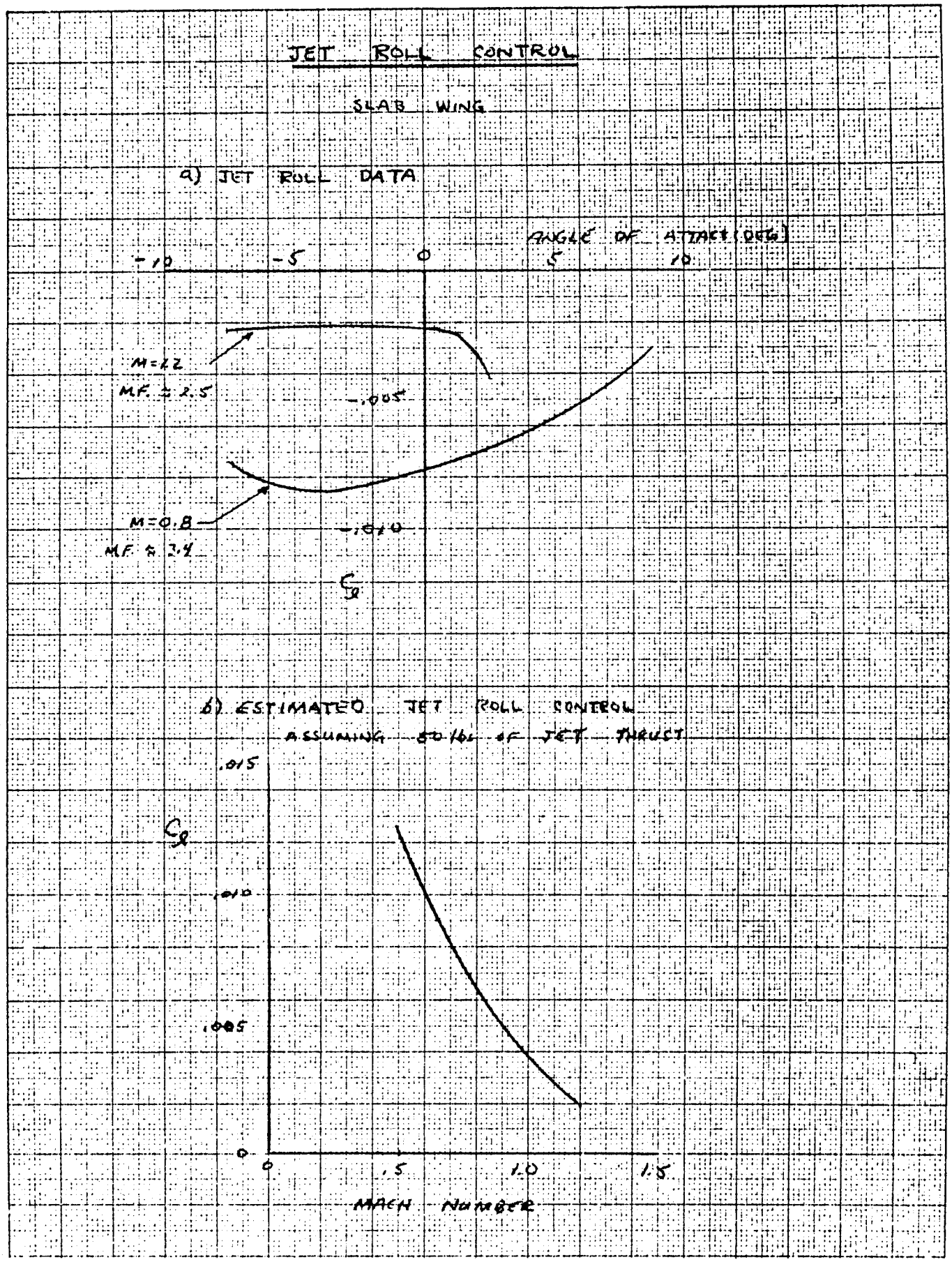

Figure 3-37. Jet Roll Control

3.3.2 Ailerons

The ailerons are shown in Figure 3-2. To reduce the hinge moments, the ailerons were approximately aerodynamically balanced. The area of each aileron was about 19.7 in.^{2} which is about 80% greater than the present Bayonet rollerons. The configuration with which the ailerons were tested was: $\delta_s = 15°$, $\delta_f = 40°$, $i_w = 16°$ and the 30% tail. The left aileron was deflected +15° and the right aileron -15°. The effect of the ailerons on rolling and yawing moment is shown in Figure 3-38. These moments were essentially independent of Mach number. The aileron induced rolling moment coefficient was approximately 0.0027. As the wing launched induced rolling moment coefficient increases with a reduction in launch Mach numbers, the ailerons are not effective enough at low flight velocities.

The spoiler control (Wagner flap) was investigated briefly before the wind tunnel test. This roll control consisted of a segmented cylinder which has its hinge point at its radius for the advantage of very low hinge moments. The roll control is provided by the lift interference from the control onto the wing; similar to a plain flap deflected 90°. This control was eliminated from the test because it was estimated that it would increase the carry drag by 50% or more.

3.4 CARRY AND GLIDE CONFIGURATION

The glide configuration is defined as the carry configuration in free flight with the top vertical tail deployed. This glide configuration is of interest for safe separation from the aircraft under jettison conditions or in the event of wing deployment failure.

3.4.1 Stability

The longitudinal stability for the glide configuration with the 30% horizontal tail is shown in Figure 3-39, at Mach 0.6, 0.8, and 1.2. The configuration was stable at all Mach numbers tested. The effect of deflecting the slat was to reduce pitching moment and trim lift coefficient. The configuration trimmed at a positive normal force coefficient at the subsonic Mach numbers which will result in good separation of the glide configuration from the launch aircraft.

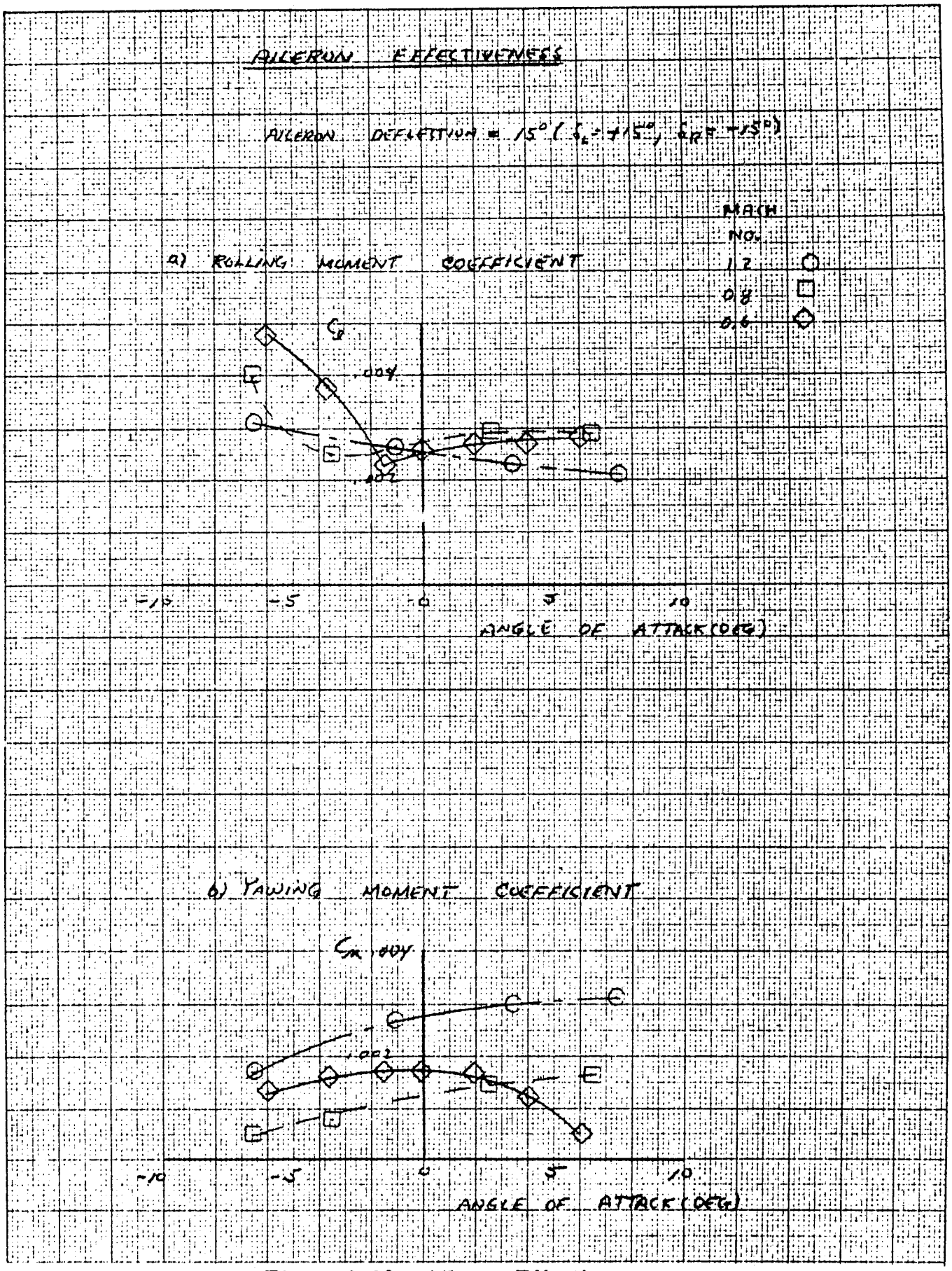

Figure 3-38. Aileron Effectiveness

UNCLASSIFIED

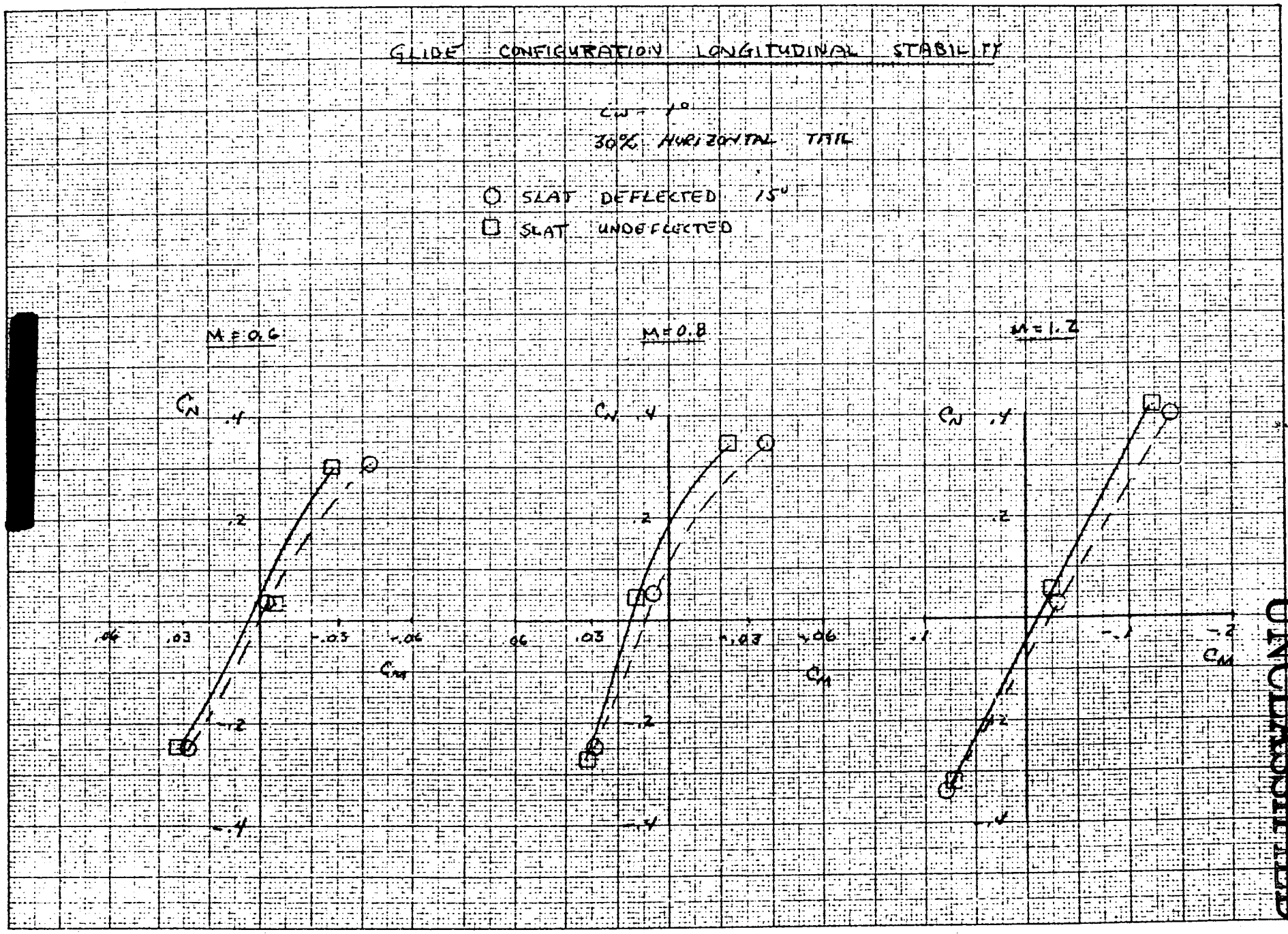

Figure 3-39. Glide Configuration Longitudinal Stability

UNCLASSIFIED

At Mach 1.2, the Bayonet configuration trimmed at a negative normal force coefficient. This trim attitude would probably result in the Bayonet colliding with the launch aircraft upon release. This can be prevented from occurring by providing a small negative deflection on the horizontal tail (positive C_M contribution), without penality.

3.4.2 Drag

The Bayonet carry or glide configuration drag at zero angle of attack is shown in Figure 3-40. This figure shows the effect of both the slat deflected and undeflected as a function of Mach number. The drag for the configuration with the slat undeflected was larger than the drag for the configuration without a slat. It is believed that most of this drag difference is caused by the slat undeflected configuration having a larger horizontal tail and also another vertical tail (on the top side). Deflecting the slat increased the carry drag approximately 45% of the subsonic Mach numbers. At Mach 1.2, the drag increase was approximately 13%.

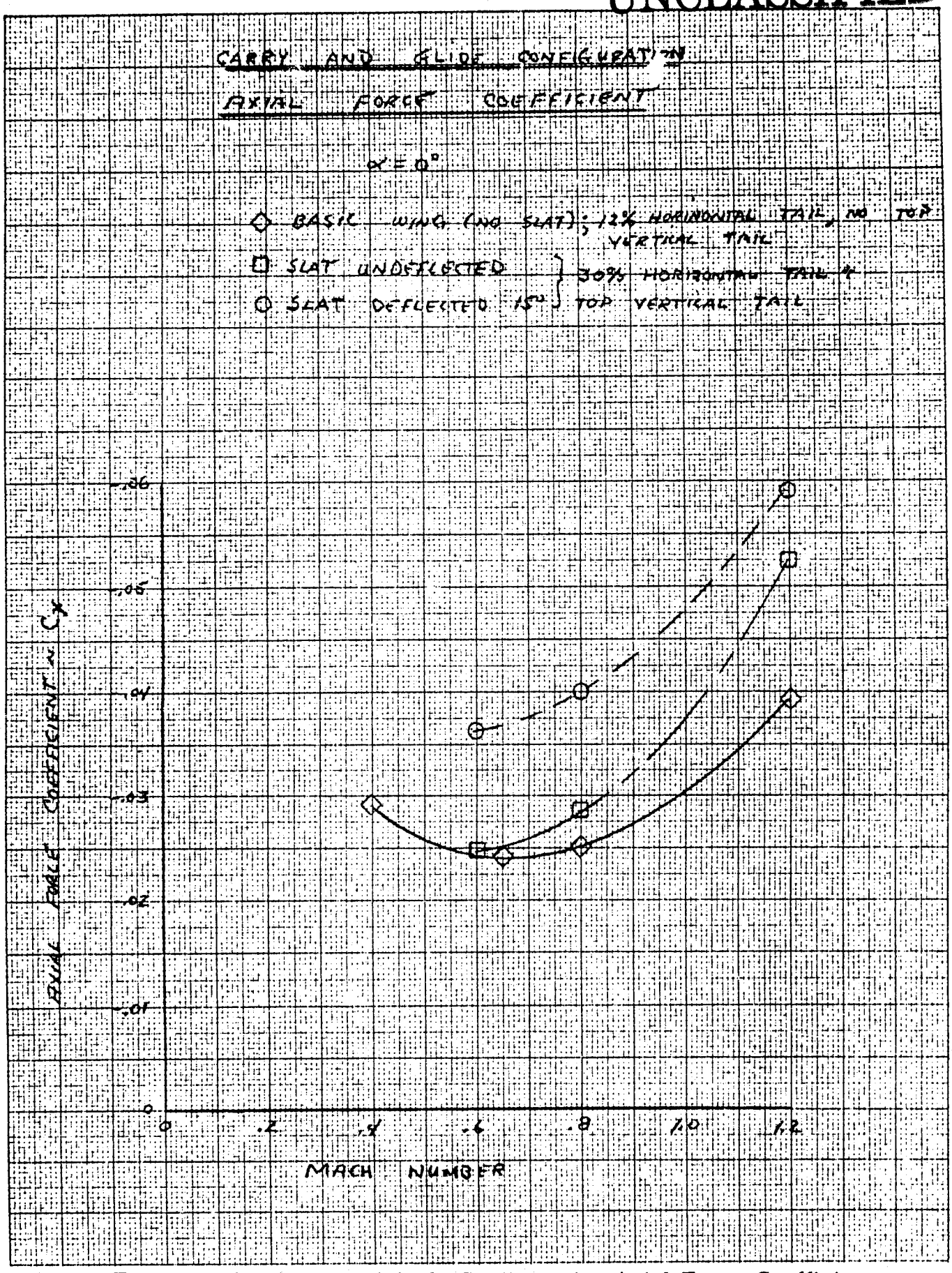

Figure 3-40. Carry and Glide Configuration Axial Force Coefficient

Section 4

ANALYSIS OF ROLL CONTROL REQUIREMENT

4.1 INTRODUCTORY REMARKS

The present Bayonet roll control system with the Sidewinder rollerons has performed satisfactorily to date; cross-range dispersion has been tolerable. This is due to four favorable circumstances: (1) the vehicle has been launched from the aircraft centerline where aerodynamic flow field is symmetric, (2) structural malalignments have been minimal, (3) extreme care has been taken to place the vehicle CG close to the roll axis, and (4) flight time is short. With the requirement for wing launch capability, the method of roll control must be re-evaluated.

From the outset of the Bayonet program, it was established that the Sidewinder rolleron-type roll control system would provide only an expedient method of augmenting inherent aerodynamic roll damping. The rolleron is only a roll-rate restrictor, and offers no positive roll position control. Large external disturbances which occur from the aerodynamic flow field during a wing launch cause sufficient roll position deviation to yield large cross-range dispersions and reduce the desired impact angle. The magnitude of potential external moments was observed in some degree during the launch of the second Bayonet vehicle. Though launched at the centerline, the aircraft pylon configuration was asymmetric which caused severe rolling moments and roll rate excursions.

Because increased roll control is required for future Bayonet vehicles, analytical studies have been undertaken to answer the following basic questions:

1. What is the cross-range dispersion during a wing launch using the present rolleron configuration?

2. Will a modified rolleron design provide significant accuracy improvement?
3. If rollerons (both old and new) exhibit unsatisfactory cross-range dispersion,
   A. What roll control configuration is required?
   B. Which mechanizations appear most promising?

4.2 ROLL CONTROL ANALYSIS

Inasmuch as a firm requirement on CEP does not as yet exist, roll control system performance is presented parametrically. Tradeoff studies of performance and mechanization complexity (cost) are necessary to the final selection of the roll control system configuration.

4.2.1 Rolleron--Existing and Modified

Evaluation of the Sidewinder rolleron configuration was accomplished with a digital simulation (IBM-7094) of the roll/rolleron equations of motion. The block diagram representation of these equations is shown in Figure 4-1. Roll disturbing moments (L_D) were estimated in the vicinity of the wing launch station and these data were included in the simulation, Figure 4-2. The disturbing moments are the moments which exist while the Bayonet is in close proximity to the launch aircraft wing during the initial phases of launch and those moments due to the structural anomalies as described in the Bayonet Final Report SM-51919, December 1965. Analysis of the flow field at the wing station considered only a Mach = 0.45 and 0.8 condition. Very preliminary estimates of the disturbing moments at Mach = 1.2 yield values of the same magnitude as those obtained for Mach = 0.45 and 0.8. Estimation of these moments (Mach = 1.2) is difficult because of the potential aerodynamic shock structure and for this reason if a supersonic launch remains a requirement, a wind tunnel test program is recommended. The largest induced rolling moments exist at the lowest launch velocity, Mach = 0.45 where aerodynamic control effectiveness is at a minimum. For this reason, most analyses were conducted for Mach = 0.45 where flight times are also at a maximum.

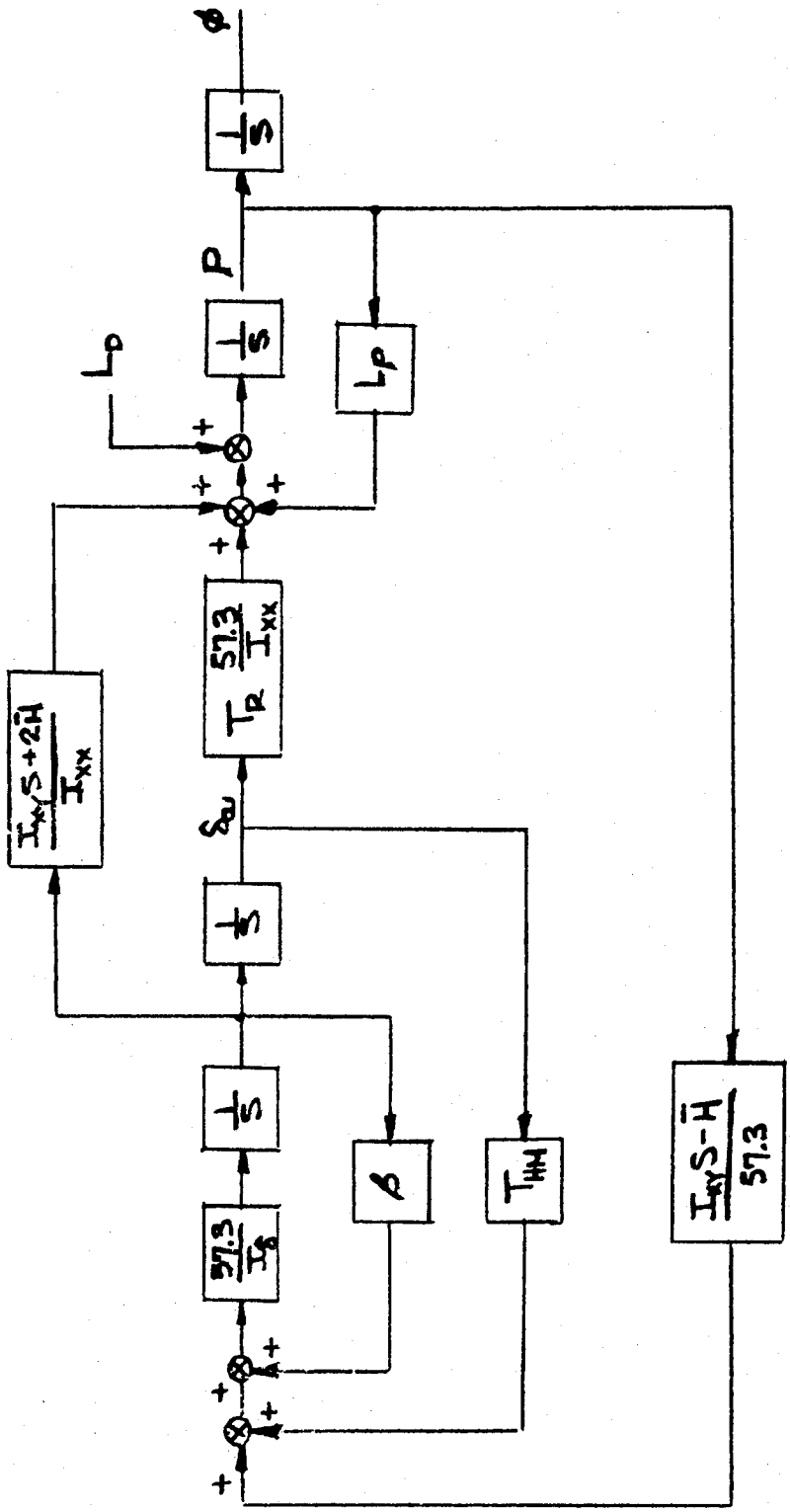

Figure 4-1. Block Diagram--Rolleron Control System

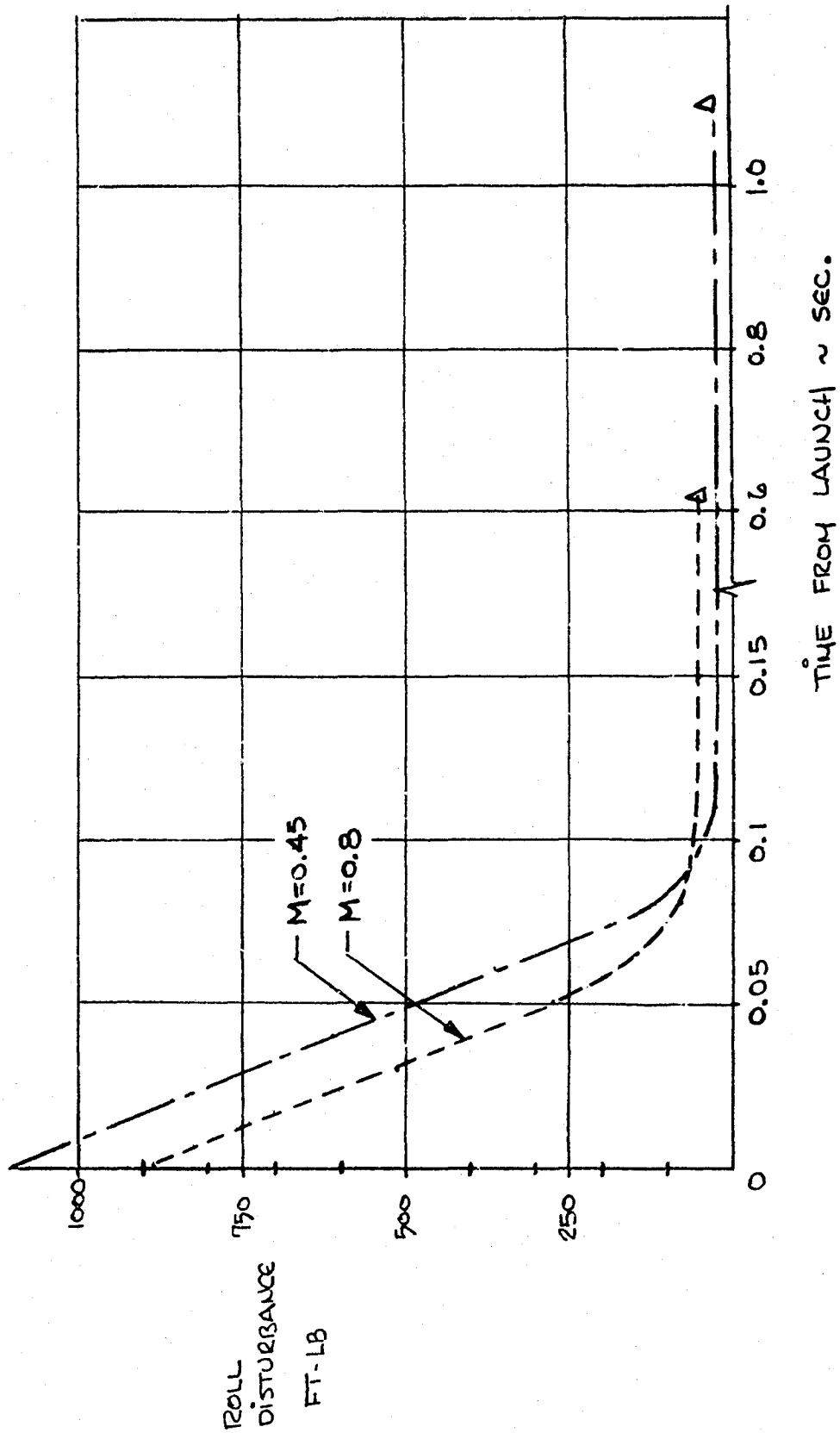

Figure 4-2. Roll Disturbance--Wing Launch

Results of the study of the existing rolleron are presented in Table 4-1. Dispersion is substantially larger than that presented in the progress reports for April and May 1966 for the following reasons:

1. A maximum launch altitude of 200 ft was used rather than the original 150 ft.
2. Initial studies did not incorporate the increased dive capability (load factor) currently achieved by the use of slats and flaps.

Table 4-1

DISPERSION--ORIGINAL ROLLERON

Launch velocity (fps)	500	500	900	900
Launch altitude (ft)	200	200	200	200
Launch position	Wing	CL	Wing	CL
Roll Position-impact (deg)	82.[illegible]	22.47	43.95	23.77
Cross-range dispersion (ft)	1.[illegible]	19.76	71.30	21.89

The rolleron planform was modified to obtain increased area (+80%), decreased aerodynamic stability (a 50% reduction in hinge moment), and better mass balancing about the hinge line. The new rolleron characteristics were analyzed to determine the effect of the modification, and the results are presented in Table 4-2. It is evident that even a major rolleron redesign achieving a substantial increase in control effectiveness (a factor of 3.4) still results in a large cross-range dispersion for the wing launch position.

Table 4-2

DISPERSION--MODIFIED ROLLERON

Launch velocity (fps)	500	500	900	900
Launch altitude (ft)	200	200	200	200
Launch position	Wing	CL	Wing	CL
Roll position-impact (deg)	45.69	13.29	24.64	13.73
Cross-range dispersion (ft)	105.30	13.48	45.93	14.17

4.2.2 Parametric Roll Analysis

To investigate various roll control systems and establish performance indices, the basic roll control system configuration shown in Figure 4-3 was formulated and coded into a second IBM 7094 digital program. Three basic control systems were investigated which are as follows:

1. Type I--Roll rate control other than rollerons. $K_R \neq 0$. $K_\phi = 0$.
2. Type II--Roll position control using only the damping afforded by aerodynamics (L_P). $K_R = 0$. $K_\phi \neq 0$.
3. Type III--Roll position control making use of artificial damping. $K_R \neq 0$. $K_\phi \neq 0$.

Inasmuch as the control capability of a reaction roll control system is relatively invariant with Mach number, it was chosen to facilitate the initial sizing and performance studies.

4.2.2.1 Roll Rate Control--Type I

A roll rate control system similar to the rolleron, but with significantly increased control capability was studied. See the block diagram in Figure 4-3, $K_\phi = 0$. The sensing of roll rate is either with a rate gyro or a rolleron; the primary control capability is generated by gas reaction. With the expected disturbance levels shown in Figure 4-2, a control thrust level of 50 lb was selected, and actuator bandwidths of $K_\delta = 50$ and 100 were investigated. Results are summarized in Table 4-3. The performance is substantially better than that of the rollerons. At a launch velocity of 500 fps, the dispersion of the Type I roll rate control system is 35.97 ft while that of the rolleron (existing and modified) is 139.0 and 105.3 ft.

4.2.2.2 Roll Position Control/Aerodynamic Damping--Type II

The second configuration investigated was one of roll position control using only aerodynamic damping. The characteristic equation for this control system configuration is:

$$S^3 + (K_\delta + L_P) S^2 + (K_R C + K_\delta L_P) S + K_\phi C. \qquad (1)$$

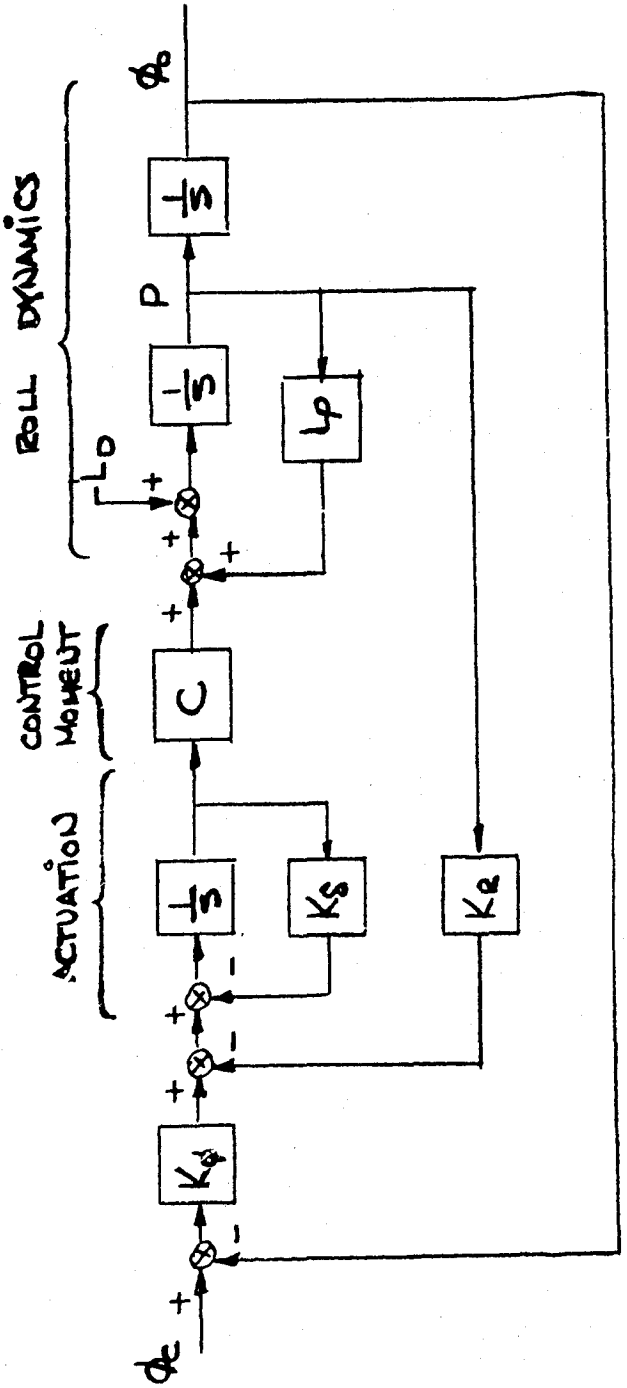

Figure 4-3. Block Diagram--Basic Control Configuration

UNCLASSIFIED

Table 4-3

SUMMARY--TYPE I ROLL CONTROL

Launch velocity (fps)	500	500	500	500	900	900	900	900
Launch altitude (ft)	200	200	200	200	200	200	200	200
Launch position	Wing	Wing	CL	CL	Wing	Wing	CL	CL
Thrust (lb)	50	50	50	50	50	50	50	50
K_δ	100	50	100	50	100	50	100	50
K_R	2.5	0.625	2.5	0.625	2.5	0.625	2.5	0.625
K_ϕ	0	0	0	0	0	0	0	0
Roll position-impact (deg)	13.28	16.4	1.48	2.87	6.59	9.94	2.56	4.83
Cross-range dispersion (ft)	35.97	42.5	1.54	2.99	14.89	20.76	2.76	5.23

UNCLASSIFIED

where:

$$C = T l \frac{k\ 57.3}{I_x}$$

$$K_R = 0$$

$$L_P = C_{l_p} \frac{Ab^2 q}{2V} \frac{57.3}{I_x}$$

By Routh's Criteria, stability is assured if:

$$(K_\delta + L_P)(K_\delta L_P) > K_\phi C \tag{2}$$

To ensure adequate stability margin, an additional factor of 4 was incorporated, to yield the following requirement on attitude gain:

$$K_\phi < \frac{(K_\delta + L_P)(K_\delta L_P)}{4C} \tag{3}$$

With a control thrust level of 50 lb and $K_\delta = 100$ (indicative of a reasonable actuator bandwidth), the inequality Equation 3 was evaluated at all launch velocities so as to determine the maximum allowable K_ϕ. This resulted in a value of $K_\phi = 6.0$. A transient response, Figure 4-4, was obtained for a wing launch at a velocity of 500 fps, the condition of the largest induced rolling moment. The cross-range dispersion was 15.5 ft; however, the roll behavior is somewhat oscillatory. A lowered attitude gain reduces the tendency to oscillate, but at the expense of additional dispersion.

4.2.2.3 Roll Position Control/Artificial Damping--Type III

To gain better damping characteristics, an active rate loop was incorporated. Inasmuch as $K_R \neq 0$, the inequality defining stability becomes:

$$(K_\delta + L_P)(K_R C + K_\delta L_P) > 4 K_\phi C \tag{4}$$

From this inequality, it is readily shown that the ability to generate damping through control action ($K_R C$) permits a substantially larger attitude gain K_ϕ.

UNCLASSIFIED

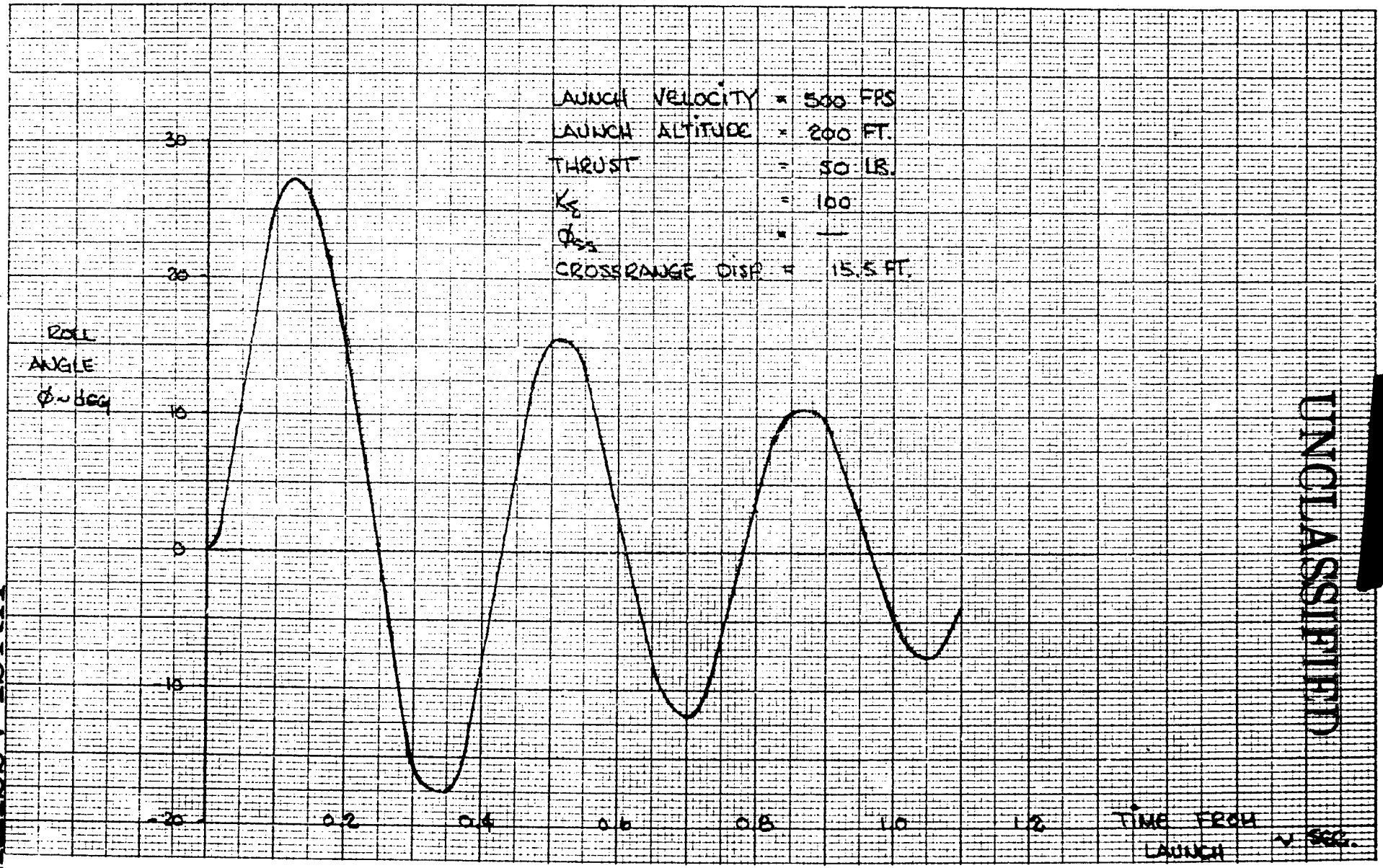

Figure 4-4. Type II--Typical Roll Transient

UNCLASSIFIED

To afford adequate stability margin, the factor of 4 has again been incorporated in selecting the attitude gain K_ϕ. With $K_\delta = 100$ and a thrust level of 50 lb, it is possible to support gains of $K_R = 0.85$ and $K_\phi = 30$. The increased attitude gain K_ϕ (from 6 to 30), with an attendant decrease in steady-state roll position error yields a substantial reduction in dispersion; 7.8 ft at M = 0.45. The increased rate gain reduces the tendency to oscillate.

The influence of actuator bandwidth (K_δ) was investigated because the amount of rate gain (K_R) and attitude gain (K_ϕ) is dependent primarily upon the actuation bandwidth. A lower actuator bandwidth means a lower rate gain; lower rate gain necessitates lower attitude gain; lower attitude gain yields larger steady-state roll errors; larger steady-state roll errors result in increased dispersion. The effect of decreasing actuator bandwidth K_δ from 100 to 50 is readily apparent by noting the transient comparison in Figure 4-5. For the lower actuator bandwidth ($K_\delta = 50$), the initial roll excursion is larger, due to slower control response. Further, steady-state error is greater because of the inability to support an attitude gain of 30 (reduced to 5.5). The net result is an increase in dispersion from 7.8 ft to 11.06 ft.

A second parameter sensitivity which was investigated is required control capability (C). A thrust level of 50 lb does not generate a control torque as large as the transient disturbing torques which exist during a wing launch; however, the time period in which the control system is overpowered is short. A thrust level of 25 lb was evaluated to determine cross-range dispersion sensitivity to basic control capability; this result is also shown in Figure 4-5. The 25 lb thrust level results in an excessively overpowered condition, and the dispersion rises from 7.8 ft to 30.3 ft.

Table 4-4 summarizes the pertinent results of the parametric analyses conducted on the Type III roll control system.

4.2.2.4 Aerodynamic Control

A third IBM 7094 program was coded to study the use of aileron control for Bayonet. Based upon the results of the preceding roll studies, only roll position control was investigated. Further, because induced rolling moments are

UNCLASSIFIED

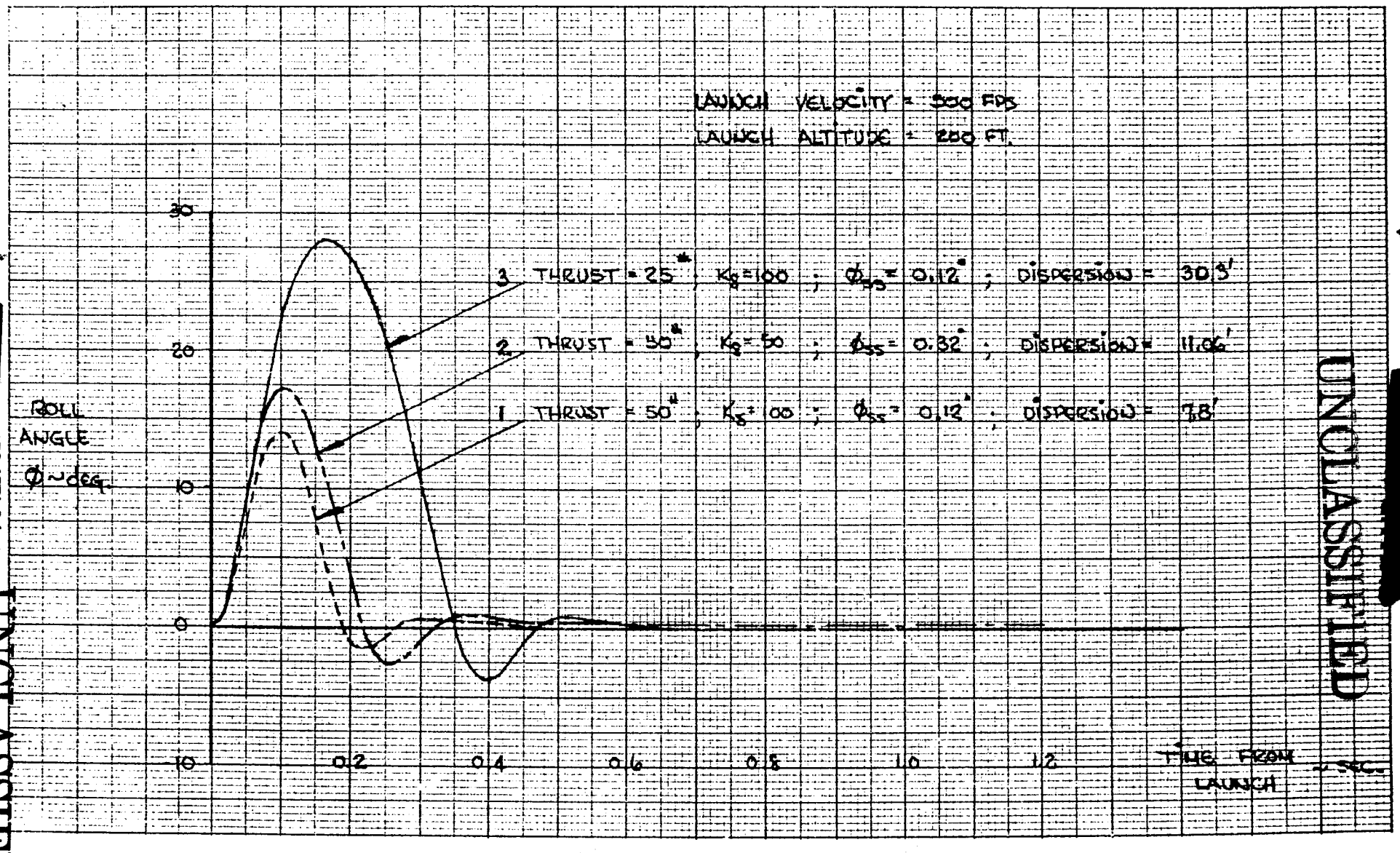

Figure 4-5. Type III--Parameter Sensitivity

UNCLASSIFIED

Table 4-4

SUMMARY--TYPE III ROLL CONTROL

Launch velocity (fps)	500	500	500	900	900	900
Launch altitude (ft)	200	200	200	200	200	200
Thrust (lb)	50	50	25	50	50	25
K_δ	100	50	100	100	50	100
K_R	0.85	0.25	1.70	0.85	0.25	1.70
K_ϕ	30	5.5	60	30	5.5	60
Launch position	Wing	Wing	Wing	Wing	Wing	Wing
Roll position-impact (deg)	0.12	0.32	0.12	0.35	1.02	0.35
Cross-range dispersion (ft)	7.8	11.06	30.03	4.49	9.43	13.6
Launch position	CL	CL	CL	CL	CL	CL
Roll position-impact (deg)	0.12	0.32	0.12	0.35	1.02	0.35
Cross-range dispersion (ft)	0.35	0.95	0.35	1.06	2.90	1.15

maximum and aerodynamic control is minimum, only M = 0.45 was studied. The characteristic equation for aileron control is similar to that for reaction control; however, control effectiveness (C) is redefined:

$$C = C_{l_{\delta_a}} \frac{Ab\,q\,57.3}{I_x} \tag{5}$$

As seen from this equation, aileron effectiveness is directly dependent upon dynamic pressure which varies approximately 8 to 1 throughout the launch envelope; therefore, stability variations with launch condition must be accounted for.

The results of the simulation are listed in Table 4-5. The aileron size used initially in the study was identical to that of the modified rolleron. It was immediately evident that the rolleron-sized aileron was inadequate. The size was increased by a factor of 6 and proved adequate (7.8 ft dispersion) if an aileron rate capability of approximately 500 deg/sec were available. By the judicious incorporation of an attitude error limiter, instability was avoided with an aileron rate limit of 250 deg/sec; however, the dispersion increased to 20.47 ft. This can be reduced to 13.82 ft by increasing the Amendment 6 aileron size tenfold.

4.2.3 Summary--Analytical Studies

The results of the analytical investigations are summarized below:

1. A roll position control system is required to achieve a cross-range dispersion of 10 ft or less from launch altitudes to 200 ft.
2. Artificial rate feedback is required.
3. A minimum control torque of 400 to 500 ft/lb is required.
4. An actuator time constant of approximately 20 to 25 msec is required. If a dispersion of 15 ft is permissible, this time constant can be relaxed to approximately 35 msec.
5. A 6- to 10-fold increase in aileron size will be required if ailerons with 250 deg/sec capability are used.

Table 4-5

SUMMARY--AERODYNAMIC ROLL CONTROL

Launch Velocity (fps)	500	500	500	500
Launch Altitude (ft)	200	200	200	200
Launch Position	Wing	Wing	Wing	Wing
Aileron Effectiveness $\left(C_{L_{\delta a}}\right)$	0.001(1)	0.001(1)	0.001(1)	0.0016(2)
Aileron Rate Limit $\left(\dot{\delta}_L\right)$	500	250	250	250
K_δ	100	100	100	100
K_R	5.5	5.5	5.5	3.4
K_ϕ	185	185	185(4)	115(4)
Roll Angle--Impact (deg)	0.35	(3)	0.35	0.35
Cross-Range Dispersion (ft)	7.8	(3)	20.47	13.82

NOTE: (1) Amendment 6 aileron effectiveness increased 6 times.
(2) Amendment 6 aileron effectiveness increased 10 times.
(3) Unstable condition.
(4) Attitude error limited: $-5° \leq \phi_\epsilon \leq +5°$.

4.3 MECHANIZATION

The mechanization of the roll control system can be broken into four basic component areas which are: (1) sensors, (2) logic, (3) moment generation, and (4) actuation.

4.3.1 Sensors

With the requirement that both roll position and roll rate information must be available, the three following alternatives exist:

1. Roll position instrument plus differentiation to obtain rates.
2. Roll rate instrument plus integration to obtain position.
3. Individual roll rate and roll position instruments.

Alternate 2 is the cheapest, most reliable of the three candidates. Integration of body rate information should yield more than adequate roll position information over the short flight time. Further, integration is usually preferred over differentiation because integration is basically a data-smoothing process while differentiation is a noise producer.

4.3.2 Logic

The primary logic alternatives are as follows:

1. Electrical.
2. Fluidic.
3. Mechanical/Fluidic.

This is the most difficult tradeoff to establish. Electronic logic necessary to mechanize the roll position control system would most probably consist of two batteries, two series voltage regulators, a multistage power amplifier, and two or three passive shaping networks. This type of system mechanization is uncomplicated and provides the flexibility to correct difficulties encountered during a flight test program. Electrical spin-up of the gyro prior to launch would probably be required. Spring-wound or pyrotechnic gyros are probably not sufficiently rapid in starting, and would probably produce an erroneous attitude reference during launch.

A fully pneumatic gyro with a pneumatic output device and the associated stages of air amplification and shaping provides a simple, cheap, reliable system: one in which the fluid is the only moving component. Cold gas would be used in the logic circuitry. It can be stored at approximately 100 psi, will represent little safety hazard and can be regulated to the desired operating pressure. A most attractive feature of a completely pneumatic instrument is that the gyro becomes fully operative with the release of the stored cold gas. This fast start capability, requiring no delay to spin-up, permits activation of the control system at launch. It must be established, however, that the frequency response (bandwidth) of this system is adequate.

A combined mechanical/fluidic approach would offer the solution to the logic design if the pneumatic gyro bandwidth is inadequate. This concept uses a mechanical output device (probably a flapper) to mechanically trigger pneumatic logic circuitry. Though a gyro of this type is not available, prototype development appears uncomplicated and relatively cheap. Further, response characteristics should be adequate and complexity low. The drawback of this type of gyro is the requirement that spin-up be accomplished prior to launch. Partial rundown of the gyro after launch is of little consequence because of the short flight time.

4.3.3 Moment Generation

The following are the two primary moment generation alternatives:

1. Aerodynamic/ailerons.
2. Reaction.

Inasmuch as the required control torque level is set at the minimum launch velocity (minimum q) because of the nature of the induced rolling moment, an aerodynamic control device sized to develop this torque level at M = 0.45 is greatly oversized at all other flight conditions. Further, analysis shows that the rolleron size tested in the Amendment 6 wind tunnel tests is inadequate for use as an aileron. It will be necessary to increase control surface size by a factor of 6 to 10, to permit a reasonable fin-rate requirement of 250 deg/sec. The increased inertia of the aileron arising from the size

modification and the associated linkage, indicates that it is unlikely that actuation bandwidth can be maintained. Lack of aileron stiffness results in decreased control system gain and increased dispersion.

On the other hand, the analytical studies have shown that reaction control has adequate response for Bayonet. Control system performance variation over the launch regime is minimal, caused only by small variations in thrust amplification factor (2.5 to 4.1). The mechanization is rather simple and relatively inexpensive.

A second level tradeoff involves the use of hot or cold gas. Cold gas, (N_2) pressurized to 3,500 psi is required to yield regulated 1,500 psi control gas for 1.5 sec duration. The storage volume required for 50 lb of thrust for this duration is 350 cu in. (5-1/2 diam x 21-5/8 long). Because of the large volume of the gas storage vessel, a comparable, but smaller blowdown (unregulated) system may be more desirable. A blowdown system requires pressurization to 6,000 psi. The initial thrust level of 75 lb decays to 20 lb within 1.5 sec. The storage volume for this system is 140 cu in. (5-1/8 diam x 13.0 long). In either case, the pressurized cold gas container represents an extreme safety hazard and the large occupied volume allows little space for other components of the system.

System performance can be improved, and required volume in the fuselage minimized, by using a solid propellant, hot gas reaction system. This system produces 50 lb of thrust for 1.5 sec. The required volume of the gas generator is substantially less than the cold gas containers: 30 cu in. (3 in. diam x 5 in. long).

Olin Mathieson can deliver PFRT qualified generators (1B-27 propellant) 8 weeks after ATP at a cost of $275 each for 12 prototype units or $220 each for 100 production units. The cost of the hermetically-sealed cold gas container and explosive cutter squib is roughly the same as the cost of the hot gas generator. If a regulated cold gas supply is selected, the cost will increase by approximately $125 (over that of the hot gas system). Development problems associated with high temperature, contaminated gas are no more severe than those encountered and solved on other missile programs.

In a successful firing test at White Sands Missile Range on 8 August 1966, the Army Missile Command demonstrated a two-axis hot gas jet attitude control system. The hot gas stages were operated from a 2,350°F, 1,000 psi, solid propellant generator. The three supersonic output stages of the fluidic logic and amplification chain were driven in a nonlinear pulse duration modulation mode.

4.3.4 Actuation

If hot gas reaction control is selected, the valving concepts are as follows:

1. Two-stage, electro/pneumatic valve.
2. Fully pneumatic valve.

This selection will be uncomplicated when the logic mechanization is determined.

If an electronic logic network is chosen, then a two stage electro-mechanical hot gas servo valve will be required to provide gas differentially to the control nozzles. The valve will be located in the fuselage and will be a flow control type designed to maintain a constant differential orifice area independent of command input. This method of flow control maintains a relatively constant chamber pressure in the gas generator, and thus the overboard gas relief valve serves only as a safety device.

The first stage of the valve positioned by an electrical torque motor is a flapper type which serves as the pilot for the second stage. A similar first stage hot gas valve was successfully developed for the Mauler program and could be used for the Bayonet application with low cost, low risk modifications.

If a fluidic logic network is used, a fully fluidic valve is the obvious choice. The final stage of amplification is a hot gas stage (similar to that demonstrated by AMC) which operates much like the secondary injection used in thrust vectoring rocket engines. The injectant used to switch the hot gas flow controlling the vehicle is simply the stored cold gas. This system of valving involves no moving parts and is compatible with a fully pneumatic control system.

4.4 PRELIMINARY ROLL CONTROL CONFIGURATION

The two leading candidate roll control configurations are presented in Figures 4-6 and 4-7. Figure 4-6 is of a fully pneumatic control system; Figure 4-7 is the more nearly standard electro/mechanical mechanization. Both systems will use a body-mounted rate gyro, integration circuitry to provide the attitude reference, and hot gas reaction control. Problems associated with the use of hot gas have been solved on other missile programs (e.g, the recent AMC test); therefore, the development risk is considered to be small. A more detailed tradeoff is required, however, to establish whether fluidic or electronic logic circuitry must be used. Detailed cost and schedule requirements must be thoroughly evaluated, and potential instrument suppliers must be contacted for the best design possible to be developed for Bayonet. If cost and schedule tradeoffs are favorable, the fully pneumatic system appears to hold a definite advantage in that it offers a simple, no-moving-parts control system. Further, it offers a very rapid activation capability. The Harry Diamond Labs, U. S. Army Materiel Command, Washington, D. C., have designed and successfully tested a fully fluidic system of this type which controlled an 80 lb hot gas reaction jet. AMC has also developed and flight tested a two-axis, hot gas reaction control system. Sensing is accomplished by a two-axis free gyro with pneumatic output.

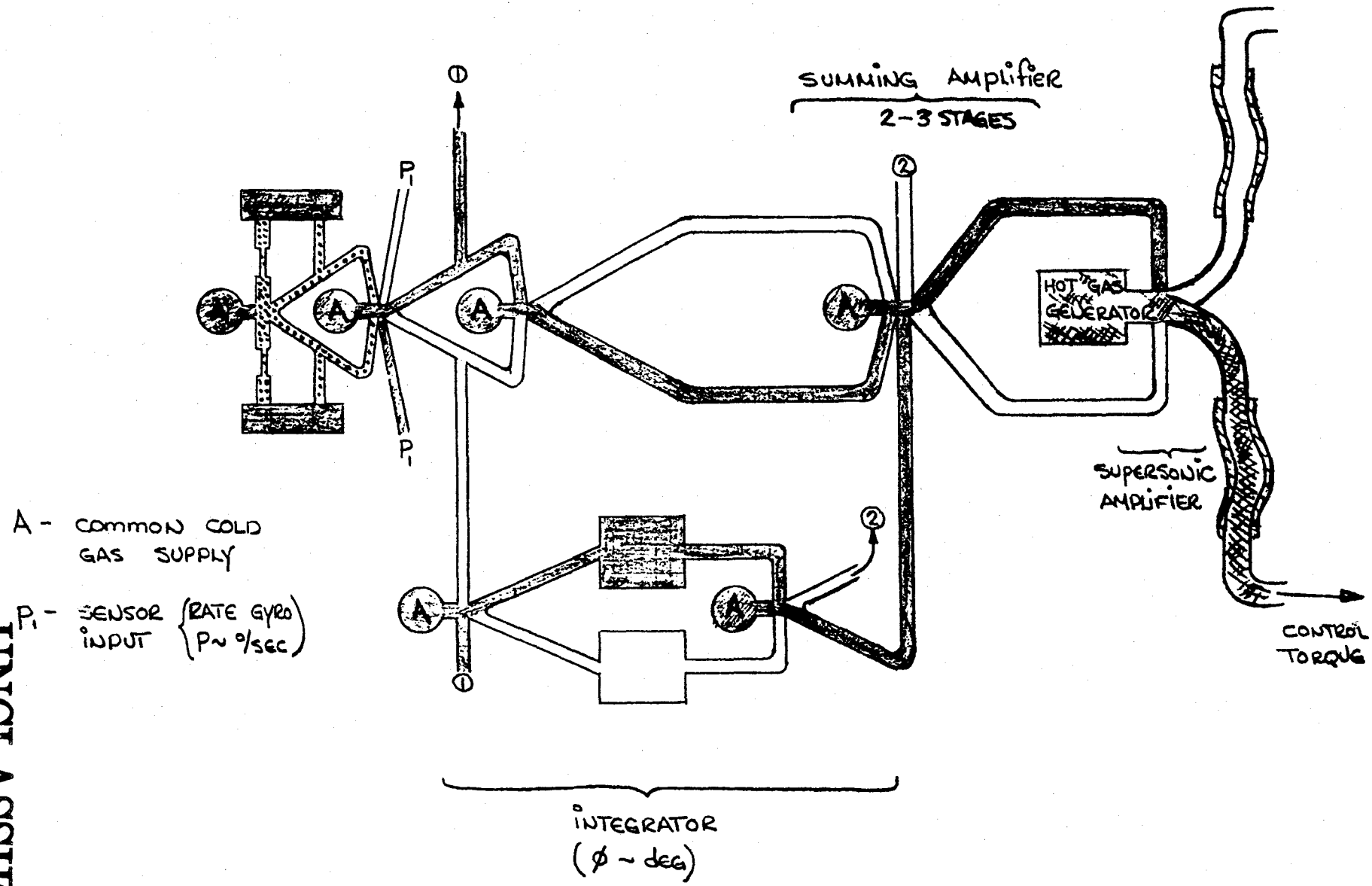

Figure 4-6. Fluidic Roll Control System

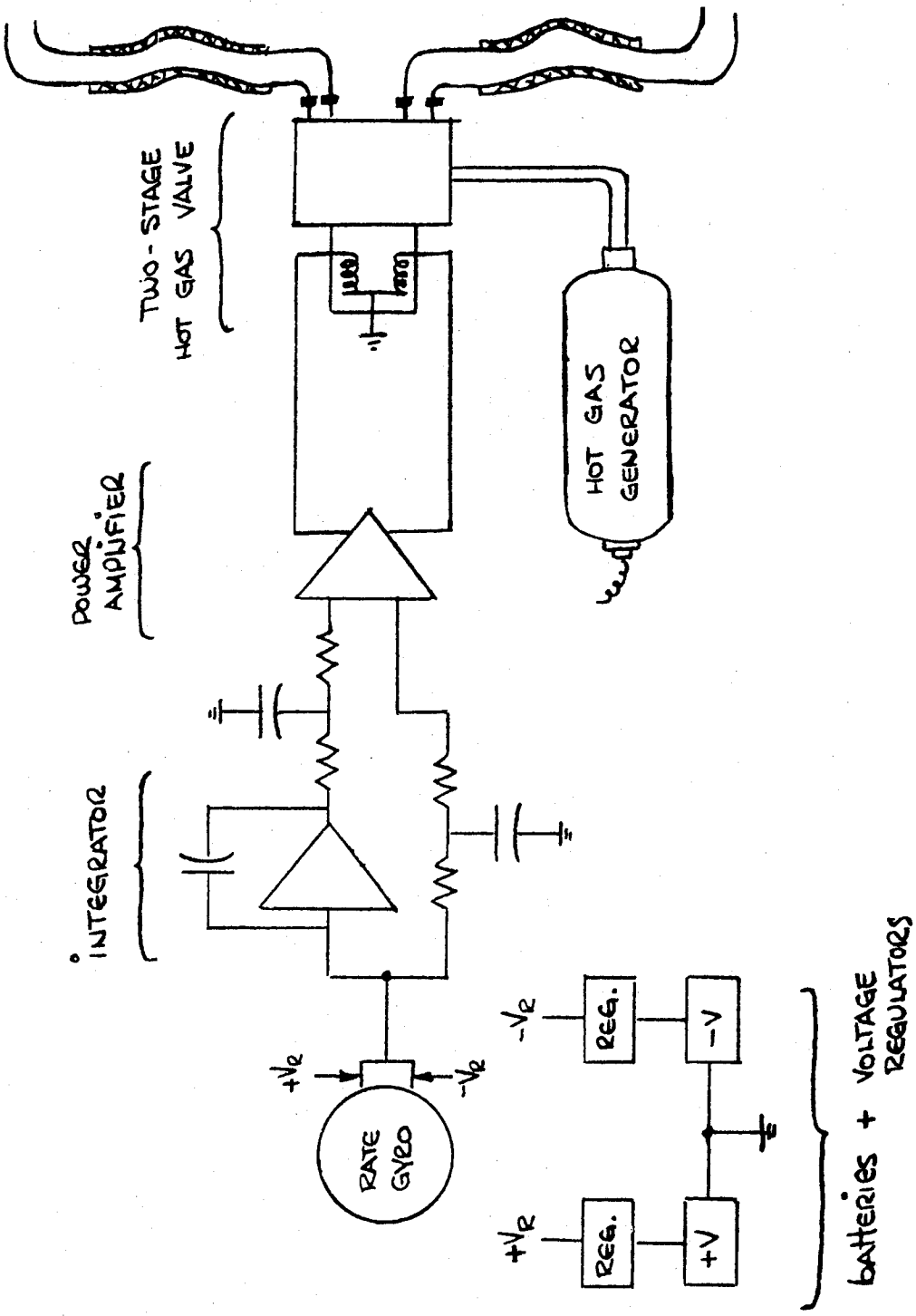

Figure 4-7. Electro/Mechanical Roll Control System

Section 5
RECOMMENDED ADVANCED BAYONET CONFIGURATION

Based on the preceding data and discussion, if minimum release altitude, wing launch capability, and minimum CEP remain as requirements, the following devices are recommended for incorporation in the Advanced Bayonet configuration:

1. Slab Wing

   The slab wing produces approximately the same lift as the contoured wing and because of its simplicity, the slab wing will be easier and cheaper to fabricate.

2. Plain Flaps

   The plain flaps are recommended because they produce considerable lift increase ($\Delta C_L = 0.4$) and because they will probably be considerably less complex than the jet flaps.

3. Slats

   Although the slats do not directly provide much lift increase, they indirectly increase lift by allowing an increase in wing incidence by providing a considerable increase in directional stability. The optimum wing incidence should be between 18° and 20°.

4. T-Tail

   To reduce trim angle-of-attack variations with Mach number, the attachment of the horizontal tail to the bottom vertical tail is recommended. This arrangement should remove the tail from the flap wake and should increase the tail effectiveness at the higher Mach numbers.

5. Jet Roll Control

   A roll jet is recommended because it can provide good roll control at the low launch velocities where the induced rolling moments from a wing launch are large. The aileron low-speed roll effectiveness appears to be too small to cope with the induced rolling moments from a low-speed wing launch.

Based on the data in Figures 3-26 through 3-28, which assume a constant horizontal tail effectiveness, the minimum launch altitude for the recommended configuration is 87, 91, and 96 ft at M = 0.6, 0.8, and 1.2. These altitudes are based on a 30° impact angle and assume the present Bayonet weight of 462 lb.

REFERENCES

1. A Proposal to Conduct a Wind-Tunnel Test Program for an Advanced Bayonet System (U), Douglas Report SM-52014P, March 1966. (C)

2. R. L. Pelley. Aerodynamic Study to Optimize Bayonet Lift, Douglas Report SM-48202, 18 October 1965.

3. Cornell Bayonet Data Report for 1965, Wind Tunnel Test. (C)

4. Preliminary Wind Tunnel Data, Transmitted from Cornell Aeronautical Laboratory, 24 June 1966.

5. Final Report - Bayonet Project, Douglas Report SM-51919, December 1965. (C)

Appendix A
NOTATION FOR RUN SCHEDULE

B_4	30 in. body plus both vertical tails
W_2	Contoured wing
W_3	Slab wing
W_4	$W_2F_2A_1S_1$
W_5	$W_3F_3A_2$
H_2	Horizontal tail, small
H_3	Horizontal tail, large
F_2	Wing flap
F_3	Slab wing jet flap
A_1	Aileron
A_2	Slab wing jet aileron
S_1	Slat
G_2	Forward wing-body fairing
G_3	Aft wing-body fairing
G_4	Fairing in wing arrestor hole
L_1	Mounting lugs
T	Boundary layer trip

Table A-1 (page 1 of 3)

RUN SCHEDULE

Configuration	Run No.	Mach No.	Schedule	β	Wing Incidence	Flap Position or Pressure	Slat Position	Comments
$B_4W_5G_2G_3T$	1	-	0	0	14°	Plugged	-	Line pressure effects
	2	-	A/B	0/-5			-	Static tare
	3	1.2	A	0			-	
	4		B	-5			-	
	5	0.8	A	0			-	
	6		B	-5			-	
	7	0.6	A	0			-	
	8		B	-5			-	
	9	1.2	0°	0°			-	Wind off thrust at P = 582 psf
	10		A				-	
	11		B	-5			-	
	12	0.8	0°	0			-	Wind off thrust at P = 743 psf
	13		A				-	
	14		B	-5			-	
	15	0.6	0°				-	Wind off thrust at P = 938 psf
	16		A				-	
	17			0°			-	
$B_4W_5G_2G_3T$	18	-	0°			Plugged	-	Aileron thrust at ATM
$B_4W_4H_2T$	19	0.8	C			0°	Closed	Oil flow
	20	-	A					Static tare
	21	1.2						
	22		B	-5				
	23	1.1	A	0				
	24		B	-5				
	25	1.0	A	0				
	26	1.0	B	-5				
	27	0.95						
	28		A	0				
	29	0.8						
	30		B	-5				
	31	0.6						
$B_4W_4H_2T$	32		A	0				
$B_4W_4H_2G_2T$	33	08						
$B_4W_4H_2G_2T$	34		B	-5				
$B_4W_4H_2G_3T$	35		A	0				
$B_4W_4H_2G_3T$	36		B	-5				
$B_4W_4H_2G_4T$	37		A	0				
$B_4W_4H_2G_4T$	38		B	-5			Closed	
$B_4W_4H_2T$	39	1.2	A	0			Open	
	40		B	-5				
$B_4W_4H_2T$	41	0.8	A	0	14°	0°	Open	

[redacted]

UNCLASSIFIED

Table A-1 (page 2 of 3)

Configuration	Run No.	Mach No.	Schedule	β	Wing Incidence	Flap Position or Pressure	Slat Position	Comments
$B_4W_4H_2T$	42		B	-5	14°	0°	Open	
	43	0.6	A	0				
	44		B	-5		0°	Open	
	45	1.2	A	0		40°	Closed	
	46		B	-5				
	47	0.8	A	0				
	48		B	-5				
	49	0.6	A	0				
	50		B	-5		40°		
	51	1.2	A	0		25°		
	52		B	-5				
	53	0.8	A	0				
	54		B	-5				
	55	0.6	A	0				
	56		B	-5		25°		
	57	1.2	A	0		50°		
	58		B	-5				
	59	0.8	A	0				
	60		B	-5				
	61	0.6	A	0				
	62		B	-5	14°	50°	Closed	
	63	1.2	A	0	16°	40°	Open	
	64		B	-5				
	65	1.1	A	0				
	66		B	-5				
	67	1.0	A	0				
	68		B	-5				
	69	0.95	A	0				
	70		B	-5				
	71	0.80	A	0				
	72		B	-5				
	73	0.6	A	0				
$B_4W_4H_2T$	74		B	-5				
$B_4W_4H_3T$	75	1.2	A	0				Grounding indication
	76	1.2	B	-5				Grounding indication
	77	1.1	A	0				Grounding indication
	78		B	-5				Grounding indication
	79	1.0	A	0				Grounding indication
	80		B	-5				Grounding indication
	81	0.95	A	0				Grounding indication
$B_4W_4H_3T$	82		B	-5	16°	40°	Open	Grounding indication

UNCLASSIFIED

[redacted]

Table A-1 (page 3 of 3)

Configuration	Run No.	Mach No.	Schedule	β	Wing Incidence	Flap Position or Pressure	Slat Position	Comments
$B_4W_4H_3T$	83		D	0	16°	40°	Open	Repeat run 79 grounding indicated
	84	0.8						Repeat run 79 grounding indicated
	85		E	-5				Repeat run 79 grounding indicated
	86	0.6	D	0				
	87		E	-5				
	88	1.2	D	0				Grounding indication
	89		E	-5				Grounding indication
	90	0.8	D	0				Grounding indication
	91		E	-5				Grounding indication
	92	0.6	D	0				
	93		E	-5	16°	40°		
	94	1.2	F	0	1°	0°		
	95	0.8	F	0				
	96	0.6	F	0			Open	
	97	1.2	F	0			Closed	
	98	0.8	F	0				
$B_4W_4H_3T$	99	0.6	F	0	1°	0°	Closed	
$B_4W_5H_2T$	100	-	0°	0°	14°	100 & 200	-	
	101	-	-	0°		-	-	Static tare
	102	1.3, 18, 0.6	0			100 & 200	-	Wind off thrust ground
	103	1.2	D			200	-	
	104		E	-5			-	
	105	0.8	D	0		75		
	106	0.8 & 0.6	-	-		36 & 75	-	Wind off thrust
	107	0.6	D	0		75	-	
$B_4W_4H_2T$	109	-	-	-	14°	0, 100, 200, 300 & 400	Lost Seal	Effects of line pressure

Angle of Attack Schedule

A = -8, -5, -3, -1, 0, 1, 3, 5, 8, 0

B = -5, -3, -1, 0, 1, 3, 5, 0

C = = 0°, ϕ = 0°, 90°, 180°
= 8°, ϕ = 180° For oil flow

D = -8, -5, -2.5, 0, 2.5, 5, 0

E = -5, 2.5, 0, 2.5, 5, 0

F = -5°, 0, 50°